

Low-rank optimization on Tucker tensor varieties

Bin Gao · Renfeng Peng · Ya-xiang Yuan

Received: date / Accepted: date

Abstract In the realm of tensor optimization, low-rank tensor decomposition, particularly Tucker decomposition, stands as a pivotal technique for reducing the number of parameters and for saving storage. We embark on an exploration of Tucker tensor varieties—the set of tensors with bounded Tucker rank—in which the geometry is notably more intricate than the well-explored geometry of matrix varieties. We give an explicit parametrization of the tangent cone of Tucker tensor varieties and leverage its geometry to develop provable gradient-related line-search methods for optimization on Tucker tensor varieties. The search directions are computed from approximate projections of antigradient onto the tangent cone, which circumvents the calculation of intractable metric projections. To the best of our knowledge, this is the first work concerning geometry and optimization on Tucker tensor varieties. In practice, low-rank tensor optimization suffers from the difficulty of choosing a reliable rank parameter. To this end, we incorporate the established geometry and propose a Tucker rank-adaptive method that is capable of identifying an appropriate rank during iterations while the convergence is also guaranteed. Numerical experiments on tensor completion with synthetic and real-world datasets reveal that the proposed methods are in favor of recovering performance over other state-of-the-art methods. Moreover, the rank-adaptive method performs the best across various rank parameter selections and is indeed able to find an appropriate rank.

This work was supported by CAS-Croucher Funding Scheme for “CAS AMSS-PolyU Joint Laboratory of Applied Mathematics: Nonlinear Optimization Theory, Algorithms and Applications”. BG was supported by the Young Elite Scientist Sponsorship Program by CAST. YY was supported by the National Natural Science Foundation of China (grant No. 12288201).

Bin Gao · Ya-xiang Yuan

State Key Laboratory of Scientific and Engineering Computing, Academy of Mathematics and Systems Science, Chinese Academy of Sciences, Beijing, China

E-mail: {gaobin,yyx}@lsec.cc.ac.cn;

Renfeng Peng

State Key Laboratory of Scientific and Engineering Computing, Academy of Mathematics and Systems Science, Chinese Academy of Sciences, and University of Chinese Academy of Sciences, Beijing, China

E-mail: pengrenfeng@lsec.cc.ac.cn

Keywords Low-rank optimization · Tucker decomposition · algebraic variety · tangent cone · rank-adaptive strategy

PACS 15A69 · 65K05 · 65F30 · 90C30

1 Introduction

Tensors are powerful tools for representing multi-dimensional data, yet they are often encumbered by high storage and computational costs. Adopting a low-rank assumption mitigates these challenges by extracting the most significant information from tensors, thereby substantially reducing storage requirements. Low-rank optimization has demonstrated its effectiveness across various applications, including image processing [VT03; Pen+14], matrix and tensor completion [KSV14; KM16; GPY23], tensor equations [KSV16], mathematical finance [GKS20], and high-dimensional partial differential equations [BEU23; Wan+23]; see [GKT13; UV20] for an overview.

In contrast with the matrix rank, different tensor decomposition formats can lead to various definitions of the rank of a tensor. The canonical polyadic decomposition [Hit28], Tucker decomposition [Tuc+64], tensor train decomposition [Ose11], and tensor ring decomposition [Zha+16] are among the most typical decomposition formats; see [KB09] for an overview. Specifically, Tucker decomposition, also referred to as higher-order principal component analysis [KNW86] or multilinear singular value decomposition [DDV00], allows us to explore the low-rank structure along each mode of a tensor. Moreover, Tucker decomposition boils down to the ubiquitous singular value decomposition (SVD) in the matrix case. Therefore, we are concerned with the following low-rank Tucker tensor optimization problem in which the search space consists of tensors with bounded Tucker rank, i.e.,

$$\begin{aligned} \min_{\mathcal{X}} \quad & f(\mathcal{X}) \\ \text{s. t.} \quad & \mathcal{X} \in \mathcal{M}_{\leq \mathbf{r}} := \{\mathcal{X} \in \mathbb{R}^{n_1 \times n_2 \times \cdots \times n_d} : \text{rank}_{\text{tc}}(\mathcal{X}) \leq \mathbf{r}\}, \end{aligned} \quad (1.1)$$

where $f : \mathbb{R}^{n_1 \times n_2 \times \cdots \times n_d} \rightarrow \mathbb{R}$ is a smooth function, $\mathbf{r} = (r_1, r_2, \dots, r_d)$ is an array of d positive integers, and $\text{rank}_{\text{tc}}(\mathcal{X})$ denotes the Tucker rank of \mathcal{X} . The set $\mathcal{M}_{\leq \mathbf{r}}$ can be constructed through the determinants of minors with size $r_k + 1$ from the mode- k unfolding matrix of a tensor for $k = 1, 2, \dots, d$, which renders $\mathcal{M}_{\leq \mathbf{r}}$ a real-algebraic variety. Hence, we refer to $\mathcal{M}_{\leq \mathbf{r}}$ as the *Tucker tensor varieties*. Note that there is another type of tensor varieties in tensor train format. Kutschan [Kut18] provided the parametrization of the tangent cone for tensor train varieties. More recently, Vermeylen et al. [Ver+23] adopted the geometric tools in tensor train varieties and proposed a rank-estimation method for third-order tensor train completion.

Related work and motivation Since the low-rank Tucker tensor optimization is closely related to the low-rank matrix optimization, we start with an overview of the existing research in the field of low-rank matrix optimization. Recall that $\mathbb{R}_r^{m \times n} := \{\mathbf{X} \in \mathbb{R}^{m \times n} : \text{rank}(\mathbf{X}) = r\}$ is a smooth manifold (see, e.g., [HS95; BV06]), one can benefit from the geometric tools and design geometric methods for minimizing f over $\mathbb{R}_r^{m \times n}$. For instance, Shalit et al. [SWC12] proposed an online-learning procedure on $\mathbb{R}_r^{m \times n}$ and applied the procedure to a multi-label image classification

task. Vandereycken [Van13] derived geometric tools on the manifold $\mathbb{R}_r^{m \times n}$ and proposed the Riemannian conjugate gradient method for low-rank matrix completion. Mishra et al. [Mis+14] studied the quotient geometry of product manifolds generated by fixed-rank matrix factorizations and proposed Riemannian methods for low-rank matrix optimization. Based on the fact that $\mathbb{R}_r^{m \times n}$ is not closed, Schneider and Uschmajew [SU15] considered minimizing f over the closure of $\mathbb{R}_r^{m \times n}$, i.e., the matrix varieties $\mathbb{R}_{\leq r}^{m \times n} := \{\mathbf{X} \in \mathbb{R}^{m \times n} : \text{rank}(\mathbf{X}) \leq r\}$, and proposed the projected gradient descent method (P²GD) in which the t -th iterate is updated with stepsize $s^{(t)}$ by

$$\mathbf{X}^{(t+1)} = \text{P}_{\mathbb{R}_{\leq r}^{m \times n}} \left(\mathbf{X}^{(t)} + s^{(t)} \text{P}_{\text{T}_{\mathbf{X}^{(t)}} \mathbb{R}_{\leq r}^{m \times n}} (-\nabla f(\mathbf{X}^{(t)})) \right)$$

that involves two metric projections onto the varieties and the tangent cone. The convergence of P²GD was proved by means of the assumption on f satisfying Łojasiewicz inequality. Zhou et al. [Zho+16] designed a Riemannian rank-adaptive method on $\mathbb{R}_{\leq r}^{m \times n}$ where the convergence is guaranteed. Recently, Hosseini and Uschmajew [HU19] proposed a gradient sampling method for optimization on general real algebraic varieties. Gao and Absil [GA22] employed the geometric illustration of tangent cone to develop a Riemannian rank-adaptive method for low-rank matrix completion, which also appears to be favorable in low-rank semidefinite programming [TT23]. More recently, Olikier and Absil [OA23] proposed a first-order algorithm by equipping P²GD with a number of rank decrease attempts and proved that every accumulation point is stationary. Furthermore, Olikier et al. [OGA23] developed a framework for first-order optimization on general stratified sets of matrices. Levin et al. [LKB23] proposed a smooth remedy in which the feasible set $\mathbb{R}_{\leq r}^{m \times n}$ was parametrized by a (product) manifold \mathcal{M} (e.g., $\mathcal{M} = \mathbb{R}^{m \times r} \times \mathbb{R}^{n \times r}$) along with a lift $\varphi : \mathcal{M} \rightarrow \mathbb{R}_{\leq r}^{m \times n}$ satisfying $\varphi(\mathcal{M}) = \mathbb{R}_{\leq r}^{m \times n}$. Subsequently, the low-rank matrix optimization problem was reformulated as minimizing $f \circ \varphi$ on the manifold \mathcal{M} , which can be solved by Riemannian optimization methods (see, e.g., [AMS09; Bou23] for an overview). Olikier et al. [OUV23] proposed Gauss–Southwell type descent methods on matrix varieties.

Due to the intricate geometric structure of Tucker tensors, the low-rank Tucker tensor optimization problems are much more challenging than the matrix case. In the light of low-rank matrix problems, the low-rank Tucker tensor optimization has several different formulations. One type is minimizing f on a smooth manifold $\mathcal{M}_{\mathbf{r}}$ of tensors with fixed Tucker rank, i.e.,

$$\begin{aligned} \min_{\mathcal{X}} \quad & f(\mathcal{X}) \\ \text{s. t.} \quad & \mathcal{X} \in \mathcal{M}_{\mathbf{r}} := \{\mathcal{X} \in \mathbb{R}^{n_1 \times n_2 \times \cdots \times n_d} : \text{rank}_{\text{tc}}(\mathcal{X}) = \mathbf{r}\}. \end{aligned} \tag{1.2}$$

Uschmajew and Vandereycken [UV13] showed that the set of tensors with fixed Tucker rank is a submanifold of $\mathbb{R}^{n_1 \times \cdots \times n_d}$ and provided explicit characterizations of the tangent space. Kressner et al. [KSV14] proposed the Riemannian conjugate gradient method for low-rank Tucker tensor completion. Kasai and Mishra [KM16] considered the quotient geometry of the product manifold from Tucker decomposition and proposed the Riemannian conjugate gradient method for tensor completion under a preconditioned metric. Interested readers are referred to [UV20] for an overview of geometric methods on fixed-rank matrix and tensor manifolds.

Nevertheless, it is worth noting that the fixed-rank Tucker manifold $\mathcal{M}_{\mathbf{r}}$ is not a closed set in $\mathbb{R}^{n_1 \times n_2 \times \dots \times n_d}$. As a consequence, the classical convergence results established in Riemannian optimization (e.g., [BAC19]) do not hold for accumulation points located on the boundary $\mathcal{M}_{\leq \mathbf{r}} \setminus \mathcal{M}_{\mathbf{r}}$.

Instead of solving the fixed-rank optimization problem (1.2), we consider minimizing f on the closure of $\mathcal{M}_{\mathbf{r}}$, i.e., solving the optimization problem (1.1). On the one hand, unlike the well-explored geometric properties of matrix varieties [SU15] or fixed-rank Tucker tensor manifold [UV13], the geometric counterpart for Tucker tensor varieties (e.g., the tangent cone at rank-deficient points) is unknown. On the other hand, $\mathcal{M}_{\leq \mathbf{r}}$ can be constructed by the intersection of d tensorized matrix varieties of all unfolding matrices along different modes. However, the relationship between the tangent cone of $\mathcal{M}_{\mathbf{r}}$ and the tangent cones of matrix varieties along different modes is unclear. Therefore, the geometry of Tucker tensor varieties can not be easily generalized from matrix varieties. The existing work in geometry and optimization on Tucker tensor varieties is quite sparse. Luo and Qi [LQ23] studied the optimality conditions of (1.1) by exploiting a subset of the normal cone while the formulation of tangent cone remains unclear. The unknown geometry of Tucker tensor varieties hampers one from designing optimization methods on Tucker tensor varieties. In summary, we are motivated to seek an explicit parametrization of the tangent cone and to employ the established results to design geometric methods for (1.1).

In addition, the question “how to choose an appropriate rank parameter \mathbf{r} in low-rank optimization” is appealing in practice. We observe that the numerical performance of optimization methods in low-rank optimization can be sensitive to the choice of rank parameter \mathbf{r} ; see, e.g., [Zho+16; GA22; Don+22]. Opting for a larger rank parameter \mathbf{r} is able to enlarge the search space and potentially leads to a better optimum. However, if \mathbf{r} is too large, it triggers more storage and computational costs. Moreover, the optimization methods may converge to rank-deficient points due to the non-closed nature of $\mathcal{M}_{\mathbf{r}}$. In view of these obstacles, we are motivated to design rank-adaptive strategies, tailored for optimization on Tucker tensor varieties, that are able to find an appropriate rank parameter during iterations.

Contributions In this paper, we delve into the geometry of Tucker tensor varieties $\mathcal{M}_{\leq \mathbf{r}}$ and propose geometric and rank-adaptive methods for optimization on Tucker tensor varieties. Specifically, we first provide new equivalent reformulations for both the tangent cone of matrix varieties and the tangent space of Tucker tensor manifold. Then, an explicit characterization of the tangent cone of $\mathcal{M}_{\leq \mathbf{r}}$ is constructed, paving the way for developing optimization methods on $\mathcal{M}_{\leq \mathbf{r}}$. In order to bypass the computationally intractable metric projection onto the tangent cone, we propose an approximate projection by choosing bases from d orthogonal complements of the corresponding d factor matrices of a Tucker tensor. To the best of our knowledge, this is the first work investigating the geometry of Tucker tensor varieties.

Reflecting on the derived geometric properties, we propose the gradient-related approximate projection (GRAP) method whose iterate reads

$$\mathcal{X}^{(t+1)} = \mathbf{P}_{\leq \mathbf{r}}^{\text{HO}} \left(\mathcal{X}^{(t)} + s^{(t)} \tilde{\mathbf{P}}_{\mathbf{T}_{\mathcal{X}^{(t)}} \mathcal{M}_{\leq \mathbf{r}}} (-\nabla f(\mathcal{X}^{(t)})) \right),$$

where $P_{\leq \mathbf{r}}^{\text{HO}}$ projects a tensor onto the Tucker tensor varieties $\mathcal{M}_{\leq \mathbf{r}}$ by the higher-order singular value decomposition and \tilde{P} is the proposed approximate projection. The GRAP method can be viewed as a generalization of the Riemannian gradient method for optimization on $\mathcal{M}_{\mathbf{r}}$, while it is capable of dealing with rank-deficient points, and the convergence can still be guaranteed via Łojasiewicz inequality. Additionally, we propose a new approximate projection operator \hat{P} by leveraging partial information of the tangent cone. Surprisingly, the operator \hat{P} is apt to develop a method without projection onto $\mathcal{M}_{\leq \mathbf{r}}$, namely, retraction-free, which iterates as

$$\mathcal{X}^{(t+1)} = \mathcal{X}^{(t)} + s^{(t)} \hat{P}_{T_{\mathcal{X}^{(t)}} \mathcal{M}_{\leq \mathbf{r}}}(-\nabla f(\mathcal{X}^{(t)}))$$

while preserving feasibility, i.e., $\mathcal{X}^{(t+1)} \in \mathcal{M}_{\leq \mathbf{r}}$, and thus saves computational costs. This method is called the retraction-free gradient-related approximate projection (rfGRAP) method and its convergence is also proved.

In order to identify an appropriate Tucker rank during iterations, we resort to the geometric illustration of the tangent cone and propose a provable Tucker rank-adaptive method (TRAM), which consists of line search on a fixed-rank manifold, rank-decreasing, and rank-increasing procedures. Specifically, a rank-decreasing procedure is aimed to save storage and eliminate singularity if an iterate is nearly rank-deficient. If an iterate appears to be nearly stationary on the fixed-rank manifold, we increase the rank in pursuit of a better optimum.

We compare the proposed GRAP, rfGRAP, and TRAM methods with existing methods in tensor completion on synthetic datasets, hyperspectral images, and movie ratings. The numerical results suggest that the proposed methods perform better than the state-of-the-art methods under different rank parameter selections. Specifically, the proposed TRAM method demonstrates its capability to find an appropriate rank in practice.

Organization We introduce the geometric tools of matrix varieties and notation in tensor operations in section 2. In section 3, an explicit parametrization of the tangent cone of Tucker tensor varieties is provided along with an approximate projection onto the tangent cone. We propose the geometric methods, GRAP and rfGRAP, in sections 4 and 5, and we design the Tucker rank-adaptive method in section 6. Section 7 reports the numerical performance of proposed methods in tensor completion. Finally, we draw the conclusion in section 8.

2 Low-rank manifolds and matrix varieties

In this section, the required geometry of matrix manifold and matrix varieties, which is closely related to the Tucker tensor varieties, is introduced first. Then, we describe the notation in tensor operations, the definition of Tucker decomposition, and the geometry of the fixed-rank Tucker manifold.

Given a nonempty subset C of $\mathbb{R}^{n_1 \times n_2 \times \cdots \times n_d}$, the (Bouligand) *tangent cone* of C at $\mathcal{X} \in C$ is defined by

$$T_{\mathcal{X}} C := \{\mathcal{V} \in \mathbb{R}^{n_1 \times n_2 \times \cdots \times n_d} : \exists t^{(i)} \rightarrow 0, \mathcal{X}^{(i)} \rightarrow \mathcal{X} \text{ in } C, \text{ s.t. } \frac{\mathcal{X}^{(i)} - \mathcal{X}}{t^{(i)}} \rightarrow \mathcal{V}\}.$$

The set $N_{\mathcal{X}}C = (T_{\mathcal{X}}C)^{\circ} := \{\mathcal{N} \in \mathbb{R}^{n_1 \times n_2 \times \dots \times n_d} : \langle \mathcal{N}, \mathcal{V} \rangle \leq 0 \text{ for all } \mathcal{V} \in T_{\mathcal{X}}C\}$ is called the *normal cone* of C at \mathcal{X} . Note that if C is a manifold, the tangent cone $T_{\mathcal{X}}C$ is referred to as the tangent space of C at \mathcal{X} . A mapping $R : \bigcup_{\mathcal{X} \in C} \{\mathcal{X}\} \times T_{\mathcal{X}}C \rightarrow C$ is called a *retraction* [SU15, Definition 2.4] if for all $\mathcal{X} \in C$ and $\mathcal{V} \in T_{\mathcal{X}}C$ it holds that $t \mapsto R_{\mathcal{X}}(t\mathcal{V})$ is continuous on $t \geq 0$ and $\lim_{t \rightarrow 0^+} (R_{\mathcal{X}}(t\mathcal{V}) - \mathcal{X} - t\mathcal{V})/t = 0$.

Definition 1 A point $\mathcal{X} \in C$ is called *stationary* for the optimization problem (1.1) if $\langle \nabla f(\mathcal{X}), \mathcal{V} \rangle \geq 0$ holds for all $\mathcal{V} \in T_{\mathcal{X}}C$, which is equivalent to $-\nabla f(\mathcal{X}) \in N_{\mathcal{X}}C$ or $\|P_{T_{\mathcal{X}}C}(-\nabla f(\mathcal{X}))\|_F = 0$.

2.1 Low-rank matrix manifold and varieties

Let m, n, r be positive integers satisfying $r \leq \min\{m, n\}$. Given a matrix $\mathbf{X} \in \mathbb{R}^{m \times n}$, the image of \mathbf{X} and its orthogonal complement are defined by $\text{span}(\mathbf{X}) := \{\mathbf{X}\mathbf{y} : \mathbf{y} \in \mathbb{R}^n\} \subseteq \mathbb{R}^m$ and $\text{span}(\mathbf{X})^{\perp} := \{\mathbf{y} \in \mathbb{R}^m : \langle \mathbf{x}, \mathbf{y} \rangle = 0 \text{ for all } \mathbf{x} \in \text{span}(\mathbf{X})\}$ respectively. The fixed-rank matrix manifold and matrix varieties are denoted by $\mathbb{R}_r^{m \times n}$ and $\mathbb{R}_{\leq r}^{m \times n}$ respectively. The set $\text{St}(r, n) := \{\mathbf{X} \in \mathbb{R}^{n \times r} : \mathbf{X}^T \mathbf{X} = \mathbf{I}_r\}$ is the *Stiefel manifold*. The orthogonal group is denoted by $\mathcal{O}(n) := \{\mathbf{Q} \in \mathbb{R}^{n \times n} : \mathbf{Q}^T \mathbf{Q} = \mathbf{Q} \mathbf{Q}^T = \mathbf{I}_n\}$.

Geometry of matrix manifold and varieties The tangent and normal cones play important roles in optimization on matrix varieties $\mathbb{R}_{\leq r}^{m \times n}$. Therefore, we introduce the explicit formulae of tangent and normal cones of matrix varieties (see [Van13, Proposition 2.1] and [SU15, Theorem 3.2]) as follows.

Proposition 1 Given $\mathbf{X} \in \mathbb{R}_{\underline{r}}^{m \times n}$ with $\underline{r} \leq r$. A thin SVD of \mathbf{X} is $\mathbf{X} = \mathbf{U} \Sigma \mathbf{V}^T$, where $\mathbf{U} \in \text{St}(\underline{r}, m)$, $\mathbf{V} \in \text{St}(\underline{r}, n)$ and $\Sigma = \text{diag}(\sigma_1, \dots, \sigma_{\underline{r}})$ with $\sigma_1 \geq \dots \geq \sigma_{\underline{r}} > 0$. It holds that

$$\begin{aligned} T_{\mathbf{X}} \mathbb{R}_{\underline{r}}^{m \times n} &= \left\{ \begin{bmatrix} \mathbf{U} & \mathbf{U}^{\perp} \end{bmatrix} \begin{bmatrix} \mathbb{R}^{\underline{r} \times \underline{r}} & \mathbb{R}^{\underline{r} \times (n-\underline{r})} \\ \mathbb{R}^{(m-\underline{r}) \times \underline{r}} & 0 \end{bmatrix} \begin{bmatrix} \mathbf{V} & \mathbf{V}^{\perp} \end{bmatrix}^T \right\}, \\ N_{\mathbf{X}} \mathbb{R}_{\underline{r}}^{m \times n} &= \left\{ \begin{bmatrix} \mathbf{U} & \mathbf{U}^{\perp} \end{bmatrix} \begin{bmatrix} 0 & 0 \\ 0 & \mathbb{R}^{(m-\underline{r}) \times (n-\underline{r})} \end{bmatrix} \begin{bmatrix} \mathbf{V} & \mathbf{V}^{\perp} \end{bmatrix}^T \right\}, \\ T_{\mathbf{X}} \mathbb{R}_{\leq r}^{m \times n} &= \left\{ \begin{bmatrix} \mathbf{U} & \mathbf{U}^{\perp} \end{bmatrix} \begin{bmatrix} \mathbb{R}^{\underline{r} \times \underline{r}} & \mathbb{R}^{\underline{r} \times (n-\underline{r})} \\ \mathbb{R}^{(m-\underline{r}) \times \underline{r}} & \mathbb{R}_{\leq (r-\underline{r})}^{(m-\underline{r}) \times (n-\underline{r})} \end{bmatrix} \begin{bmatrix} \mathbf{V} & \mathbf{V}^{\perp} \end{bmatrix}^T \right\}, \\ N_{\mathbf{X}} \mathbb{R}_{\leq r}^{m \times n} &= \begin{cases} N_{\mathbf{X}} \mathbb{R}_r^{m \times n}, & \text{if } \underline{r} = r; \\ \{0\}, & \text{if } \underline{r} < r, \end{cases} \end{aligned}$$

for any $\mathbf{U}^{\perp} \in \text{St}(m - \underline{r}, m)$ with $\text{span}(\mathbf{U}^{\perp}) = \text{span}(\mathbf{U})^{\perp}$ and $\mathbf{V}^{\perp} \in \text{St}(n - \underline{r}, n)$ with $\text{span}(\mathbf{V}^{\perp}) = \text{span}(\mathbf{V})^{\perp}$.

Note that $(\mathbf{U}^{\perp})^T \mathbf{U} = 0$ and $(\mathbf{V}^{\perp})^T \mathbf{V} = 0$. The choice of \mathbf{U}^{\perp} and \mathbf{V}^{\perp} is not unique, but the results in Proposition 1 are independent of a specific choice of \mathbf{U}^{\perp}

and \mathbf{V}^\perp . Actually, the tangent space and normal space can be uniquely represented in the sense of tensor product by

$$\begin{aligned} \mathbf{T}_{\mathbf{X}} \mathbb{R}_r^{m \times n} &= \text{span}(\mathbf{U}) \otimes \text{span}(\mathbf{V}) + \text{span}(\mathbf{U})^\perp \otimes \text{span}(\mathbf{V}) + \text{span}(\mathbf{U}) \otimes \text{span}(\mathbf{V})^\perp, \\ \mathbf{N}_{\mathbf{X}} \mathbb{R}_r^{m \times n} &= \text{span}(\mathbf{U})^\perp \otimes \text{span}(\mathbf{V})^\perp. \end{aligned}$$

The direct sum of tangent and normal spaces forms the Euclidean space $\mathbb{R}^{m \times n}$, i.e.,

$$\begin{aligned} \mathbb{R}^{m \times n} &= \mathbf{T}_{\mathbf{X}} \mathbb{R}_r^{m \times n} + \mathbf{N}_{\mathbf{X}} \mathbb{R}_r^{m \times n} \\ &= \left\{ \begin{bmatrix} \mathbf{U} & \mathbf{U}^\perp \end{bmatrix} \begin{bmatrix} \text{shaded} & \text{blank} \\ \text{blank} & \text{shaded} \end{bmatrix} \begin{bmatrix} \mathbf{V} & \mathbf{V}^\perp \end{bmatrix}^\top \right\} + \left\{ \begin{bmatrix} \mathbf{U} & \mathbf{U}^\perp \end{bmatrix} \begin{bmatrix} \text{blank} & \text{blank} \\ \text{blank} & \text{shaded} \end{bmatrix} \begin{bmatrix} \mathbf{V} & \mathbf{V}^\perp \end{bmatrix}^\top \right\}, \end{aligned}$$

where the shaded square represents an arbitrary matrix and the blank represents the matrix with zero elements.

Moreover, we propose a new reduced representation of the tangent cone of matrix varieties. For any element Ξ in the tangent cone $\mathbf{T}_{\mathbf{X}} \mathbb{R}_{\leq r}^{m \times n}$, there exists $\mathbf{C} \in \mathbb{R}^{r \times r}$, $\mathbf{D} \in \mathbb{R}^{(m-r) \times r}$, $\mathbf{E} \in \mathbb{R}^{r \times (n-r)}$ and $\mathbf{F} \in \mathbb{R}_{\leq (r-r)}^{(m-r) \times (n-r)}$, such that

$$\Xi = \mathbf{UCV}^\top + \mathbf{U}^\perp \mathbf{DV}^\top + \mathbf{UE}(\mathbf{V}^\perp)^\top + \mathbf{U}^\perp \mathbf{F}(\mathbf{V}^\perp)^\top. \quad (2.1)$$

Note that $\ell := \text{rank}(\mathbf{F}) \leq (r-r) \leq \min\{m-r, n-r\}$. Therefore, we can further decompose Ξ by using the SVD of $\mathbf{F} = \tilde{\mathbf{U}} \tilde{\Sigma} \tilde{\mathbf{V}}^\top$, where $\tilde{\mathbf{U}} \in \text{St}(\ell, m-r)$, $\tilde{\mathbf{V}} \in \text{St}(\ell, n-r)$ and $\tilde{\Sigma} \in \mathbb{R}^{\ell \times \ell}$ is a diagonal matrix. Specifically, since $\ell \leq \min\{m-r, n-r\}$, there exists matrices $\tilde{\mathbf{U}}_2 \in \text{St}(m-r-\ell, m-r)$ and $\tilde{\mathbf{V}}_2 \in \text{St}(n-r-\ell, n-r)$, such that $[\tilde{\mathbf{U}} \ \tilde{\mathbf{U}}_2] \in \mathcal{O}(m-r)$ and $[\tilde{\mathbf{V}} \ \tilde{\mathbf{V}}_2] \in \mathcal{O}(n-r)$. In fact, it holds that $\text{span}(\tilde{\mathbf{U}}_2) = \text{span}(\tilde{\mathbf{U}})^\perp$ and $\text{span}(\tilde{\mathbf{V}}_2) = \text{span}(\tilde{\mathbf{V}})^\perp$. As a result, we yield a new equivalent (reduced) representation of Ξ as follows

$$\begin{aligned} \Xi &= \mathbf{UCV}^\top + \mathbf{U}^\perp \mathbf{DV}^\top + \mathbf{UE}(\mathbf{V}^\perp)^\top + \mathbf{U}^\perp \tilde{\mathbf{U}} \tilde{\Sigma} \tilde{\mathbf{V}}^\top (\mathbf{V}^\perp)^\top \\ &= \mathbf{UCV}^\top + \mathbf{U}^\perp [\tilde{\mathbf{U}} \ \tilde{\mathbf{U}}_2] [\tilde{\mathbf{U}} \ \tilde{\mathbf{U}}_2]^\top \mathbf{DV}^\top \\ &\quad + \mathbf{UE}[\tilde{\mathbf{V}} \ \tilde{\mathbf{V}}_2] [\tilde{\mathbf{V}} \ \tilde{\mathbf{V}}_2]^\top (\mathbf{V}^\perp)^\top + \mathbf{U}^\perp \tilde{\mathbf{U}} \tilde{\Sigma} \tilde{\mathbf{V}}^\top (\mathbf{V}^\perp)^\top \\ &= \begin{bmatrix} \mathbf{U} & \mathbf{U}^\perp \tilde{\mathbf{U}} & \mathbf{U}^\perp \tilde{\mathbf{U}}_2 \end{bmatrix} \begin{bmatrix} \mathbf{C} & \mathbf{E} \tilde{\mathbf{V}} & \mathbf{E} \tilde{\mathbf{V}}_2 \\ \tilde{\mathbf{U}}^\top \mathbf{D} & \tilde{\Sigma} & 0 \\ \tilde{\mathbf{U}}_2^\top \mathbf{D} & 0 & 0 \end{bmatrix} \begin{bmatrix} \mathbf{V} & \mathbf{V}^\perp \tilde{\mathbf{V}} & \mathbf{V}^\perp \tilde{\mathbf{V}}_2 \end{bmatrix}^\top. \end{aligned}$$

Therefore, the tangent cone can also be represented by

$$\mathbf{T}_{\mathbf{X}} \mathbb{R}_{\leq r}^{m \times n} = \left\{ \begin{bmatrix} \mathbf{U} & \mathbf{U}_1 & \mathbf{U}_2 \end{bmatrix} \begin{bmatrix} \text{shaded} & \text{shaded} & \text{shaded} \\ \text{shaded} & \text{shaded} & \text{shaded} \\ \text{shaded} & \text{shaded} & \text{shaded} \end{bmatrix} \begin{bmatrix} \mathbf{V} & \mathbf{V}_1 & \mathbf{V}_2 \end{bmatrix}^\top \right\}, \quad (2.2)$$

where $\mathbf{U}_1 := \mathbf{U}^\perp \tilde{\mathbf{U}}$, $\mathbf{U}_2 := \mathbf{U}^\perp \tilde{\mathbf{U}}_2$, $\mathbf{V}_1 := \mathbf{V}^\perp \tilde{\mathbf{V}}$, and $\mathbf{V}_2 := \mathbf{V}^\perp \tilde{\mathbf{V}}_2$. It is worth noting that $\text{span}(\mathbf{U}^\perp) = \text{span}([\mathbf{U}_1 \ \mathbf{U}_2])$ and $\text{span}(\mathbf{V}^\perp) = \text{span}([\mathbf{V}_1 \ \mathbf{V}_2])$, i.e., we extract the singular vectors of \mathbf{F} and simplify $\mathbf{U}^\perp \mathbf{F}(\mathbf{V}^\perp)^\top$ by $\mathbf{U}_1 \tilde{\Sigma} \mathbf{V}_1^\top$ in (2.1). Consequently, it follows from the new representation (2.2) that

$$\mathbf{T}_{\mathbf{X}} \mathbb{R}_{\leq r}^{m \times n} = \mathbf{T}_{\mathbf{X}} \mathbb{R}_r^{m \times n} + \text{span}(\mathbf{U}_1) \otimes \text{span}(\mathbf{V}_1),$$

which is vital to the development of the tangent cone of Tucker tensor varieties; see Theorem 1 for details.

Remark 1 We observe that the tangent cone can be alternatively decomposed as

$$\mathbf{T}_{\mathbf{X}\mathbb{R}_{\leq r}^{m \times n}} = \mathbf{T}_{\mathbf{X}\mathbb{R}_{\underline{r}}^{m \times n}} + \mathbf{N}_{\leq(r-\underline{r})}(\mathbf{X}),$$

where $\mathbf{N}_{\leq(r-\underline{r})}(\mathbf{X}) := \left\{ \mathbf{N} \in \mathbf{N}_{\mathbf{X}\mathbb{R}_{\underline{r}}^{m \times n}} : \text{rank}(\mathbf{N}) \leq (r - \underline{r}) \right\}$. As [GA22] suggests, given a matrix $\mathbf{X} \in \mathbb{R}_{\underline{r}}^{m \times n}$ with $\underline{r} < r$ and a vector in the cone $\mathbf{V} \in \mathbf{N}_{\leq(r-\underline{r})}(\mathbf{X}) \setminus \{0\}$, it holds that

$$\text{rank}(\mathbf{X} + s\mathbf{V}) \in (\underline{r}, r]$$

for $s > 0$. The principle can be applied to increase the rank of \mathbf{X} . A similar observation can be found in tensor cases; see section 6.3 for details.

Metric projections Given a matrix $\mathbf{A} = \sum_{k=1}^I \sigma_k \mathbf{u}_k \mathbf{v}_k^\top \in \mathbb{R}^{m \times n}$, where $\sigma_1 \geq \dots \geq \sigma_I > 0$, $\mathbf{u}_k \in \mathbb{R}^m$ and $\mathbf{v}_k \in \mathbb{R}^n$ are singular vectors of \mathbf{A} . The *metric projection* of \mathbf{A} onto the matrix varieties $\mathbb{R}_{\leq r}^{m \times n}$ is defined by

$$\mathbf{P}_{\leq r}(\mathbf{A}) := \arg \min_{\mathbf{X} \in \mathbb{R}_{\leq r}^{m \times n}} \|\mathbf{A} - \mathbf{X}\|_F^2.$$

By using Eckart–Young theorem, the metric projection exists and reads

$$\mathbf{P}_{\leq r}(\mathbf{A}) = \begin{cases} \mathbf{A}, & \text{if } I \leq r, \\ \sum_{k=1}^r \sigma_k \mathbf{u}_k \mathbf{v}_k^\top, & \text{if } I > r. \end{cases}$$

Note that $\mathbf{P}_{\leq r}(\mathbf{A})$ is not unique when the singular value σ_r is equal to σ_{r+1} , but we can always choose $\sum_{k=1}^r \sigma_k \mathbf{u}_k \mathbf{v}_k^\top$ in practice. The metric projection of \mathbf{A} onto the fixed-rank manifold $\mathbb{R}_r^{m \times n}$ is similar to the metric projection onto $\mathbb{R}_{\leq r}^{m \times n}$, i.e., $\mathbf{P}_r(\mathbf{A}) = \mathbf{P}_{\leq r}(\mathbf{A})$ for $I \geq r$.

Moreover, in view of Proposition 1, given a matrix $\mathbf{A} \in \mathbb{R}^{m \times n}$, the orthogonal projections onto the tangent space and tangent cone are given by

$$\begin{aligned} \mathbf{P}_{\mathbf{T}_{\mathbf{X}\mathbb{R}_{\underline{r}}^{m \times n}}} \mathbf{A} &= \mathbf{P}_{\mathbf{U}} \mathbf{A} \mathbf{P}_{\mathbf{V}} + \mathbf{P}_{\mathbf{U}}^\perp \mathbf{A} \mathbf{P}_{\mathbf{V}} + \mathbf{P}_{\mathbf{U}} \mathbf{A} \mathbf{P}_{\mathbf{V}}^\perp, \\ \mathbf{P}_{\mathbf{T}_{\mathbf{X}\mathbb{R}_{\leq r}^{m \times n}}} \mathbf{A} &= \mathbf{P}_{\mathbf{T}_{\mathbf{X}\mathbb{R}_{\underline{r}}^{m \times n}}} \mathbf{A} + \mathbf{P}_{\leq(r-\underline{r})} \left(\mathbf{P}_{\mathbf{U}}^\perp \mathbf{A} \mathbf{P}_{\mathbf{V}}^\perp \right), \end{aligned} \quad (2.3)$$

where $\mathbf{P}_{\mathbf{U}} := \mathbf{U}\mathbf{U}^\top$, $\mathbf{P}_{\mathbf{U}}^\perp := \mathbf{I}_m - \mathbf{U}\mathbf{U}^\top$, $\mathbf{P}_{\mathbf{V}} := \mathbf{V}\mathbf{V}^\top$, and $\mathbf{P}_{\mathbf{V}}^\perp := \mathbf{I}_n - \mathbf{V}\mathbf{V}^\top$.

2.2 Tucker decomposition: definition and geometry

We introduce notation in tensor operations. Denote the index set $\{1, 2, \dots, n\}$ by $[n]$. The inner product between two tensors $\mathcal{X}, \mathcal{Y} \in \mathbb{R}^{n_1 \times \dots \times n_d}$ is defined by $\langle \mathcal{X}, \mathcal{Y} \rangle := \sum_{i_1=1}^{n_1} \dots \sum_{i_d=1}^{n_d} \mathcal{X}(i_1, \dots, i_d) \mathcal{Y}(i_1, \dots, i_d)$. The Frobenius norm of a tensor \mathcal{X} is defined by $\|\mathcal{X}\|_F := \sqrt{\langle \mathcal{X}, \mathcal{X} \rangle}$. The mode- k unfolding of a tensor $\mathcal{X} \in \mathbb{R}^{n_1 \times \dots \times n_d}$ is denoted by a matrix $\mathbf{X}_{(k)} \in \mathbb{R}^{n_k \times n_{-k}}$ for $k = 1, \dots, d$, where $n_{-k} := \prod_{i \neq k} n_i$. The (i_1, i_2, \dots, i_d) -th entry of \mathcal{X} corresponds to the (i_k, j) -th entry of $\mathbf{X}_{(k)}$, where $j = 1 + \sum_{\ell \neq k, \ell=1}^d (i_\ell - 1)J_\ell$ with $J_\ell = \prod_{m=1, m \neq k}^{\ell-1} n_m$. The

tensorization operator maps a matrix $\mathbf{X}_k \in \mathbb{R}^{n_k \times n_{-k}}$ to a tensor $\text{ten}_{(k)}(\mathbf{X}_k) \in \mathbb{R}^{n_1 \times \dots \times n_d}$ defined by $\text{ten}_{(k)}(\mathbf{X}_k)(i_1, \dots, i_d) = \mathbf{X}_k(i_k, 1 + \sum_{\ell \neq k, \ell=1}^d (i_\ell - 1)J_\ell)$ for $(i_1, \dots, i_d) \in [n_1] \times \dots \times [n_d]$. Note that $\text{ten}_{(k)}(\mathbf{X}_{(k)}) = \mathcal{X}$ holds for fixed n_1, \dots, n_d . Therefore, the tensorization operator is invertible. The k -mode product of a tensor \mathcal{X} and a matrix $\mathbf{A} \in \mathbb{R}^{n_k \times M}$ is denoted by $\mathcal{X} \times_k \mathbf{A} \in \mathbb{R}^{n_1 \times \dots \times M \times \dots \times n_d}$, where the $(i_1, \dots, i_{k-1}, j, i_{k+1}, \dots, i_d)$ -th entry of $\mathcal{X} \times_k \mathbf{A}$ is $\sum_{i_k=1}^{n_k} x_{i_1 \dots i_d} a_{ji_k}$. It holds that $(\mathcal{X} \times_k \mathbf{A})_{(k)} = \mathbf{A} \mathbf{X}_{(k)}$. Given $\mathbf{u}_1 \in \mathbb{R}^{n_1} \setminus \{0\}, \dots, \mathbf{u}_d \in \mathbb{R}^{n_d} \setminus \{0\}$, a rank-1 tensor of size $n_1 \times \dots \times n_d$ is defined by the outer product $\mathcal{V} := \mathbf{u}_1 \circ \dots \circ \mathbf{u}_d$, or $v_{i_1, \dots, i_d} := u_{1, i_1} \dots u_{d, i_d}$ equivalently. The Kronecker product of two matrices $\mathbf{A} \in \mathbb{R}^{m_1 \times n_1}$ and $\mathbf{B} \in \mathbb{R}^{m_2 \times n_2}$ is an $(m_1 m_2)$ -by- $(n_1 n_2)$ matrix defined by $\mathbf{A} \otimes \mathbf{B} := (a_{ij} \mathbf{B})_{ij}$. The vector $\mathbf{e}_i \in \mathbb{R}^n$ is defined by the i -th column of n -by- n identity matrix \mathbf{I}_n .

Definition 2 (Tucker decomposition) Given a tensor $\mathcal{X} \in \mathbb{R}^{n_1 \times \dots \times n_d}$, the Tucker decomposition is

$$\mathcal{X} = \mathcal{G} \times_1 \mathbf{U}_1 \cdots \times_d \mathbf{U}_d,$$

where $\mathcal{G} \in \mathbb{R}^{r_1 \times \dots \times r_d}$ is a core tensor, $\mathbf{U}_k \in \text{St}(r_k, n_k)$ are factor matrices with orthogonal columns and $r_k = \text{rank}(\mathbf{X}_{(k)})$.

The Tucker rank of a tensor \mathcal{X} is defined by

$$\text{rank}_{\text{tc}}(\mathcal{X}) := \mathbf{r} = (r_1, r_2, \dots, r_d) = (\text{rank}(\mathbf{X}_{(1)}), \text{rank}(\mathbf{X}_{(2)}), \dots, \text{rank}(\mathbf{X}_{(d)})).$$

Figure 1 depicts the Tucker decomposition of a third-order tensor. Note that the mode- k unfolding of a tensor $\mathcal{X} = \mathcal{G} \times_1 \mathbf{U}_1 \cdots \times_d \mathbf{U}_d$ satisfies

$$\mathbf{X}_{(k)} = \mathbf{U}_k \mathbf{G}_{(k)} (\mathbf{U}_d \otimes \dots \otimes \mathbf{U}_{k+1} \otimes \mathbf{U}_{k-1} \otimes \dots \otimes \mathbf{U}_1)^\top = \mathbf{U}_k \mathbf{G}_{(k)} ((\mathbf{U}_j)^{\otimes j \neq k})^\top,$$

where $(\mathbf{U}_j)^{\otimes j \neq k} := \mathbf{U}_d \otimes \dots \otimes \mathbf{U}_{k+1} \otimes \mathbf{U}_{k-1} \otimes \dots \otimes \mathbf{U}_1$ for $k \in [d]$. Notably, for a d -th order tensor \mathcal{A} , it holds that

$$\mathcal{A} \in \bigotimes_{k=1}^d \text{span}(\mathbf{U}_k) \iff \mathcal{A} = \mathcal{C} \times_{k=1}^d \mathbf{U}_k \quad (2.4)$$

with $\mathcal{C} \in \mathbb{R}^{r_1 \times \dots \times r_d}$.

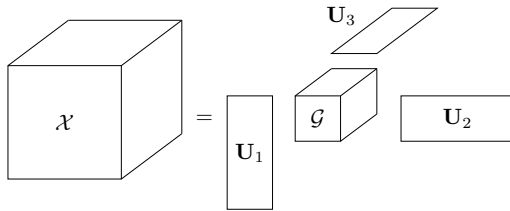


Fig. 1 Tucker decomposition of a third-order tensor

Fixed-rank Tucker manifold Since $\mathcal{M}_{\mathbf{r}} = \{\mathcal{X} \in \mathbb{R}^{n_1 \times n_2 \times \dots \times n_d} : \text{rank}_{\text{tc}}(\mathcal{X}) = \mathbf{r}\}$ forms a smooth manifold with dimension $\dim(\mathcal{M}_{\mathbf{r}}) = r_1 \dots r_d + \sum_{k=1}^d (n_k r_k - r_k^2)$, Koch and Lubich [KL10] provided that the tangent space of $\mathcal{M}_{\mathbf{r}}$ at \mathcal{X} is characterized by

$$\text{T}_{\mathcal{X}}\mathcal{M}_{\mathbf{r}} = \left\{ \begin{array}{l} \dot{\mathcal{G}} \times_1 \mathbf{U}_1 \cdots \times_d \mathbf{U}_d + \sum_{k=1}^d \mathcal{G} \times_k \dot{\mathbf{U}}_k \times_{j \neq k} \mathbf{U}_j : \\ \dot{\mathcal{G}} \in \mathbb{R}^{r_1 \times \dots \times r_d}, \dot{\mathbf{U}}_k \in \mathbb{R}^{n_k \times r_k}, \dot{\mathbf{U}}_k^{\top} \mathbf{U}_k = 0 \end{array} \right\}. \quad (2.5)$$

Though the Tucker decomposition of a tensor is not unique, the definition of $\text{T}_{\mathcal{X}}\mathcal{M}_{\mathbf{r}}$ does not rely on a specific Tucker decomposition.

Metric projections Given a tensor $\mathcal{A} \in \mathbb{R}^{n_1 \times \dots \times n_d}$, the metric projection of \mathcal{A} onto the Tucker tensor varieties $\mathcal{M}_{\leq \mathbf{r}} = \{\mathcal{X} \in \mathbb{R}^{n_1 \times n_2 \times \dots \times n_d} : \text{rank}_{\text{tc}}(\mathcal{X}) \leq \mathbf{r}\}$ is defined by

$$\text{P}_{\leq \mathbf{r}}(\mathcal{A}) := \arg \min_{\mathcal{X} \in \mathcal{M}_{\leq \mathbf{r}}} \|\mathcal{A} - \mathcal{X}\|_{\text{F}}^2. \quad (2.6)$$

In contrast with the matrix case in section 2.1, $\text{P}_{\leq \mathbf{r}}(\mathcal{A})$ does not have a closed-form expression in general [DDV00]. Nevertheless, one can apply *higher-order singular value decomposition* (HOSVD) to yield a quasi-optimal solution. Specifically, the HOSVD procedure sequentially applies the best rank- r_k approximation operator $\text{P}_{\leq r_k}^k$ to each mode of \mathcal{A} for $k = 1, 2, \dots, d$, i.e.,

$$\text{P}_{\leq \mathbf{r}}^{\text{HO}}(\mathcal{A}) := \text{P}_{\leq r_d}^d (\text{P}_{\leq r_{d-1}}^{d-1} \cdots (\text{P}_{\leq r_1}^1(\mathcal{A}))), \quad (2.7)$$

where $\text{P}_{\leq r_k}^k(\mathcal{A}) := \text{ten}_{(k)}(\text{P}_{\leq r_k}(\mathbf{A}_{(k)}))$. Since the quasi-optimality

$$\|\mathcal{A} - \text{P}_{\leq \mathbf{r}}^{\text{HO}}(\mathcal{A})\|_{\text{F}} \leq \sqrt{d} \|\mathcal{A} - \text{P}_{\leq \mathbf{r}}(\mathcal{A})\|_{\text{F}} \quad (2.8)$$

holds [DDV00, Property 10], HOSVD can be served as an approximate projection onto $\mathcal{M}_{\leq \mathbf{r}}$. Moreover, we can prove that HOSVD is also a retraction on $\mathcal{M}_{\leq \mathbf{r}}$ around \mathcal{X} .

Proposition 2 *The mapping $\text{R}_{\mathcal{X}}^{\text{HO}} : \text{T}_{\mathcal{X}}\mathcal{M}_{\leq \mathbf{r}} \rightarrow \mathcal{M}_{\leq \mathbf{r}} : \mathcal{V} \mapsto \text{P}_{\leq \mathbf{r}}^{\text{HO}}(\mathcal{X} + \mathcal{V})$ is a retraction on $\mathcal{M}_{\leq \mathbf{r}}$.*

Proof See Appendix A. □

In addition, the metric projection of a tensor $\mathcal{A} \in \mathbb{R}^{n_1 \times n_2 \times \dots \times n_d}$ onto $\text{T}_{\mathcal{X}}\mathcal{M}_{\mathbf{r}}$ is given by [KL10, §2.3]

$$\text{P}_{\text{T}_{\mathcal{X}}\mathcal{M}_{\mathbf{r}}} \mathcal{A} = \mathcal{A} \times_{k=1}^d \text{P}_{\mathbf{U}_k} + \sum_{k=1}^d \mathcal{G} \times_k \left(\text{P}_{\mathbf{U}_k}^{\perp} \left(\mathcal{A} \times_{j \neq k} \mathbf{U}_j^{\top} \right)_{(k)} \mathbf{G}_{(k)}^{\dagger} \right) \times_{j \neq k} \mathbf{U}_j, \quad (2.9)$$

where $\mathbf{G}_{(k)}^{\dagger} = \mathbf{G}_{(k)}^{\top} (\mathbf{G}_{(k)} \mathbf{G}_{(k)}^{\top})^{-1}$ is the Moore–Penrose pseudoinverse of $\mathbf{G}_{(k)}$, the mode- k unfolding matrix of \mathcal{G} .

3 Geometry of Tucker tensor varieties

We first revisit the tangent space of the fixed-rank Tucker manifold from a new geometric perspective. Then, an explicit representation of the tangent cone of Tucker varieties is developed. Moreover, we propose an approximate projection onto the tangent cone.

3.1 A new formulation of the tangent space of fixed-rank Tucker manifold

In this subsection, we give an equivalent formulation for the tangent space to fixed-rank Tucker manifold $\mathcal{M}_{\mathbf{r}}$. Given a tensor $\mathcal{X} \in \mathbb{R}^{n_1 \times n_2 \times \cdots \times n_d}$ with $\text{rank}_{\text{tc}}(\mathcal{X}) = \mathbf{r}$ and Tucker decomposition $\mathcal{X} = \mathcal{G} \times_{k=1}^d \mathbf{U}_k$, it follows from (2.5) that $\text{span}(\dot{\mathbf{U}}_k) \subseteq \text{span}(\mathbf{U}_k)^\perp$, i.e., the set $\{\dot{\mathbf{U}}_k \in \mathbb{R}^{n_k \times \mathcal{L}_k} : \dot{\mathbf{U}}_k^\top \mathbf{U}_k = 0\}$ can be presented as $\{\dot{\mathbf{U}}_k = \mathbf{U}_k^\perp \dot{\mathbf{R}}_k : \dot{\mathbf{R}}_k \in \mathbb{R}^{(n_k - \mathcal{L}_k) \times \mathcal{L}_k}\}$, where \mathbf{U}_k^\perp is defined in a same fashion as Proposition 1 for $k \in [d]$. Subsequently, for any tangent vector $\mathcal{V} \in \text{T}_{\mathcal{X}}\mathcal{M}_{\mathbf{r}}$, we have

$$\begin{aligned} \mathcal{V} &= \dot{\mathcal{G}} \times_1 \mathbf{U}_1 \cdots \times_d \mathbf{U}_d + \sum_{k=1}^d \mathcal{G} \times_k \dot{\mathbf{U}}_k \times_{j \neq k} \mathbf{U}_j \\ &= \dot{\mathcal{G}} \times_1 \mathbf{U}_1 \cdots \times_d \mathbf{U}_d + \sum_{k=1}^d \mathcal{G} \times_k (\mathbf{U}_k^\perp \dot{\mathbf{R}}_k) \times_{j \neq k} \mathbf{U}_j \\ &= \dot{\mathcal{G}} \times_1 \mathbf{U}_1 \cdots \times_d \mathbf{U}_d + \sum_{k=1}^d (\mathcal{G} \times_k \dot{\mathbf{R}}_k) \times_k \mathbf{U}_k^\perp \times_{j \neq k} \mathbf{U}_j. \end{aligned}$$

It turns out that the tangent space $\text{T}_{\mathcal{X}}\mathcal{M}_{\mathbf{r}}$ can also be parametrized by

$$\text{T}_{\mathcal{X}}\mathcal{M}_{\mathbf{r}} = \left\{ \dot{\mathcal{G}} \times_1 \mathbf{U}_1 \cdots \times_d \mathbf{U}_d + \sum_{k=1}^d (\mathcal{G} \times_k \dot{\mathbf{R}}_k) \times_k \mathbf{U}_k^\perp \times_{j \neq k} \mathbf{U}_j : \begin{array}{l} \dot{\mathcal{G}} \in \mathbb{R}^{\mathcal{L}_1 \times \cdots \times \mathcal{L}_d}, \dot{\mathbf{R}}_k \in \mathbb{R}^{(n_k - \mathcal{L}_k) \times \mathcal{L}_k} \end{array} \right\}. \quad (3.1)$$

Specifically, a tangent vector in $\text{T}_{\mathcal{X}}\mathcal{M}_{\mathbf{r}}$ for $d = 3$ is illustrated in Fig. 2, where the shaded cube represents an arbitrary tensor $\dot{\mathcal{G}} \in \mathbb{R}^{\mathcal{L}_1 \times \cdots \times \mathcal{L}_d}$ and the blank represents the tensor with zero elements. For the sake of brevity, we adopt these symbols to represent a tensor.

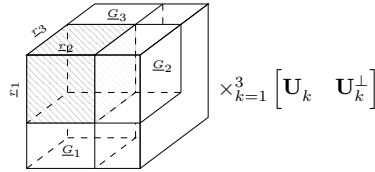


Fig. 2 Illustration of a tangent vector in $\text{T}_{\mathcal{X}}\mathcal{M}_{\mathbf{r}}$ at $\mathcal{X} = \mathcal{G} \times_{k=1}^d \mathbf{U}_k$ for $d = 3$. $\underline{G}_k := \mathcal{G} \times_k \dot{\mathbf{R}}_k$ with arbitrary $\dot{\mathbf{R}}_k$

3.2 Tangent cone of Tucker tensor varieties

In this subsection, we study the tangent cone of $\mathcal{M}_{\leq \mathbf{r}}$. Since $\mathcal{M}_{\leq \mathbf{r}}$ can be constructed through d matrix varieties $\mathbb{R}_{\leq r_k}^{n_k \times n_{-k}}$ of unfolding matrices, i.e.,

$$\mathcal{M}_{\leq \mathbf{r}} = \bigcap_{k=1}^d \text{ten}_{(k)} \left(\mathbb{R}_{\leq r_k}^{n_k \times n_{-k}} \right),$$

it is ready to know the following lemma.

Lemma 1 *Given a tensor $\mathcal{X} \in \mathcal{M}_{\leq \mathbf{r}}$, the tangent cone of $\mathcal{M}_{\leq \mathbf{r}}$ is a subset of the intersection of tensorized tangent cones of unfolding matrices along different modes, i.e.,*

$$\text{T}_{\mathcal{X}} \mathcal{M}_{\leq \mathbf{r}} \subseteq \bigcap_{k=1}^d \text{ten}_{(k)} \left(\text{T}_{\mathbf{X}_{(k)}} \mathbb{R}_{\leq r_k}^{n_k \times n_{-k}} \right).$$

Then, we can give an explicit parametrization of the tangent cone of Tucker tensor varieties as follows.

Theorem 1 *Given a Tucker tensor $\mathcal{X} = \mathcal{G} \times_1 \mathbf{U}_1 \cdots \times_d \mathbf{U}_d \in \mathbb{R}^{n_1 \times \cdots \times n_d}$ with $\text{rank}_{\text{tc}}(\mathcal{X}) = \mathbf{r} \leq \mathbf{r}$, any \mathcal{V} in the tangent cone of $\mathcal{M}_{\leq \mathbf{r}}$ at \mathcal{X} can be expressed by*

$$\mathcal{V} = \mathcal{C} \times_{k=1}^d \begin{bmatrix} \mathbf{U}_k & \mathbf{U}_{k,1} \end{bmatrix} + \sum_{k=1}^d \mathcal{G} \times_k (\mathbf{U}_{k,2} \mathbf{R}_{k,2}) \times_{j \neq k} \mathbf{U}_j, \quad (3.2)$$

where $\mathcal{C} \in \mathbb{R}^{r_1 \times \cdots \times r_d}$, $\mathbf{R}_{k,2} \in \mathbb{R}^{(n_k - r_k) \times r_k}$, $\mathbf{U}_{k,1} \in \text{St}(r_k - r_k, n_k)$ and $\mathbf{U}_{k,2} \in \text{St}(n_k - r_k, n_k)$ are arbitrary that satisfy $[\mathbf{U}_k \ \mathbf{U}_{k,1} \ \mathbf{U}_{k,2}] \in \mathcal{O}(n_k)$ for $k \in [d]$.

Proof For all $\mathcal{V} = \mathcal{C} \times_{k=1}^d [\mathbf{U}_k \ \mathbf{U}_{k,1}] + \sum_{k=1}^d \mathcal{G} \times_k (\mathbf{U}_{k,2} \mathbf{R}_{k,2}) \times_{j \neq k} \mathbf{U}_j$, $t^{(i)} = 1/i$ for $i \in \mathbb{N}$, we consider a sequence

$$\begin{aligned} \mathcal{X}^{(i)} &= t_i \mathcal{C} \times_{k=1}^d \begin{bmatrix} \mathbf{U}_k + t_i \mathbf{U}_{k,2} \mathbf{R}_{k,2} & \mathbf{U}_{k,1} \end{bmatrix} + \mathcal{G} \times_{k=1}^d (\mathbf{U}_k + t_i \mathbf{U}_{k,2} \mathbf{R}_{k,2}) \\ &\in \bigotimes_{k=1}^d \text{span} \left(\begin{bmatrix} \mathbf{U}_k + t_i \mathbf{U}_{k,2} \mathbf{R}_{k,2} & \mathbf{U}_{k,1} \end{bmatrix} \right) \subseteq \mathcal{M}_{\leq \mathbf{r}}, \end{aligned}$$

where we use the facts (2.4) and $\text{rank}([\mathbf{U}_k + t_i \mathbf{U}_{k,2} \mathbf{R}_{k,2} \ \mathbf{U}_{k,1}]) \leq r_k$. By direct calculations, we yield that $\lim_{i \rightarrow \infty} (\mathcal{X}^{(i)} - \mathcal{X})/t^{(i)} = \mathcal{V}$ and thus $\mathcal{V} \in \text{T}_{\mathcal{X}} \mathcal{M}_{\leq \mathbf{r}}$.

Then, we prove that any $\mathcal{V} \in \text{T}_{\mathcal{X}} \mathcal{M}_{\leq \mathbf{r}}$ can be represented by (3.2). Denote the mode- k unfolding matrix of \mathcal{V} by $\Xi_k := \mathbf{V}_{(k)}$. It follows from Lemma 1 that $\Xi_k \in \text{T}_{\mathbf{X}_{(k)}} \mathbb{R}_{\leq r_k}^{n_k \times n_{-k}}$ for $k \in [d]$. Since the k -th unfolding matrix $\mathbf{X}_{(k)}$ of \mathcal{X} admits the decomposition

$$\mathbf{X}_{(k)} = \mathbf{U}_k \mathbf{G}_{(k)} \mathbf{V}_k^T = \mathbf{U}_k \tilde{\mathbf{U}}_k \tilde{\Sigma}_k \tilde{\mathbf{V}}_k^T \mathbf{V}_k^T,$$

where $\mathbf{G}_{(k)} = \tilde{\mathbf{U}}_k \tilde{\Sigma}_k \tilde{\mathbf{V}}_k^T$ is the SVD of the unfolding matrix $\mathbf{G}_{(k)}$ of \mathcal{G} with $\tilde{\mathbf{U}}_k \in \mathcal{O}(r_k)$, and $\mathbf{V}_k := (\mathbf{U}_j)^{\otimes_{j \neq k}}$, it follows from $\Xi_k \in \text{T}_{\mathbf{X}_{(k)}} \mathbb{R}_{\leq r_k}^{n_k \times n_{-k}}$ and (2.2) that there exists $\mathbf{C}_k \in \mathbb{R}^{r_k \times r_k}$, $\mathbf{D}_{k,1} \in \mathbb{R}^{(r_k - r_k) \times r_k}$, $\mathbf{D}_{k,2} \in \mathbb{R}^{(n_k - r_k) \times r_k}$, $\mathbf{E}_{k,1} \in$

$\mathbb{R}^{r_k \times (r_k - r_k)}$, $\mathbf{E}_{k,2} \in \mathbb{R}^{r_k \times (n_k - r_k)}$, $\mathbf{F}_k \in \mathbb{R}^{(r_k - r_k) \times (r_k - r_k)}$, $\mathbf{U}_{k,1} \in \text{St}(r_k - r_k, n_k)$, $\mathbf{U}_{k,2} \in \text{St}(n_k - r_k, n_k)$, $\mathbf{V}_{k,1} \in \text{St}(r_k - r_k, n_k)$, $\mathbf{V}_{k,2} \in \text{St}(n_k - r_k, n_k)$ that satisfy $[\mathbf{U}_k \tilde{\mathbf{U}}_k \mathbf{U}_{k,1} \mathbf{U}_{k,2}] \in \mathcal{O}(n_k)$ and $[\mathbf{V}_k \tilde{\mathbf{V}}_k \mathbf{V}_{k,1} \mathbf{V}_{k,2}] \in \mathcal{O}(n_k)$, such that

$$\Xi_k = \begin{bmatrix} \mathbf{U}_k \tilde{\mathbf{U}}_k & \mathbf{U}_{k,1} & \mathbf{U}_{k,2} \end{bmatrix} \begin{bmatrix} \mathbf{C}_k & \mathbf{E}_{k,1} & \mathbf{E}_{k,2} \\ \mathbf{D}_{k,1} & \mathbf{F}_k & 0 \\ \mathbf{D}_{k,2} & 0 & 0 \end{bmatrix} \begin{bmatrix} \mathbf{V}_k \tilde{\mathbf{V}}_k & \mathbf{V}_{k,1} & \mathbf{V}_{k,2} \end{bmatrix}^\top.$$

We aim to find the unknowns \mathcal{C} and $\mathbf{R}_{k,2}$ in (3.2) by leveraging the structure of Ξ_k . To this end, we first claim that

$$\mathcal{W} := \mathcal{V} - \sum_{k=1}^d \mathcal{G} \times_k (\mathbf{U}_{k,2} \mathbf{R}_{k,2}) \times_{j \neq k} \mathbf{U}_j \in \bigotimes_{k=1}^d \text{span}([\mathbf{U}_k \mathbf{U}_{k,1}])$$

with $\mathbf{R}_{k,2} = \mathbf{D}_{k,2} \tilde{\Sigma}_k^{-1} \tilde{\mathbf{U}}_k^\top$. In view of (2.4), there exists $\mathcal{C} \in \mathbb{R}^{r_1 \times \dots \times r_d}$ such that

$$\mathcal{C} \times_{k=1}^d [\mathbf{U}_k \mathbf{U}_{k,1}] = \mathcal{W} = \mathcal{V} - \sum_{k=1}^d \mathcal{G} \times_k (\mathbf{U}_{k,2} \mathbf{R}_{k,2}) \times_{j \neq k} \mathbf{U}_j.$$

Hence, \mathcal{V} can be interpreted by (3.2).

Specifically, the claim can be validated as follows. We observe that

$$\begin{aligned} \mathbf{P}_{\mathbf{U}_{k,2}} \mathbf{W}_{(k)} &= \mathbf{P}_{\mathbf{U}_{k,2}} \left(\mathcal{V} - \sum_{i=1}^d \mathcal{G} \times_i \mathbf{U}_{i,2} \mathbf{R}_{i,2} \times_{j \neq i} \mathbf{U}_j \right)_{(k)} \\ &= \mathbf{P}_{\mathbf{U}_{k,2}} \Xi_k - \mathbf{U}_{k,2} \mathbf{R}_{k,2} \mathbf{G}_{(k)} \mathbf{V}_k^\top \\ &= \mathbf{U}_{k,2} \mathbf{D}_{k,2} \tilde{\mathbf{V}}_k^\top \mathbf{V}_k^\top - \mathbf{U}_{k,2} \mathbf{R}_{k,2} \mathbf{G}_{(k)} \mathbf{V}_k^\top \\ &= \mathbf{U}_{k,2} \mathbf{D}_{k,2} \tilde{\Sigma}_k^{-1} \tilde{\mathbf{U}}_k^\top \tilde{\mathbf{U}}_k \tilde{\Sigma}_k \tilde{\mathbf{V}}_k^\top \mathbf{V}_k^\top - \mathbf{U}_{k,2} \mathbf{R}_{k,2} \mathbf{G}_{(k)} \mathbf{V}_k^\top \\ &= \mathbf{U}_{k,2} \mathbf{D}_{k,2} \tilde{\Sigma}_k^{-1} \tilde{\mathbf{U}}_k^\top \mathbf{G}_{(k)} \mathbf{V}_k^\top - \mathbf{U}_{k,2} \mathbf{R}_{k,2} \mathbf{G}_{(k)} \mathbf{V}_k^\top \\ &= \mathbf{U}_{k,2} \left(\mathbf{D}_{k,2} \tilde{\Sigma}_k^{-1} \tilde{\mathbf{U}}_k^\top - \mathbf{R}_{k,2} \right) \mathbf{G}_{(k)} \mathbf{V}_k^\top \\ &= 0 \end{aligned}$$

holds for all $k \in [d]$. The equalities come from $\mathbf{V}_{(k)} = \Xi_k$, $\mathbf{P}_{\mathbf{U}_{k,2}} \mathbf{U}_k = 0$, $\mathbf{V}_k = (\mathbf{U}_j)^{\otimes_{j \neq k}}$, $\mathbf{G}_{(k)} = \tilde{\mathbf{U}}_k \tilde{\Sigma}_k \tilde{\mathbf{V}}_k^\top$, and $\mathbf{R}_{k,2} = \mathbf{D}_{k,2} \tilde{\Sigma}_k^{-1} \tilde{\mathbf{U}}_k^\top$. It turns out that

$$\mathbf{W}_{(k)} \in \text{span}(\mathbf{U}_{k,2})^\perp = \text{span}([\mathbf{U}_k \tilde{\mathbf{U}}_k \mathbf{U}_{k,1}]) = \text{span}([\mathbf{U}_k \mathbf{U}_{k,1}])$$

and thus

$$\mathcal{W} = \mathcal{V} - \sum_{k=1}^d \mathcal{G} \times_k (\mathbf{U}_{k,2} \mathbf{R}_{k,2}) \times_{j \neq k} \mathbf{U}_j \in \bigotimes_{k=1}^d \text{span}([\mathbf{U}_k \mathbf{U}_{k,1}]).$$

□

Remarkably, in the proof of Theorem 1, we employ the low-rank structure (2.2) of unfolding matrices in the tangent cone of Tucker tensor varieties. In other words, the new reformulation (2.2) of the tangent cone of matrix varieties is crucial to develop (3.2) in tensor case. We give a geometric illustration of the tangent cone $T_{\mathcal{X}}\mathcal{M}_{\leq \mathbf{r}}$ for $d = 3$ in Fig. 3, where the shaded cube represents an arbitrary tensor $\mathcal{C} \in \mathbb{R}^{r_1 \times \dots \times r_d}$. Note that (3.2) boils down to the tangent space (3.1) for $\underline{\mathbf{r}} = \mathbf{r}$ in the sense of $\mathbf{U}_{k,2} = \mathbf{U}_k^\perp$, $\mathbf{R}_{k,2} = \mathbf{R}_k$, $\mathcal{C} = \dot{\mathcal{G}}$, and removing $\mathbf{U}_{k,1}$. Moreover, the results are reduced to the tangent space and tangent cone of the matrix case for $d = 2$. In fact, the tangent cone of matrix varieties (2.2) can be informally interpreted by compressing the cube from back to front in Fig. 3 akin to “playing the accordion”.

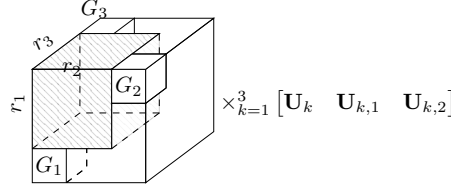


Fig. 3 Illustration of an element in $T_{\mathcal{X}}\mathcal{M}_{\leq \mathbf{r}}$ at $\mathcal{X} = \mathcal{G} \times_{k=1}^d \mathbf{U}_k$ for $d = 3$. $G_k := \mathcal{G} \times_k \mathbf{R}_{k,2}$ with arbitrary $\mathbf{R}_{k,2}$

In addition, we observe from the proof of Theorem 1 that the tangent cone inclusion in Lemma 1 is actually an equality, which is claimed in the following corollary. Precisely, for any tensor $\mathcal{V} \in \mathbb{R}^{n_1 \times n_2 \times \dots \times n_d}$ that satisfies $\mathbf{V}_{(k)} \in T_{\mathbf{X}_{(k)}} \mathbb{R}_{\leq r_k}^{n_k \times n_{-k}}$, it holds that \mathcal{V} can be represented by (3.2), i.e., $\mathcal{V} \in T_{\mathcal{X}}\mathcal{M}_{\leq \mathbf{r}}$.

Corollary 1 *The tangent cone of Tucker tensor varieties equals the intersection of tensorized tangent cones of unfolding matrices along different modes, i.e.,*

$$T_{\mathcal{X}}\mathcal{M}_{\leq \mathbf{r}} = \bigcap_{k=1}^d \text{ten}_{(k)} \left(T_{\mathbf{X}_{(k)}} \mathcal{M}_{\leq r_k} \right).$$

By using Corollary 1, we can prove the following stationary condition for the optimization problem (1.1).

Corollary 2 *Let \mathcal{X}^* be a stationary point of (1.1) with $\underline{\mathbf{r}}^* := \text{rank}_{\text{tc}}(\mathcal{X}^*) < \mathbf{r}$. Then, it holds that*

$$\nabla f(\mathcal{X}^*) = 0.$$

Proof Since any tensor $\mathcal{A} \in \mathbb{R}^{n_1 \times n_2 \times \dots \times n_d}$ can be represented by

$$\mathcal{A} = \sum_{i_1=1}^{n_1} \dots \sum_{i_d=1}^{n_d} y_{i_1, \dots, i_d} \mathbf{e}_{i_1} \circ \dots \circ \mathbf{e}_{i_d}$$

with bases $\mathbf{e}_{i_1} \circ \dots \circ \mathbf{e}_{i_d} \in \mathcal{M}_1$ and $(i_1, \dots, i_d) \in [n_1] \times \dots \times [n_d]$, it suffices to prove that $\langle \mathbf{e}_{i_1} \circ \dots \circ \mathbf{e}_{i_d}, \nabla f(\mathcal{X}^*) \rangle = 0$.

In fact, we observe from (2.2) and $\underline{r}_k^* < r_k$ that ℓ can be one. Therefore, $\mathbf{T}_{\mathbf{X}_{(k)}^*} \mathbb{R}_{\leq r_k}^{n_k \times n-k}$ contains all rank-1 matrices and thus contains $\pm(\mathbf{e}_{i_1} \circ \cdots \circ \mathbf{e}_{i_d})_{(k)}$ for $k \in [d]$. Subsequently, it follows from Corollary 1 that

$$\pm \mathbf{e}_{i_1} \circ \cdots \circ \mathbf{e}_{i_d} \in \bigcap_{k=1}^d \text{ten}_{(k)} \left(\mathbf{T}_{\mathbf{X}_{(k)}^*} \mathcal{M}_{\leq r_k} \right) = \mathbf{T}_{\mathcal{X}^*} \mathcal{M}_{\leq \mathbf{r}}.$$

According to Definition 1 and the stationarity of \mathcal{X}^* , it yields

$$\langle \mathbf{e}_{i_1} \circ \cdots \circ \mathbf{e}_{i_d}, \nabla f(\mathcal{X}^*) \rangle = 0.$$

□

The explicit form of the tangent cone in Theorem 1 allows us to obtain several attractive results. Recall the parametrization (3.2) that

$$\mathcal{V} = \mathcal{V}_0 + \sum_{k=1}^d \mathcal{V}_k := \mathcal{C} \times_{k=1}^d [\mathbf{U}_k \ \mathbf{U}_{k,1}] + \sum_{k=1}^d \mathcal{G} \times_k (\mathbf{U}_{k,2} \mathbf{R}_{k,2}) \times_{j \neq k} \mathbf{U}_j. \quad (3.3)$$

Note that $\langle \mathcal{V}_i, \mathcal{V}_j \rangle = 0$ for $i \neq j$ and thus $\|\mathcal{V}\|_{\mathbb{F}}^2 = \sum_{k=0}^d \|\mathcal{V}_k\|_{\mathbb{F}}^2$. Surprisingly, searching along the two types of directions in \mathcal{V} does not leave the Tucker tensor varieties: 1) it follows from (2.4) and Tucker decomposition $\mathcal{X} = \mathcal{G} \times_{k=1}^d \mathbf{U}_k$ that

$$\begin{aligned} \mathcal{X} + \mathcal{V}_0 &= \mathcal{G} \times_{k=1}^d \mathbf{U}_k + \mathcal{C} \times_{k=1}^d [\mathbf{U}_k \ \mathbf{U}_{k,1}] \\ &\in \bigotimes_{k=1}^d \text{span}([\mathbf{U}_k \ \mathbf{U}_{k,1}]) \subseteq \mathcal{M}_{\leq \mathbf{r}}; \end{aligned} \quad (3.4)$$

2) for all $k \in [d]$, we observe from $\text{rank}(\mathbf{U}_k + \mathbf{U}_{k,2} \mathbf{R}_{k,2}) \leq r_k$ that

$$\begin{aligned} \mathcal{X} + \mathcal{V}_k &= \mathcal{G} \times_{i=1}^d \mathbf{U}_i + \mathcal{G} \times_k (\mathbf{U}_{k,2} \mathbf{R}_{k,2}) \times_{j \neq k} \mathbf{U}_j \\ &= \mathcal{G} \times_k (\mathbf{U}_k + \mathbf{U}_{k,2} \mathbf{R}_{k,2}) \times_{j \neq k} \mathbf{U}_j \\ &\in \mathcal{M}_{\leq \mathbf{r}}. \end{aligned} \quad (3.5)$$

It is worth noting that (3.4) and (3.5) provide $d+1$ *retraction-free* search directions in $\mathbf{T}_{\mathcal{X}} \mathcal{M}_{\leq \mathbf{r}}$, which can be adopted to develop line-search methods on $\mathcal{M}_{\leq \mathbf{r}}$ without retractions; see section 5 for details. Additionally, the following corollary gives a bound for the retraction $\mathbf{R}_{\mathcal{X}}^{\text{HO}}$ and is of great importance to prove the convergence for line-search methods on $\mathcal{M}_{\leq \mathbf{r}}$.

Corollary 3 *There exists a constant $M = 1 + \frac{d}{\sqrt{d+1}} > 0$, such that*

$$\|\mathcal{X} - \mathbf{P}_{\leq \mathbf{r}}^{\text{HO}}(\mathcal{X} + \mathcal{V})\|_{\mathbb{F}} \leq M \|\mathcal{V}\|_{\mathbb{F}}$$

for all $\mathcal{X} \in \mathcal{M}_{\leq \mathbf{r}}$ and $\mathcal{V} \in \mathbf{T}_{\mathcal{X}} \mathcal{M}_{\leq \mathbf{r}}$.

Proof By combining (2.6)–(2.8), (3.4)–(3.5) and $\|\mathcal{V}\|_{\mathbb{F}}^2 = \sum_{k=0}^d \|\mathcal{V}_k\|_{\mathbb{F}}^2$, we yield

$$\begin{aligned}
& \left\| \mathcal{X} + \mathcal{V} - \mathbf{P}_{\leq \mathbf{r}}^{\text{HO}}(\mathcal{X} + \mathcal{V}) \right\|_{\mathbb{F}}^2 \leq d \|\mathcal{X} + \mathcal{V} - \mathbf{P}_{\leq \mathbf{r}}(\mathcal{X} + \mathcal{V})\|_{\mathbb{F}}^2 \\
& \leq d \min_{k=0,1,\dots,d} \{ \|\mathcal{X} + \mathcal{V} - (\mathcal{X} + \mathcal{V}_k)\|_{\mathbb{F}}^2 \} \\
& = d \min_{k=0,1,\dots,d} \left\{ \sum_{j=0, j \neq k}^d \|\mathcal{V}_j\|_{\mathbb{F}}^2 \right\} \\
& \leq \frac{d}{d+1} \sum_{k=0}^d \sum_{j=0, j \neq k}^d \|\mathcal{V}_j\|_{\mathbb{F}}^2 \\
& = \frac{d^2}{d+1} \|\mathcal{V}\|_{\mathbb{F}}^2.
\end{aligned}$$

Therefore, it holds that

$$\|\mathcal{X} - \mathbf{P}_{\leq \mathbf{r}}^{\text{HO}}(\mathcal{X} + \mathcal{V})\|_{\mathbb{F}} \leq \|\mathcal{X} + \mathcal{V} - \mathbf{P}_{\leq \mathbf{r}}^{\text{HO}}(\mathcal{X} + \mathcal{V})\|_{\mathbb{F}} + \|\mathcal{V}\|_{\mathbb{F}} \leq (1 + \frac{d}{\sqrt{d+1}}) \|\mathcal{V}\|_{\mathbb{F}}.$$

□

3.3 Metric projection onto the tangent cone

For the sake of fulfilling the basic requirement of the projected gradient method on $\mathcal{M}_{\leq \mathbf{r}}$, we consider the metric projection of a tensor $\mathcal{A} \in \mathbb{R}^{n_1 \times \dots \times n_d}$ onto the tangent cone $\mathbf{T}_{\mathcal{X}} \mathcal{M}_{\leq \mathbf{r}}$ at $\mathcal{X} = \mathcal{G} \times_{k=1}^d \mathbf{U}_k$, which is determined by the following optimization problem

$$\mathbf{P}_{\mathbf{T}_{\mathcal{X}} \mathcal{M}_{\leq \mathbf{r}}} \mathcal{A} := \arg \min_{\mathcal{V} \in \mathbf{T}_{\mathcal{X}} \mathcal{M}_{\leq \mathbf{r}}} \|\mathcal{A} - \mathcal{V}\|_{\mathbb{F}}^2. \quad (3.6)$$

Since the tangent cone $\mathbf{T}_{\mathcal{X}} \mathcal{M}_{\leq \mathbf{r}}$ is closed, the metric projection exists. We explore the metric projection by taking the parametrization (3.2) and (3.3) into (3.6), and it yields

$$\begin{aligned}
\|\mathcal{A} - \mathcal{V}\|_{\mathbb{F}}^2 &= \|\mathcal{A} - \sum_{k=0}^d \mathcal{V}_k\|_{\mathbb{F}}^2 \\
&= \|\mathcal{A}\|_{\mathbb{F}}^2 + \|\mathcal{V}_0\|_{\mathbb{F}}^2 + \sum_{k=1}^d \|\mathcal{V}_k\|_{\mathbb{F}}^2 - 2 \langle \mathcal{A}, \mathcal{V}_0 \rangle - 2 \sum_{k=1}^d \langle \mathcal{A}, \mathcal{V}_k \rangle \\
&= \|\mathcal{A}\|_{\mathbb{F}}^2 + \|\mathcal{C}\|_{\mathbb{F}}^2 - 2 \left\langle \mathcal{A} \times_{k=1}^d [\mathbf{U}_k \ \mathbf{U}_{k,1}]^{\top}, \mathcal{C} \right\rangle \\
&\quad + \sum_{k=1}^d \left(\|\mathcal{G} \times_k \mathbf{R}_{k,2}\|_{\mathbb{F}}^2 - 2 \left\langle \mathcal{A} \times_k \mathbf{U}_{k,2}^{\top} \times_{j \neq k} \mathbf{U}_j^{\top}, \mathcal{G} \times_k \mathbf{R}_{k,2} \right\rangle \right).
\end{aligned} \quad (3.7)$$

In order to solve (3.6), we aim to find the unknowns \mathcal{C} , $\mathbf{U}_{k,1}$, $\mathbf{U}_{k,2}$ and $\mathbf{R}_{k,2}$ for $k \in [d]$ and $j = 1, 2$ in (3.7). Generally speaking, the computation of $\mathbf{P}_{\mathbf{T}_{\mathcal{X}} \mathcal{M}_{\leq \mathbf{r}}} \mathcal{A}$ is divided into two steps: 1) by fixing $\mathbf{U}_{k,1}$ and $\mathbf{U}_{k,2}$, we yield closed-form solutions of \mathcal{C} and $\mathbf{R}_{k,2}$; 2) we take the solutions into (3.7) and determine $\mathbf{U}_{k,1}$ by an optimization problem.

Step 1: representing \mathcal{C} and $\mathbf{R}_{k,2}$ by $\mathbf{U}_{k,1}$ and $\mathbf{U}_{k,2}$ By fixing $\mathbf{U}_{k,1}$ and $\mathbf{U}_{k,2}$ for $k \in [d]$, we observe that (3.7) is a separable quadratic function with respect to \mathcal{C} and $\mathbf{R}_{k,2}$. Therefore, \mathcal{C} and $\mathbf{R}_{k,2}$ in the metric projection (3.6) can be uniquely expressed by

$$\begin{aligned}\mathcal{C} &= \mathcal{A} \times_{k=1}^d \left[\mathbf{U}_k \mathbf{U}_{k,1} \right]^\top, \\ \mathbf{R}_{k,2} &= \left(\mathcal{A} \times_k \mathbf{U}_{k,2}^\top \times_{j \neq k} \mathbf{U}_j^\top \right)_{(k)} \mathbf{G}_{(k)}^\dagger.\end{aligned}\quad (3.8)$$

Step 2: determining $\mathbf{U}_{k,1}$ We determine $\mathbf{U}_{k,1}$ by taking (3.8) into (3.7) and obtain

$$\begin{aligned}\|\mathcal{A} - \mathcal{V}\|_F^2 &= \|\mathcal{A}\|_F^2 - \|\mathcal{C}\|_F^2 - \sum_{k=1}^d \|\mathcal{G} \times_k \mathbf{R}_{k,2}\|_F^2 \\ &= \|\mathcal{A}\|_F^2 - \|\mathcal{C}\|_F^2 - \sum_{k=1}^d \left\| \left(\mathcal{A} \times_k \mathbf{U}_{k,2}^\top \times_{j \neq k} \mathbf{U}_j^\top \right)_{(k)} \mathbf{G}_{(k)}^\dagger \mathbf{G}_{(k)} \right\|_F^2 \\ &= \|\mathcal{A}\|_F^2 - \|\mathcal{C}\|_F^2 - \sum_{k=1}^d \left\langle \mathbf{A}_{\neq k} \mathbf{P}_{\mathbf{G}_{(k)}^\top}, \mathbf{U}_{k,2} \mathbf{U}_{k,2}^\top \mathbf{A}_{\neq k} \mathbf{P}_{\mathbf{G}_{(k)}^\top} \right\rangle \\ &= \|\mathcal{A}\|_F^2 - \|\mathcal{C}\|_F^2 - \sum_{k=1}^d \left\langle \mathbf{A}_{\neq k} \mathbf{P}_{\mathbf{G}_{(k)}^\top}, (\mathbf{I}_{n_k} - \mathbf{U}_k \mathbf{U}_k^\top - \mathbf{U}_{k,1} \mathbf{U}_{k,1}^\top) \mathbf{A}_{\neq k} \mathbf{P}_{\mathbf{G}_{(k)}^\top} \right\rangle \\ &= \|\mathcal{A}\|_F^2 - \left\| \mathcal{A} \times_{k=1}^d \left[\mathbf{U}_k \mathbf{U}_{k,1} \right]^\top \right\|_F^2 \\ &\quad - \sum_{k=1}^d \left\| \mathbf{A}_{\neq k} \mathbf{P}_{\mathbf{G}_{(k)}^\top} \right\|_F^2 + \sum_{k=1}^d \left\| \mathbf{U}_k^\top \mathbf{A}_{\neq k} \mathbf{P}_{\mathbf{G}_{(k)}^\top} \right\|_F^2 + \sum_{k=1}^d \left\| \mathbf{U}_{k,1}^\top \mathbf{A}_{\neq k} \mathbf{P}_{\mathbf{G}_{(k)}^\top} \right\|_F^2,\end{aligned}$$

where $\mathbf{A}_{\neq k} := \left(\mathcal{A} \times_{j \neq k} \mathbf{U}_j^\top \right)_{(k)} \in \mathbb{R}^{n_k \times r-k}$ and $\mathbf{P}_{\mathbf{G}_{(k)}^\top} := \mathbf{G}_{(k)}^\dagger \mathbf{G}_{(k)}$. Note that $\mathbf{U}_{k,2}$ is eliminated by \mathbf{U}_k and $\mathbf{U}_{k,1}$. Alternatively, one can also eliminate $\mathbf{U}_{k,1}$ by \mathbf{U}_k and $\mathbf{U}_{k,2}$. Nevertheless, the number of parameters of $\mathbf{U}_{k,1} \in \mathbb{R}^{n_k \times (r_k - r_k)}$ is smaller than $\mathbf{U}_{k,2} \in \mathbb{R}^{n_k \times (n_k - r_k)}$ when $r_k \ll n_k$. Therefore, it is computationally favorable to formulate (3.6) as

$$\begin{aligned}\min \quad & F(\mathbf{U}_{1,1}, \dots, \mathbf{U}_{d,1}) := - \left\| \mathcal{A} \times_{k=1}^d \left[\mathbf{U}_k \mathbf{U}_{k,1} \right]^\top \right\|_F^2 + \sum_{k=1}^d \left\| \mathbf{U}_{k,1}^\top \mathbf{A}_{\neq k} \mathbf{P}_{\mathbf{G}_{(k)}^\top} \right\|_F^2 \\ \text{s. t.} \quad & \left[\mathbf{U}_k \mathbf{U}_{k,1} \right]^\top \left[\mathbf{U}_k \mathbf{U}_{k,1} \right] = \mathbf{I}_{r_k} \text{ for } k \in [d].\end{aligned}\quad (3.9)$$

Since the feasible set of (3.9) is compact, a global minimizer of (3.9) exists.

Let $(\mathbf{U}_{1,1}^*, \dots, \mathbf{U}_{d,1}^*)$ be a global minima of (3.9). By using (3.2) and (3.8), the projection onto the tangent cone $\text{T}_{\mathcal{X}\mathcal{M}_{\leq r}}$ reads

$$\text{P}_{\text{T}_{\mathcal{X}\mathcal{M}_{\leq r}}} \mathcal{A} = \mathcal{A} \times_{k=1}^d \mathbf{P}_{\mathbf{S}_k^*} + \sum_{k=1}^d \mathcal{G} \times_k \left(\mathbf{P}_{\mathbf{S}_k^*}^\perp \left(\mathcal{A} \times_{j \neq k} \mathbf{U}_j^\top \right)_{(k)} \mathbf{G}_{(k)}^\dagger \right) \times_{j \neq k} \mathbf{U}_j, \quad (3.10)$$

where $\mathbf{S}_k^* := [\mathbf{U}_k \ \mathbf{U}_{k,1}^*]$. We observe that the metric projection (3.10) relies on the projection $\mathbf{P}_{\mathbf{S}_k^*}$ but not a specific $\mathbf{U}_{k,1}$. Additionally, (3.10) boils down to the projection onto the tangent space (2.9) when $\mathbf{r} = \underline{\mathbf{r}}$.

Connection to matrix varieties It is worth noting that the projection (3.10) also coincides with (2.3) in matrix case. Specifically, given a matrix $\mathbf{X} \in \mathbb{R}_{\underline{\mathbf{r}}}^{m \times n}$ and the SVD of $\mathbf{X} = \mathbf{U}\Sigma\mathbf{V}^\top$, by following the steps in tensor case, (3.9) boils down to

$$\max_{\mathbf{U}_{1,1}, \mathbf{V}_{2,1}} \|\mathbf{U}_{1,1}^\top \mathbf{A} \mathbf{V}_{2,1}\|_{\mathbb{F}}^2, \quad \text{s.t.} \quad \begin{bmatrix} \mathbf{U} & \mathbf{U}_{1,1} \end{bmatrix}^\top \begin{bmatrix} \mathbf{U} & \mathbf{U}_{1,1} \end{bmatrix} = \begin{bmatrix} \mathbf{V} & \mathbf{V}_{2,1} \end{bmatrix}^\top \begin{bmatrix} \mathbf{V} & \mathbf{V}_{2,1} \end{bmatrix} = \mathbf{I}_r. \quad (3.11)$$

In fact, (3.11) has a closed-form solution $(\mathbf{U}^*, \mathbf{V}^*)$, which is the leading $(r - \underline{r})$ singular vectors of the matrix $\mathbf{P}_{\mathbf{U}}^\perp \mathbf{A} \mathbf{P}_{\mathbf{V}}^\perp$. Specifically, it is ready to know $\mathbf{U}^\top \mathbf{U}^* = 0$ and $\mathbf{V}^\top \mathbf{V}^* = 0$, i.e., $(\mathbf{U}^*, \mathbf{V}^*)$ is a feasible point of (3.11). Furthermore, for all feasible points $(\mathbf{U}_{1,1}, \mathbf{V}_{2,1})$, it follows from $\mathbf{P}_{\mathbf{U}}^\perp \mathbf{U}_{1,1} = \mathbf{U}_{1,1}$, $\mathbf{P}_{\mathbf{V}}^\perp \mathbf{V}_{2,1} = \mathbf{V}_{2,1}$, and the Eckart–Young theorem that

$$\|\mathbf{U}_{1,1}^\top \mathbf{A} \mathbf{V}_{2,1}\|_{\mathbb{F}}^2 = \|\mathbf{U}_{1,1}^\top \mathbf{P}_{\mathbf{U}}^\perp \mathbf{A} \mathbf{P}_{\mathbf{V}}^\perp \mathbf{V}_{2,1}\|_{\mathbb{F}}^2 \leq \|(\mathbf{U}^*)^\top \mathbf{P}_{\mathbf{U}}^\perp \mathbf{A} \mathbf{P}_{\mathbf{V}}^\perp \mathbf{V}^*\|_{\mathbb{F}}^2 = \|(\mathbf{U}^*)^\top \mathbf{A} \mathbf{V}^*\|_{\mathbb{F}}^2.$$

Therefore, the optimality of $(\mathbf{U}^*, \mathbf{V}^*)$ of (3.11) is verified.

We yield from (3.10) that

$$\begin{aligned} \mathbf{P}_{\mathbf{T}_{\mathbf{X}} \mathbb{R}_{\leq \underline{\mathbf{r}}}^{m \times n}} \mathbf{A} &= \mathbf{P}_{[\mathbf{U} \ \mathbf{U}^*]} \mathbf{A} \mathbf{P}_{[\mathbf{V} \ \mathbf{V}^*]} + \mathbf{P}_{[\mathbf{U} \ \mathbf{U}^*]}^\perp \mathbf{A} \mathbf{P}_{\mathbf{V}} + \mathbf{P}_{\mathbf{U}} \mathbf{A} \mathbf{P}_{[\mathbf{V} \ \mathbf{V}^*]}^\perp \\ &= \mathbf{P}_{\mathbf{T}_{\mathbf{X}} \mathbb{R}_{\underline{\mathbf{r}}}^{m \times n}} \mathbf{A} + \mathbf{P}_{\leq (r - \underline{r})} \left(\mathbf{P}_{\mathbf{U}}^\perp \mathbf{A} \mathbf{P}_{\mathbf{V}}^\perp \right), \end{aligned}$$

which coincides with the known results in (2.3).

In contrast with the matrix case, the global minima of (3.9) for $d \geq 3$ is computationally intractable. Therefore, pursuing an approximate projection emerges as a more practical way to approach the metric projection.

3.4 An approximate projection

The projection in (3.6) is unavailable in general, and hence it is natural to consider an approximation. To this end, given $\mathcal{X} = \mathcal{G} \times_{k=1}^d \mathbf{U}_k$ and any $\tilde{\mathbf{U}}_{k,1} \in \text{St}(r_k - \underline{r}_k, n_k)$ that satisfies $\mathbf{P}_{\mathbf{U}_k} \tilde{\mathbf{U}}_{k,1} = 0$ for $k \in [d]$, we construct an approximate projection via (3.10) by substituting $\tilde{\mathbf{U}}_{k,1}$ for $\mathbf{U}_{k,1}^*$ as follows.

Proposition 3 *Given $\tilde{\mathbf{U}}_{k,1} \in \text{St}(r_k - \underline{r}_k, n_k)$ that satisfies $\mathbf{P}_{\mathbf{U}_k} \tilde{\mathbf{U}}_{k,1} = 0$ for $k \in [d]$, the approximate projection, defined by*

$$\tilde{\mathbf{P}}_{\mathbf{T}_{\mathcal{X}} \mathcal{M}_{\leq \underline{\mathbf{r}}}} \mathcal{A} := \mathcal{A} \times_{k=1}^d \mathbf{P}_{\tilde{\mathbf{S}}_k} + \sum_{k=1}^d \mathcal{G} \times_k \left(\mathbf{P}_{\tilde{\mathbf{S}}_k}^\perp \left(\mathcal{A} \times_{j \neq k} \mathbf{U}_j^\top \right)_{(k)} \mathbf{G}_{(k)}^\dagger \right) \times_{j \neq k} \mathbf{U}_j, \quad (3.12)$$

satisfies $\tilde{\mathbf{P}}_{\mathbf{T}_{\mathcal{X}} \mathcal{M}_{\leq \underline{\mathbf{r}}}} \mathcal{A} \in \mathbf{T}_{\mathcal{X}} \mathcal{M}_{\leq \underline{\mathbf{r}}}$ and $\langle \mathcal{A}, \tilde{\mathbf{P}}_{\mathbf{T}_{\mathcal{X}} \mathcal{M}_{\leq \underline{\mathbf{r}}}} \mathcal{A} \rangle = \|\tilde{\mathbf{P}}_{\mathbf{T}_{\mathcal{X}} \mathcal{M}_{\leq \underline{\mathbf{r}}}} \mathcal{A}\|_{\mathbb{F}}^2$, where $\tilde{\mathbf{S}}_k := [\mathbf{U}_k \ \tilde{\mathbf{U}}_{k,1}]$.

Proof For the sake of brevity, we introduce the notation $\tilde{\mathbf{P}}_{\mathcal{T}_{\mathcal{X}}\mathcal{M}_{\leq \mathbf{r}}} \mathcal{A} = \tilde{\mathcal{V}}_0 + \sum_{k=1}^d \tilde{\mathcal{V}}_k$ in a similar fashion as (3.3) for (3.12). It is direct to verify that

$$\begin{aligned}\tilde{\mathcal{V}}_0 &= \left(\mathcal{A} \times_{j=1}^d [\mathbf{U}_j \ \tilde{\mathbf{U}}_{j,1}]^\top \right) \times_{i=1}^d [\mathbf{U}_i \ \tilde{\mathbf{U}}_{i,1}], \\ \tilde{\mathcal{V}}_k &= \mathcal{G} \times_k \left(\tilde{\mathbf{U}}_{k,2} \tilde{\mathbf{U}}_{k,2}^\top \left(\mathcal{A} \times_{j \neq k} \mathbf{U}_j^\top \right)_{(k)} \mathbf{G}_{(k)}^\dagger \right) \times_{j \neq k} \mathbf{U}_j,\end{aligned}$$

where $\tilde{\mathbf{U}}_{k,2} \in \text{St}(n_k - r_k, n_k)$ satisfies $[\mathbf{U}_k \ \tilde{\mathbf{U}}_{k,1} \ \tilde{\mathbf{U}}_{k,2}] \in \mathcal{O}(n_k)$. Hence, $\tilde{\mathbf{P}}_{\mathcal{T}_{\mathcal{X}}\mathcal{M}_{\leq \mathbf{r}}} \mathcal{A}$ is of the form (3.2) in the tangent cone $\mathcal{T}_{\mathcal{X}}\mathcal{M}_{\leq \mathbf{r}}$.

Note that $\langle \tilde{\mathcal{V}}_i, \tilde{\mathcal{V}}_j \rangle = 0$ for $i \neq j$ and thus $\|\tilde{\mathbf{P}}_{\mathcal{T}_{\mathcal{X}}\mathcal{M}_{\leq \mathbf{r}}} \mathcal{A}\|_{\text{F}}^2 = \sum_{k=0}^d \|\tilde{\mathcal{V}}_k\|_{\text{F}}^2$. By using $\mathbf{P}_{\tilde{\mathbf{S}}_k}^2 = \mathbf{P}_{\tilde{\mathbf{S}}_k} = \mathbf{P}_{\tilde{\mathbf{S}}_k}^\top$, $(\mathbf{P}_{\tilde{\mathbf{S}}_k}^\perp)^2 = \mathbf{P}_{\tilde{\mathbf{S}}_k}^\perp = (\mathbf{P}_{\tilde{\mathbf{S}}_k}^\perp)^\top$, $(\mathbf{G}_{(k)}^\dagger \mathbf{G}_{(k)})^2 = \mathbf{G}_{(k)}^\dagger \mathbf{G}_{(k)} = (\mathbf{G}_{(k)}^\dagger \mathbf{G}_{(k)})^\top$, and $\mathbf{V}_k^\top \mathbf{V}_k = \mathbf{I}_{r-k}$ with $\mathbf{V}_k = (\mathbf{U}_j)^{\otimes j \neq k}$, we yield that

$$\begin{aligned}\langle \mathcal{A}, \tilde{\mathbf{P}}_{\mathcal{T}_{\mathcal{X}}\mathcal{M}_{\leq \mathbf{r}}} \mathcal{A} \rangle &= \left\langle \mathcal{A}, \tilde{\mathcal{V}}_0 + \sum_{k=1}^d \tilde{\mathcal{V}}_k \right\rangle = \langle \mathcal{A}, \mathcal{A} \times_{k=1}^d \mathbf{P}_{\tilde{\mathbf{S}}_k} \rangle + \sum_{k=1}^d \langle \mathcal{A}, \tilde{\mathcal{V}}_k \rangle \\ &= \|\tilde{\mathcal{V}}_0\|_{\text{F}}^2 + \sum_{k=1}^d \left\langle \mathbf{A}_{(k)}, \left(\mathbf{P}_{\tilde{\mathbf{S}}_k}^\perp \mathbf{A}_{(k)} \mathbf{V}_k \mathbf{G}_{(k)}^\dagger \right) \mathbf{G}_{(k)} \mathbf{V}_k^\top \right\rangle \\ &= \|\tilde{\mathcal{V}}_0\|_{\text{F}}^2 + \sum_{k=1}^d \left\| \left(\mathbf{P}_{\tilde{\mathbf{S}}_k}^\perp \mathbf{A}_{(k)} \mathbf{V}_k \mathbf{G}_{(k)}^\dagger \right) \mathbf{G}_{(k)} \mathbf{V}_k^\top \right\|_{\text{F}}^2 \\ &= \|\tilde{\mathcal{V}}_0\|_{\text{F}}^2 + \sum_{k=1}^d \left\| \mathcal{G} \times_k \left(\mathbf{P}_{\tilde{\mathbf{S}}_k}^\perp \left(\mathcal{A} \times_{j \neq k} \mathbf{U}_j^\top \right)_{(k)} \mathbf{G}_{(k)}^\dagger \right) \times_{j \neq k} \mathbf{U}_j \right\|_{\text{F}}^2 \\ &= \|\tilde{\mathcal{V}}_0\|_{\text{F}}^2 + \sum_{k=1}^d \|\tilde{\mathcal{V}}_k\|_{\text{F}}^2 \\ &= \left\| \tilde{\mathbf{P}}_{\mathcal{T}_{\mathcal{X}}\mathcal{M}_{\leq \mathbf{r}}} \mathcal{A} \right\|_{\text{F}}^2.\end{aligned}$$

□

The approximate projection can be explicitly computed by Algorithm 1. Moreover, let $\mathcal{A} = -\nabla f(\mathcal{X})$, it turns out that $\tilde{\mathbf{P}}_{\mathcal{T}_{\mathcal{X}}\mathcal{M}_{\leq \mathbf{r}}}(-\nabla f(\mathcal{X})) \in \mathcal{T}_{\mathcal{X}}\mathcal{M}_{\leq \mathbf{r}}$ is a descent direction for f since

$$\langle -\nabla f(\mathcal{X}), \tilde{\mathbf{P}}_{\mathcal{T}_{\mathcal{X}}\mathcal{M}_{\leq \mathbf{r}}}(-\nabla f(\mathcal{X})) \rangle = \|\tilde{\mathbf{P}}_{\mathcal{T}_{\mathcal{X}}\mathcal{M}_{\leq \mathbf{r}}}(-\nabla f(\mathcal{X}))\|_{\text{F}}^2 \geq 0.$$

Algorithm 1 The approximate projection onto $\mathcal{T}_{\mathcal{X}}\mathcal{M}_{\leq \mathbf{r}}$

Input: $\mathcal{X} = \mathcal{G} \times_1 \mathbf{U}_1 \cdots \times_d \mathbf{U}_d$ with $\text{rank}_{\text{tc}}(\mathcal{X}) = \mathbf{r} \leq \mathbf{r}$, and a tensor $\mathcal{A} \in \mathbb{R}^{n_1 \times \cdots \times n_d}$.

1: Choose $\tilde{\mathbf{U}}_{1,1}, \dots, \tilde{\mathbf{U}}_{d,1}$ from Proposition 3.

2: Compute the approximate projection by (3.12).

Output: $\tilde{\mathbf{P}}_{\mathcal{T}_{\mathcal{X}}\mathcal{M}_{\leq \mathbf{r}}}(\mathcal{A})$.

4 Gradient-related approximate projection method

In this section, we aim to design line search methods by taking advantage of the tangent cone in Theorem 1. One instinctive approach is the projected gradient descent method

$$\mathcal{X}^{(t+1)} = P_{\mathcal{M}_{\leq \mathbf{r}}} \left(\mathcal{X}^{(t)} + s^{(t)} P_{T_{\mathcal{X}^{(t)}} \mathcal{M}_{\leq \mathbf{r}}} (-\nabla f(\mathcal{X}^{(t)})) \right),$$

which is a generalization of the Riemannian gradient descent for minimizing f on $\mathcal{M}_{\mathbf{r}}$; see, e.g., [SU15; OGA23] for matrix varieties. However, the metric projections $P_{T_{\mathcal{X}^{(t)}} \mathcal{M}_{\leq \mathbf{r}}}$ and $P_{\mathcal{M}_{\leq \mathbf{r}}}$ do not enjoy closed-form expressions. Therefore, we propose the gradient-related approximate projection method by exploiting the approximate projection (3.12) and HOSVD.

4.1 Algorithm

Algorithm 2 lists the proposed gradient-related approximate projection method (GRAP) for solving (1.1).

Algorithm 2 gradient-related approximate projection method (GRAP)

Input: Initial guess $\mathcal{X}^{(0)} \in \mathcal{M}_{\leq \mathbf{r}}$, $\omega = (0, 1]$, backtracking parameters $\rho, a \in (0, 1)$, $s_{\min} > 0$.

- 1: **while** the stopping criteria are not satisfied **do**
 - 2: Compute $g^{(t)} = \tilde{P}_{T_{\mathcal{X}^{(t)}} \mathcal{M}_{\leq \mathbf{r}}} (-\nabla f(\mathcal{X}^{(t)}))$ by Algorithm 1.
 - 3: **if** the angle condition is not satisfied **then**
 - 4: Set $g^{(t)} = -\nabla f(\mathcal{X}^{(t)})$ as a restart.
 - 5: **end if**
 - 6: Choose stepsize $s^{(t)}$ by Armijo backtracking line search (4.2).
 - 7: Update $\mathcal{X}^{(t+1)} = P_{\leq \mathbf{r}}^{\text{HO}} \left(\mathcal{X}^{(t)} + s^{(t)} g^{(t)} \right)$. $t = t + 1$.
 - 8: **end while**
- Output:** $\mathcal{X}^{(t)}$.
-

Instead of solving (3.10) for exact metric projection, the GRAP method substitutes (3.10) by the approximate projection (3.12). Additionally, the metric projection $P_{\mathcal{M}_{\leq \mathbf{r}}}$ is replaced by $P_{\mathcal{M}_{\leq \mathbf{r}}}^{\text{HO}}$. In summary, the update of iterates in GRAP is

$$\mathcal{X}^{(t+1)} = P_{\leq \mathbf{r}}^{\text{HO}} \left(\mathcal{X}^{(t)} + s^{(t)} \tilde{P}_{T_{\mathcal{X}^{(t)}} \mathcal{M}_{\leq \mathbf{r}}} (-\nabla f(\mathcal{X}^{(t)})) \right).$$

Moreover, to ensure that the search directions $\{g^{(t)} = \tilde{P}_{T_{\mathcal{X}^{(t)}} \mathcal{M}_{\leq \mathbf{r}}} (-\nabla f(\mathcal{X}^{(t)}))\}_{t \geq 0}$ are sufficiently gradient-related, the *angle condition*

$$\langle -\nabla f(\mathcal{X}^{(t)}), g^{(t)} \rangle \geq \omega \|P_{T_{\mathcal{X}^{(t)}} \mathcal{M}_{\leq \mathbf{r}}} (-\nabla f(\mathcal{X}^{(t)}))\|_{\mathbf{F}} \|g^{(t)}\|_{\mathbf{F}} \quad (4.1)$$

is imposed with $\omega \in (0, 1]$. It follows from Proposition 3 that (4.1) is equivalent to

$$\|g^{(t)}\|_{\mathbf{F}} \geq \omega \|P_{T_{\mathcal{X}^{(t)}} \mathcal{M}_{\leq \mathbf{r}}} (-\nabla f(\mathcal{X}^{(t)}))\|_{\mathbf{F}}.$$

If $g^{(t)}$ is rejected by the angle condition, we reset $g^{(t)}$ to be the full antigradient $g^{(t)} = -\nabla f(\mathcal{X}^{(t)})$ as a restart. One the one hand, if $\mathcal{X}^{(t)} \in \mathcal{M}_{\mathbf{r}}$, the search direction

$g^{(t)} = \tilde{P}_{T_{\mathcal{X}^{(t)}}\mathcal{M}_{\leq r}}(-\nabla f(\mathcal{X}^{(t)}))$ boils down to the negative Riemannian gradient $-\text{grad}f(\mathcal{X}) := -P_{T_{\mathcal{X}}\mathcal{M}_r}(\nabla f(\mathcal{X}))$ and thus satisfies the angle condition with $\omega = 1$. Hence, the restart is never activated for points on \mathcal{M}_r . On the other hand, if $\mathcal{X} \in \mathcal{M}_{< r}$, we observe from Corollary 2 that the condition $\nabla f(\mathcal{X}) = 0$ necessarily and sufficiently depicts a stationary point. Therefore, searching along the antigradient as a restart is reasonable.

For the selection of stepsize, we consider the Armijo backtracking line search. Specifically, given an initial stepsize $s_0^{(t)} > 0$, find the smallest integer l , such that for $s^{(t)} = \rho^l s_0^{(t)} > s_{\min}$, the inequality

$$f(\mathcal{X}^{(t)}) - f(P_{\leq r}^{\text{HO}}(\mathcal{X}^{(t)} + s^{(t)}g^{(t)})) \geq s^{(t)}a \left\langle -\nabla f(\mathcal{X}^{(t)}), g^{(t)} \right\rangle \quad (4.2)$$

holds, where $\rho, a \in (0, 1)$, $s_{\min} > 0$ are backtracking parameters.

4.2 Global convergence

Let $\{\mathcal{X}^{(t)}\}_{t \geq 0}$ be an infinite sequence generated by Algorithm 2. We prove that the stationary measure $\|P_{T_{\mathcal{X}^{(t)}}\mathcal{M}_{\leq r}}(-\nabla f(\mathcal{X}^{(t)}))\|_F$ converges to 0.

Theorem 2 *Let $\{\mathcal{X}^{(t)}\}_{t \geq 0}$ be an infinite sequence generated by Algorithm 2. Assume f is bounded below from f^* , it holds that*

$$\lim_{t \rightarrow \infty} \|P_{T_{\mathcal{X}^{(t)}}\mathcal{M}_{\leq r}}(-\nabla f(\mathcal{X}^{(t)}))\|_F = 0.$$

Moreover, Algorithm 2 returns $\mathcal{X}^{(t)} \in \mathcal{M}_{\leq r}$ satisfying $\|P_{T_{\mathcal{X}^{(t)}}\mathcal{M}_{\leq r}}(-\nabla f(\mathcal{X}^{(t)}))\|_F < \epsilon$ after $\left\lceil f(\mathcal{X}^{(0)})/(s_{\min}a\omega^2\epsilon^2) \right\rceil$ iterations at most.

Proof It follows from (4.1) and (4.2) that

$$\begin{aligned} f(\mathcal{X}^{(t)}) - f(\mathcal{X}^{(t+1)}) &\geq s^{(t)}a \left\langle -\nabla f(\mathcal{X}^{(t)}), g^{(t)} \right\rangle \\ &\geq s_{\min}a \|g^{(t)}\|_F^2 \\ &\geq s_{\min}a\omega^2 \|P_{T_{\mathcal{X}^{(t)}}\mathcal{M}_{\leq r}}(-\nabla f(\mathcal{X}^{(t)}))\|_F^2. \end{aligned}$$

Therefore, it yields

$$f(\mathcal{X}^{(0)}) - f^* \geq \sum_{t=0}^{\infty} s_{\min}a\omega^2 \|P_{T_{\mathcal{X}^{(t)}}\mathcal{M}_{\leq r}}(-\nabla f(\mathcal{X}^{(t)}))\|_F^2,$$

and thus $\|P_{T_{\mathcal{X}^{(t)}}\mathcal{M}_{\leq r}}(-\nabla f(\mathcal{X}^{(t)}))\|_F$ converges to 0.

Moreover, assume $\|P_{T_{\mathcal{X}^{(t)}}\mathcal{M}_{\leq r}}(-\nabla f(\mathcal{X}^{(t)}))\|_F \geq \epsilon$ holds for $t = 0, \dots, T$. We have

$$f(\mathcal{X}^{(0)}) - f(\mathcal{X}^{(T)}) \geq s_{\min}a\omega^2\epsilon^2 T,$$

and thus $T \leq f(\mathcal{X}^{(0)})/(s_{\min}a\omega^2\epsilon^2)$. \square

It is worth noting that it requires $\mathcal{O}(\epsilon^{-2})$ steps to achieve an ϵ -stationary point, which coincides with the classical results in Riemannian optimization; see, e.g., [BAC19, Theorem 2.5].

4.3 Local convergence

Given an infinite sequence $\{\mathcal{X}^{(t)}\}_{t \geq 0}$ generated by Algorithm 2, we analyze the local convergence by exploiting the *Łojasiewicz gradient inequality* [SU15, Definition 2.1]. A point $\mathcal{X} \in \mathcal{M}_{\leq \mathbf{r}}$ is said to satisfy the Łojasiewicz gradient inequality if there exists $\delta, L > 0$ and $\theta \in (0, 1/2]$ such that

$$|f(\mathcal{X}) - f(\mathcal{Y})|^{1-\theta} \leq L \|\mathbf{P}_{\mathbf{T}_{\mathcal{X}} \mathcal{M}_{\leq \mathbf{r}}}(-\nabla f(\mathcal{Y}))\|_{\mathbf{F}} \quad (4.3)$$

holds for all $\mathcal{Y} \in \mathcal{M}_{\leq \mathbf{r}}$ with $\|\mathcal{Y} - \mathcal{X}\|_{\mathbf{F}} \leq \delta$. Under the assumption that f satisfies (4.3), we can prove the local convergence of Algorithm 2 is as follows.

Theorem 3 *Let $\{\mathcal{X}^{(t)}\}_{t \geq 0}$ be an infinite sequence generated by Algorithm 2. Assume that f is bounded below from f^* and satisfies the Łojasiewicz gradient inequality. Assume $\text{rank}_{\text{tc}}(\mathcal{X}^{(t)}) < \mathbf{r}$ or $\text{rank}_{\text{tc}}(\mathcal{X}^{(t)}) = \mathbf{r}$ for sufficiently large t . If $\{\mathcal{X}^{(t)}\}_{t \geq 0}$ has an accumulation point \mathcal{X}^* , then $\mathcal{X}^{(t)}$ converges to \mathcal{X}^* . Furthermore, if $\text{rank}_{\text{tc}}(\mathcal{X}^*) = \mathbf{r}$, then the stationary measure $\|\mathbf{P}_{\mathbf{T}_{\mathcal{X}^*} \mathcal{M}_{\leq \mathbf{r}}}(-\nabla f(\mathcal{X}^*))\|_{\mathbf{F}} = \|\text{grad} f(\mathcal{X}^*)\|_{\mathbf{F}} = 0$ and*

$$\|\mathcal{X}^{(t)} - \mathcal{X}^*\|_{\mathbf{F}} \leq C \begin{cases} e^{-ct}, & \text{if } \theta = \frac{1}{2}, \\ t^{-\frac{\theta}{1-2\theta}}, & \text{if } 0 < \theta < \frac{1}{2} \end{cases}$$

hold for some $C, c > 0$.

Proof Using [SU15, Theorem 2.3, Corollary 2.11], it suffices to prove the following three claims: 1) there exists $c > 0$, such that

$$f(\mathcal{X}^{(t)}) - f(\mathcal{X}^{(t+1)}) \geq c \|\mathbf{P}_{\mathbf{T}_{\mathcal{X}^{(t)}} \mathcal{M}_{\leq \mathbf{r}}}(-\nabla f(\mathcal{X}^{(t)}))\|_{\mathbf{F}} \|\mathcal{X}^{(t)} - \mathcal{X}^{(t+1)}\|_{\mathbf{F}};$$

2) the stationary measure $\|\mathbf{P}_{\mathbf{T}_{\mathcal{X}^{(t)}} \mathcal{M}_{\leq \mathbf{r}}}(-\nabla f(\mathcal{X}^{(t)}))\|_{\mathbf{F}} = 0$ implies $\mathcal{X}^{(t+1)} = \mathcal{X}^{(t)}$ for sufficiently large t ; 3) if $\text{rank}_{\text{tc}}(\mathcal{X}^*) = \mathbf{r}$, $\mathcal{X}^{(t)} \in \mathcal{M}_{\mathbf{r}}$ for sufficiently large t .

For the first claim, we discuss two scenarios: i) if the approximate projection (3.12) is adopted, i.e., $g^{(t)} = \tilde{\mathbf{P}}_{\mathbf{T}_{\mathcal{X}^{(t)}} \mathcal{M}_{\leq \mathbf{r}}}(-\nabla f(\mathcal{X}^{(t)}))$, it follows from (4.1)–(4.2) and Corollary 3 that

$$\begin{aligned} f(\mathcal{X}^{(t)}) - f(\mathcal{X}^{(t+1)}) &\geq a\omega \|\mathbf{P}_{\mathbf{T}_{\mathcal{X}^{(t)}} \mathcal{M}_{\leq \mathbf{r}}}(-\nabla f(\mathcal{X}^{(t)}))\|_{\mathbf{F}} \|s^{(t)} g^{(t)}\|_{\mathbf{F}} \\ &\geq \frac{a\omega}{M} \|\mathbf{P}_{\mathbf{T}_{\mathcal{X}^{(t)}} \mathcal{M}_{\leq \mathbf{r}}}(-\nabla f(\mathcal{X}^{(t)}))\|_{\mathbf{F}} \|\mathcal{X}^{(t)} - \mathcal{X}^{(t+1)}\|_{\mathbf{F}}; \end{aligned}$$

ii) if a restart occurs, i.e., $g^{(t)} = -\nabla f(\mathcal{X}^{(t)})$, it holds that

$$\begin{aligned} \|\mathcal{X}^{(t+1)} - \mathcal{X}^{(t)}\|_{\mathbf{F}} &= \|\mathbf{P}_{\leq \mathbf{r}}^{\text{HO}}(\mathcal{X}^{(t)} + s^{(t)} g^{(t)}) - \mathcal{X}^{(t)}\|_{\mathbf{F}} \\ &\leq \|\mathbf{P}_{\leq \mathbf{r}}^{\text{HO}}(\mathcal{X}^{(t)} + s^{(t)} g^{(t)}) - (\mathcal{X}^{(t)} + s^{(t)} g^{(t)})\|_{\mathbf{F}} + \|s^{(t)} g^{(t)}\|_{\mathbf{F}} \\ &\leq \sqrt{d} \|\mathbf{P}_{\leq \mathbf{r}}(\mathcal{X}^{(t)} + s^{(t)} g^{(t)}) - (\mathcal{X}^{(t)} + s^{(t)} g^{(t)})\|_{\mathbf{F}} + \|s^{(t)} g^{(t)}\|_{\mathbf{F}} \\ &\leq \sqrt{d} \|\mathcal{X}^{(t)} - (\mathcal{X}^{(t)} + s^{(t)} g^{(t)})\|_{\mathbf{F}} + \|s^{(t)} g^{(t)}\|_{\mathbf{F}} \\ &\leq (\sqrt{d} + 1) \|s^{(t)} g^{(t)}\|_{\mathbf{F}}, \end{aligned}$$

where we use (2.8) and the definition of metric projection in (3.6). It turns out that

$$\begin{aligned} f(\mathcal{X}^{(t)}) - f(\mathcal{X}^{(t+1)}) &\geq s^{(t)} a \|g^{(t)}\|_F^2 \\ &\geq s^{(t)} a \|P_{T_{\mathcal{X}^{(t)}} \mathcal{M}_{\leq \mathbf{r}}}(-\nabla f(\mathcal{X}^{(t)}))\|_F \|g^{(t)}\|_F \\ &\geq \frac{a}{\sqrt{d}+1} \|P_{T_{\mathcal{X}^{(t)}} \mathcal{M}_{\leq \mathbf{r}}}(-\nabla f(\mathcal{X}^{(t)}))\|_F \|\mathcal{X}^{(t)} - \mathcal{X}^{(t+1)}\|_F. \end{aligned}$$

Moreover, assume that $\|P_{T_{\mathcal{X}^{(t)}} \mathcal{M}_{\leq \mathbf{r}}}(-\nabla f(\mathcal{X}^{(t)}))\|_F = 0$, holds for some large t . If $\text{rank}_{\text{tc}}(\mathcal{X}^{(t)}) = \mathbf{r}$, it holds that $g^{(t)} = -\text{grad}f(\mathcal{X}^{(t)})$ and $\mathcal{X}^{(t+1)} = \mathcal{X}^{(t)}$. If $\text{rank}_{\text{tc}}(\mathcal{X}^{(t)}) < \mathbf{r}$, then it follows from Corollary 2 that $\nabla f(\mathcal{X}^{(t)}) = 0$ and thus $g^{(t)} = 0$ and $\mathcal{X}^{(t+1)} = \mathcal{X}^{(t)}$.

The third claim is ready since $\mathcal{M}_{\mathbf{r}}$ is open in $\mathcal{M}_{\leq \mathbf{r}}$. \square

4.4 Discussion: apocalypse

Observe that even though $\{\mathcal{X}^{(t)}\}_{t \geq 0}$ has an accumulation point \mathcal{X}^* , the condition $\lim_{t \rightarrow \infty} \|P_{T_{\mathcal{X}^{(t)}} \mathcal{M}_{\leq \mathbf{r}}}(-\nabla f(\mathcal{X}^{(t)}))\|_F = 0$ does not necessarily guarantee that \mathcal{X}^* is a stationary point of f , i.e., $\|P_{T_{\mathcal{X}^*} \mathcal{M}_{\leq \mathbf{r}}}(-\nabla f(\mathcal{X}^*))\|_F$ can be nonzero; see the following example.

Example 1 Given $\mathcal{A} = \mathbf{e}_1 \circ \mathbf{e}_1 \circ \mathbf{e}_1 + \mathbf{e}_3 \circ \mathbf{e}_3 \circ \mathbf{e}_3 \in \mathbb{R}^{n \times n \times n}$ and $\mathbf{r} = (2, 2, 2)$, consider the objective function $f(\mathcal{X}) = \|\mathcal{X} - \mathcal{A}\|_F^2$, and initial guess $\mathcal{X}^{(0)} = \mathbf{e}_1 \circ \mathbf{e}_1 \circ \mathbf{e}_1 + \mathbf{e}_2 \circ \mathbf{e}_2 \circ \mathbf{e}_2$. Then, the sequence generated by Algorithm 2 with a constant stepsize $s^{(t)} = \alpha \in (0, 1)$ is explicitly

$$\mathcal{X}^{(t)} = \mathbf{e}_1 \circ \mathbf{e}_1 \circ \mathbf{e}_1 + (1 - \alpha)^t \mathbf{e}_2 \circ \mathbf{e}_2 \circ \mathbf{e}_2,$$

which converges to $\mathcal{X}^* = \mathbf{e}_1 \circ \mathbf{e}_1 \circ \mathbf{e}_1$. According to Theorem 2, the sequence satisfies that $\lim_{t \rightarrow \infty} \|P_{T_{\mathcal{X}^{(t)}} \mathcal{M}_{\leq \mathbf{r}}}(-\nabla f(\mathcal{X}^{(t)}))\|_F = 0$. However, since $\nabla f(\mathcal{X}^*) \neq 0$, \mathcal{X}^* is not a stationary point of f by using Corollary 2.

More recently, such a phenomenon has been investigated and named by *apocalypse* [LKB23]. Specifically, a point $\mathcal{X}^* \in \mathcal{M}_{\leq \mathbf{r}}$ is called *apocalyptic* if there exists a sequence $\{\mathcal{X}^{(t)}\} \subseteq \mathcal{M}_{\leq \mathbf{r}}$ converging to \mathcal{X}^* and a smooth function f , such that

$$\lim_{t \rightarrow \infty} \|P_{T_{\mathcal{X}^{(t)}} \mathcal{M}_{\leq \mathbf{r}}}(-\nabla f(\mathcal{X}^{(t)}))\|_F = 0 \quad \text{but} \quad \|P_{T_{\mathcal{X}^*} \mathcal{M}_{\leq \mathbf{r}}}(-\nabla f(\mathcal{X}^*))\|_F > 0.$$

The triplet $(\mathcal{X}^*, \{\mathcal{X}^{(t)}\}, f)$ is called an apocalypse. Similar to the matrix varieties, we observe that the Tucker tensor varieties suffer from apocalypse at rank deficient points in $\mathcal{M}_{\leq \mathbf{r}}$.

Proposition 4 *If $\mathcal{X}^* \in \mathcal{M}_{\leq \mathbf{r}}$ has $\text{rank}_{\text{tc}}(\mathcal{X}^*) = \underline{\mathbf{r}} < \mathbf{r}$, then \mathcal{X}^* is apocalyptic.*

Proof See Appendix B. \square

Circumventing apocalypse for Tucker tensor varieties is far beyond the main purpose of this paper. Hence, we leave it for future research.

5 A retraction-free gradient-related approximate projection method

In Algorithm 2, the retraction $R_{\mathcal{X}}^{\text{HO}}$, which requires computation of HOSVD to a d -dimensional tensor with size $(r_1 + r_1) \times \dots \times (r_d + r_d)$, is inevitable to preserve the constraint, Tucker tensor variety. One is curious about exploiting information of the tangent cone $T_{\mathcal{X}\mathcal{M}_{\leq \mathbf{r}}}$ to construct search directions and facilitate line search without retraction to save computational cost. In this section, we consider partial projections to develop retraction-free line search method on $\mathcal{M}_{\leq \mathbf{r}}$.

5.1 New partial projections

Recall that any \mathcal{V} in the tangent cone $T_{\mathcal{X}\mathcal{M}_{\leq \mathbf{r}}}$ at $\mathcal{X} = \mathcal{G} \times_{k=1}^d \mathbf{U}_k$ with $\text{rank}_{\text{tc}}(\mathcal{X}) = \mathbf{r}$ can be parametrized in terms of $(\mathcal{C}, \{\mathbf{U}_{k,1}\}_{k=1}^d, \{\mathbf{U}_{k,2}\}_{k=1}^d, \{\mathbf{R}_{k,2}\}_{k=1}^d)$ by (3.2), i.e.,

$$\mathcal{V} = \mathcal{V}_0 + \sum_{k=1}^d \mathcal{V}_k = \mathcal{C} \times_{k=1}^d \begin{bmatrix} \mathbf{U}_k & \mathbf{U}_{k,1} \end{bmatrix} + \sum_{k=1}^d \mathcal{G} \times_k (\mathbf{U}_{k,2} \mathbf{R}_{k,2}) \times_{j \neq k} \mathbf{U}_j.$$

In view of (3.4)–(3.5), searching along such $d+1$ directions $\{\mathcal{V}_k\}$ is able to get rid of retractions. In the light of this, we consider partial projections that are of the form in $\{\mathcal{V}_k\}$.

Given $\mathcal{A} \in \mathbb{R}^{n_1 \times \dots \times n_d}$, the partial projections are defined as follows.

$$P_0(\mathcal{A}) := \arg \min_{\mathcal{V}_0} \left\{ \|\mathcal{V}_0 - \mathcal{A}\| : \mathcal{V}_0 = \mathcal{C} \times_{k=1}^d \begin{bmatrix} \mathbf{U}_k & \mathbf{U}_{k,1} \end{bmatrix} \in T_{\mathcal{X}\mathcal{M}_{\leq \mathbf{r}}} \right\}, \quad (5.1)$$

$$P_k(\mathcal{A}) := \arg \min_{\mathcal{V}_k} \left\{ \|\mathcal{V}_k - \mathcal{A}\| : \mathcal{V}_k = \mathcal{G} \times_k (\mathbf{U}_{k,2} \mathbf{R}_{k,2}) \times_{j \neq k} \mathbf{U}_j \in T_{\mathcal{X}\mathcal{M}_{\leq \mathbf{r}}} \right\}. \quad (5.2)$$

Since (5.1) does not enjoy a closed-form solution, we consider its approximation

$$\tilde{P}_0(\mathcal{A}) := \mathcal{A} \times_{k=1}^d P_{\tilde{\mathbf{S}}_k}, \quad (5.3)$$

which is exactly the first term of the approximate projection $\tilde{P}_{T_{\mathcal{X}\mathcal{M}_{\leq \mathbf{r}}}}(\mathcal{A})$ in (3.12) for given $\tilde{\mathbf{U}}_{k,1} \in \text{St}(r_k - r_k, n_k)$ with $\tilde{\mathbf{U}}_{k,1}^T \mathbf{U}_k = 0$, where $\tilde{\mathbf{S}}_k := [\mathbf{U}_k \ \tilde{\mathbf{U}}_{k,1}]$ for $k \in [d]$. It is worth noting that $\tilde{P}_0(\mathcal{A})$ requires the parameters $\{\tilde{\mathbf{U}}_{k,1}\}_{k=1}^d$ a priori. Moreover, by fixing $\mathbf{U}_{k,2}$ in (5.2) and using $[\mathbf{U}_k \ \mathbf{U}_{k,1} \ \mathbf{U}_{k,2}] \in \mathcal{O}(n_k)$ and (3.10), $P_k(\mathcal{A})$ is in the form of

$$P_k(\mathcal{A}) = \mathcal{G} \times_k \left(P_{\mathbf{U}_{k,2}} \left(\mathcal{A} \times_{j \neq k} \mathbf{U}_j^T \right)_{(k)} \mathbf{G}_{(k)}^\dagger \right) \times_{j \neq k} \mathbf{U}_j.$$

Similarly, since $\mathbf{U}_{k,2}$ is unknown, we consider substituting the projection $P_{\mathbf{U}_{k,2}}$ by $P_{\mathbf{U}_k}^\perp$ and yield an approximation

$$\tilde{P}_k(\mathcal{A}) = \mathcal{G} \times_k \left(P_{\mathbf{U}_k}^\perp \left(\mathcal{A} \times_{j \neq k} \mathbf{U}_j^T \right)_{(k)} \mathbf{G}_{(k)}^\dagger \right) \times_{j \neq k} \mathbf{U}_j. \quad (5.4)$$

Note that for $k = 0, 1, \dots, d$, $\tilde{P}_k(\mathcal{A}) \in \mathcal{T}_{\mathcal{X}}\mathcal{M}_{\leq \mathbf{r}}$ and $\langle \mathcal{A}, \tilde{P}_k(\mathcal{A}) \rangle = \|\tilde{P}_k(\mathcal{A})\|_F^2$, which can be proved in a similar fashion as Proposition 3. Additionally, we can prove $\text{rank}_{\text{tc}}(\mathcal{X} + \tilde{P}_k(\mathcal{A})) \leq \mathbf{r}$, i.e.,

$$\mathcal{X} + \tilde{P}_k(\mathcal{A}) \in \mathcal{M}_{\leq \mathbf{r}},$$

in a similar fashion as (3.4)–(3.5). However, this property does not necessarily hold for two different partial projections $\tilde{P}_j(\mathcal{A})$ and $\tilde{P}_k(\mathcal{A})$ with $j \neq k$, i.e., $\text{rank}_{\text{tc}}(\mathcal{X} + \tilde{P}_j(\mathcal{A}) + \tilde{P}_k(\mathcal{A}))$ can be larger than \mathbf{r} .

5.2 Algorithm and convergence results

To sum up, we propose the partial projection operator defined by

$$\hat{P}_{\mathcal{T}_{\mathcal{X}}\mathcal{M}_{\leq \mathbf{r}}}(\mathcal{A}) := \arg \max_{\mathcal{V} \in \{\tilde{P}_0(\mathcal{A}), \dots, \tilde{P}_d(\mathcal{A})\}} \|\mathcal{V}\|_F. \quad (5.5)$$

By using the partial projection (5.5), we propose a retraction-free gradient-related approximate projection method (rfGRAP) in Algorithm 3. The iteration of the proposed rfGRAP method is

$$\mathcal{X}^{(t+1)} = \mathcal{X}^{(t)} + s^{(t)} \hat{P}_{\mathcal{T}_{\mathcal{X}^{(t)}}\mathcal{M}_{\leq \mathbf{r}}}(-\nabla f(\mathcal{X}^{(t)})),$$

where $s^{(t)}$ is also computed by Armijo backtracking line search (4.2). In contrast with the proposed GRAP method (Algorithm 2), there is no retraction in Algorithm 3.

Algorithm 3 Retraction-free gradient-related approximate projection method (rfGRAP)

Input: Initial guess $\mathcal{X}^{(0)} \in \mathcal{M}_{\leq \mathbf{r}}$, backtracking parameters $\rho, a \in (0, 1)$, $s_{\min} > 0$.

```

1: while the stopping criteria are not satisfied do
2:   Compute  $\hat{P}_{\mathcal{T}_{\mathcal{X}^{(t)}}\mathcal{M}_{\leq \mathbf{r}}}(-\nabla f(\mathcal{X}^{(t)}))$  by (5.5).
3:   if the angle condition is not satisfied then
4:     Set  $g^{(t)} = -\nabla f(\mathcal{X}^{(t)})$ .
5:   end if
6:   Choose stepsize  $s^{(t)}$  by Armijo backtracking line search (4.2).
7:   Update  $\mathcal{X}^{(t+1)} = \mathcal{X}^{(t)} + s^{(t)}g^{(t)}$ .  $t = t + 1$ .
8: end while
Output:  $\mathcal{X}^{(t)}$ 

```

The global and local convergence of the rfGRAP method can be proved in a similar fashion as Theorem 2 and Theorem 3.

Theorem 4 *Let $\{\mathcal{X}^{(t)}\}_{t \geq 0}$ be an infinite sequence generated by Algorithm 3. Assume f is bounded below from f^* and satisfies the Lojasiewicz gradient inequality. It holds that*

$$\lim_{t \rightarrow \infty} \|\mathcal{P}_{\mathcal{T}_{\mathcal{X}^{(t)}}\mathcal{M}_{\leq \mathbf{r}}}(-\nabla f(\mathcal{X}^{(t)}))\|_F = 0.$$

The method returns $\mathcal{X}^{(t)} \in \mathcal{M}_{\leq \mathbf{r}}$ satisfying $\|\mathcal{P}_{\mathcal{T}_{\mathcal{X}^{(t)}}\mathcal{M}_{\leq \mathbf{r}}}(-\nabla f(\mathcal{X}^{(t)}))\|_F < \epsilon$ after $\left\lceil f(\mathcal{X}^{(0)})/(s_{\min} a \omega^2 \epsilon^2) \right\rceil$ iterations at most. If $\{\mathcal{X}^{(t)}\}_{t \geq 0}$ has an accumulation point

\mathcal{X}^* and either $\text{rank}_{\text{tc}}(\mathcal{X}^{(t)}) < \mathbf{r}$ or $\text{rank}_{\text{tc}}(\mathcal{X}^{(t)}) = \mathbf{r}$ for sufficiently large t , then $\mathcal{X}^{(t)}$ converges to \mathcal{X}^* . Furthermore, if $\text{rank}_{\text{tc}}(\mathcal{X}^*) = \mathbf{r}$, then $\|\text{P}_{\text{T}_{\mathcal{X}^*}\mathcal{M}_{\leq \mathbf{r}}}(-\nabla f(\mathcal{X}^*))\|_{\text{F}} = \|\text{grad}f(\mathcal{X}^*)\|_{\text{F}} = 0$ and

$$\|\mathcal{X}^{(t)} - \mathcal{X}^*\|_{\text{F}} \leq C \begin{cases} e^{-ct}, & \text{if } \theta = \frac{1}{2}, \\ t^{-\frac{\theta}{1-2\theta}}, & \text{if } 0 < \theta < \frac{1}{2}. \end{cases}$$

5.3 Connection to matrix varieties

We investigate the connection between the proposed rfGRAP method and other existing methods in the matrix case.

Specifically, given a matrix $\mathbf{A} \in \mathbb{R}^{m \times n}$ and the SVD $\mathbf{X} = \mathbf{U}\Sigma\mathbf{V}^T$ of $\mathbf{X} \in \mathbb{R}_{\underline{r}}^{m \times n}$, the proposed partial projections $\{\tilde{\text{P}}_k(\mathbf{A})\}_{k=0}^d$ in (5.3)–(5.4) boils down to

$$\begin{aligned} \tilde{\text{P}}_0(\mathbf{A}) &= \text{P}_{[\mathbf{U} \ \mathbf{U}_1]} \mathbf{A} \text{P}_{[\mathbf{V} \ \mathbf{V}_1]}, \\ \tilde{\text{P}}_1(\mathbf{A}) &= \text{P}_{\mathbf{U}}^\perp \mathbf{A} \text{P}_{\mathbf{V}}, \\ \tilde{\text{P}}_2(\mathbf{A}) &= \text{P}_{\mathbf{U}} \mathbf{A} \text{P}_{\mathbf{V}}^\perp \end{aligned}$$

when $d = 2$, where $\mathbf{U}_1 \in \text{St}(r - \underline{r}, m)$, $\mathbf{V}_1 \in \text{St}(r - \underline{r}, n)$, i.e., $\tilde{\mathbf{U}}_{1,1}$ and $\tilde{\mathbf{U}}_{2,1}$ in (5.3), are selected by the leading $(r - \underline{r})$ left and right singular vectors of $\text{P}_{\mathbf{U}}^\perp \mathbf{A} \text{P}_{\mathbf{V}}^\perp$. Given $\mathbf{U}_2 \in \text{St}(m - r, m)$ with $[\mathbf{U} \ \mathbf{U}_1 \ \mathbf{U}_2] \in \mathcal{O}(m)$ and $\mathbf{V}_2 \in \text{St}(n - r, n)$ with $[\mathbf{V} \ \mathbf{V}_1 \ \mathbf{V}_2] \in \mathcal{O}(n)$. Subsequently, the partial projections can be illustrated by

$$\begin{aligned} \tilde{\text{P}}_0(\mathbf{A}) &= [\mathbf{U} \ \mathbf{U}_1 \ \mathbf{U}_2] \begin{bmatrix} \text{shaded} & & \\ & \text{shaded} & \\ & & \text{shaded} \end{bmatrix} [\mathbf{V} \ \mathbf{V}_1 \ \mathbf{V}_2]^T, \\ \tilde{\text{P}}_1(\mathbf{A}) &= [\mathbf{U} \ \mathbf{U}_1 \ \mathbf{U}_2] \begin{bmatrix} & & \\ & \text{shaded} & \\ & & \text{shaded} \end{bmatrix} [\mathbf{V} \ \mathbf{V}_1 \ \mathbf{V}_2]^T, \\ \tilde{\text{P}}_2(\mathbf{A}) &= [\mathbf{U} \ \mathbf{U}_1 \ \mathbf{U}_2] \begin{bmatrix} & & \\ & & \text{shaded} \\ \text{shaded} & & \end{bmatrix} [\mathbf{V} \ \mathbf{V}_1 \ \mathbf{V}_2]^T \end{aligned}$$

in the sense of (2.2), which is different from the “partial projections”

$$\begin{aligned} \check{\text{P}}_1(\mathbf{A}) &= [\mathbf{U} \ \mathbf{U}_1 \ \mathbf{U}_2] \begin{bmatrix} \text{shaded} & & \\ & \text{shaded} & \\ & & \text{shaded} \end{bmatrix} [\mathbf{V} \ \mathbf{V}_1 \ \mathbf{V}_2]^T, \\ \check{\text{P}}_2(\mathbf{A}) &= [\mathbf{U} \ \mathbf{U}_1 \ \mathbf{U}_2] \begin{bmatrix} & & \\ & \text{shaded} & \\ \text{shaded} & & \end{bmatrix} [\mathbf{V} \ \mathbf{V}_1 \ \mathbf{V}_2]^T \end{aligned}$$

in [SU15, §3.4]. Therefore, the proposed partial projection $\hat{\text{P}}_{\text{T}_{\mathbf{X}}\mathcal{M}_{\leq r}}$ is also able to serve as a new retraction-free search direction in optimization on matrix varieties.

6 A Tucker rank-adaptive method

In practice, choosing an appropriate rank parameter \mathbf{r} appears to be a challenging task. A larger \mathbf{r} can expand the search space and potentially yield a better optimum while simultaneously increasing computational costs. In addition, as shown in Example 1, even though a sequence generated by GRAP satisfies that $\|P_{T_{\mathcal{X}^{(t)}}\mathcal{M}_{\leq \mathbf{r}}}(-\nabla f(\mathcal{X}^{(t)}))\|_F$ converges to 0, the rank deficiency at an accumulation point can hamper it to be a stationary point. A similar challenge arises in Riemannian optimization methods applied on the fixed-rank Tucker tensor manifold $\mathcal{M}_{\mathbf{r}}$; see, e.g., [Don+22, Section 5.1]. Therefore, in this section, we are motivated to propose a rank-adaptive method to adjust the rank of an iterate $\mathcal{X}^{(t)} = \mathcal{G}^{(t)} \times_{k=1}^d \mathbf{U}_k^{(t)}$ by designing new rank-adaptive strategies with the search directions in

$$T_{\mathcal{X}^{(t)}}\mathcal{M}_{\mathbf{r}^{(t)}} + N_{\leq \ell^{(t)}}(\mathcal{X}^{(t)}) \subseteq T_{\mathcal{X}^{(t)}}\mathcal{M}_{\leq \mathbf{r}}, \quad (6.1)$$

where $N_{\leq \ell^{(t)}}(\mathcal{X}^{(t)}) := \mathcal{M}_{\leq \ell^{(t)}} \cap \left(\bigotimes_{k=1}^d \text{span}(\mathbf{U}_k^{(t)})^\perp \right) \subseteq N_{\mathcal{X}^{(t)}}\mathcal{M}_{\mathbf{r}^{(t)}}$ and $\ell^{(t)} \in \mathbb{N}_+^d$ satisfies $\ell^{(t)} \leq \mathbf{r} - \mathbf{r}^{(t)}$.

Generally speaking, we first apply Riemannian optimization on $\mathcal{M}_{\mathbf{r}^{(t)}}$ in section 6.1. Then, rank-decreasing and rank-increasing procedures are developed to automatically adjust the rank of an iterate $\mathcal{X}^{(t)}$ in sections 6.2 and 6.3. In summary, a new Tucker rank-adaptive method (TRAM) is proposed and analyzed in sections 6.4 and 6.5. The implementation details of TRAM are provided in section 6.6.

6.1 Line search on fixed-rank manifold

Given a point $\tilde{\mathcal{X}}^{(t)} \in \mathcal{M}_{\mathbf{r}^{(t)}}$, we observe from (3.2) that $T_{\tilde{\mathcal{X}}^{(t)}}\mathcal{M}_{\mathbf{r}^{(t)}} \subseteq T_{\tilde{\mathcal{X}}^{(t)}}\mathcal{M}_{\leq \mathbf{r}}$. Therefore, the negative Riemannian gradient of f at $\tilde{\mathcal{X}}^{(t)}$ on $\mathcal{M}_{\mathbf{r}^{(t)}}$ provides a convincing search direction that enjoys a closed-form expression (2.9). The Riemannian gradient descent method (RGD) on $\mathcal{M}_{\mathbf{r}^{(t)}}$ is shown in Algorithm 4.

Algorithm 4 Riemannian gradient descent method (RGD) on $\mathcal{M}_{\mathbf{r}^{(t)}}$

Input: Initial guess $\mathcal{Y}^{(0)} = \tilde{\mathcal{X}}^{(t)} \in \mathcal{M}_{\mathbf{r}^{(t)}}$; backtracking parameters $\rho, a \in (0, 1), s_{\min} > 0$.

- 1: **while** the stopping criteria are not satisfied **do**
- 2: Compute $g^{(i)} = -\text{grad}f(\mathcal{Y}^{(i)}) = P_{T_{\mathcal{Y}^{(i)}}\mathcal{M}_{\mathbf{r}^{(t)}}}(-\nabla f(\mathcal{Y}^{(i)}))$ by (2.9).
- 3: Choose stepsize $s^{(i)}$ by Armijo backtracking line search (4.2).
- 4: Update $\mathcal{Y}^{(i+1)} = P_{\mathbf{r}^{(t)}}^{\text{HO}}(\mathcal{Y}^{(i)} + s^{(i)}g^{(i)})$, $i = i + 1$.
- 5: **end while**

Output: The last iterate $\mathcal{X}^{(t)} = \mathcal{Y}^{(i)}$.

Let $\{\mathcal{Y}^{(i)}\}_{i \geq 0}$ be the sequence generated by RGD with $\mathcal{Y}^{(0)} = \tilde{\mathcal{X}}^{(t)}$. The RGD method updates $\mathcal{Y}^{(i)}$ by

$$\mathcal{Y}^{(i+1)} = P_{\mathbf{r}^{(t)}}^{\text{HO}}\left(\mathcal{Y}^{(i)} - s^{(i)} \text{grad}f(\mathcal{Y}^{(i)})\right).$$

For the selection of stepsize, we apply the Armijo backtracking line search (4.2) to ensure the convergence. The algorithm terminates if: 1) rank deficiency is detected, namely, at least one of the mode- k unfolding matrices of \mathcal{Y} satisfies $\sigma_{\min}(\mathbf{Y}_{(k)}^{(i)})/\sigma_{\max}(\mathbf{Y}_{(k)}^{(i)}) \leq \Delta$; 2) the Riemannian gradient satisfies $\|\text{grad}f(\mathcal{Y}^{(i)})\|_F \leq \varepsilon_R^{(t)}$ with threshold $\varepsilon_R^{(t)} > 0$. Note that we always check the rank deficiency in prior to the stationarity.

6.2 Rank-decreasing procedure

Given $\mathcal{X}^{(t)} = \mathcal{G}^{(t)} \times_{k=1}^d \mathbf{U}_k^{(t)}$ returned by Algorithm 4, if the RGD method terminates upon detecting rank deficiency, we proceed by implementing a rank-decreasing procedure, which is able to reduce the number of parameters and thus save storage. Specifically, we produce a rank- $\hat{\mathbf{r}}$ truncation of $\mathcal{X}^{(t)}$ with

$$\hat{r}_k := \min\{i : \sigma_{i,k} < \Delta\sigma_{1,k}\} \quad \text{or} \quad \hat{r}_k := r_k^{(t)} \quad \text{if} \quad \sigma_{r_k^{(t)},k} \geq \Delta\sigma_{1,k},$$

where $\sigma_{1,k} \geq \dots \geq \sigma_{r_k^{(t)},k}$ are the singular values of $\mathbf{X}_{(k)}^{(t)}$ and $\Delta \in (0, 1)$ is a threshold. Subsequently, we yield a truncated low-rank tensor $\mathbf{P}_{\leq \hat{\mathbf{r}}}^{\text{HO}}(\mathcal{X}^{(t)})$. To ensure the convergence, we adaptively shrink Δ by $\rho_1 \Delta$ with $\rho_1 \in (0, 1)$ until it holds that $f(\mathcal{X}^{(t)}) \geq f(\mathbf{P}_{\leq \hat{\mathbf{r}}}^{\text{HO}}(\mathcal{X}^{(t)}))$. Then, we set

$$\tilde{\mathcal{X}}^{(t+1)} = \mathbf{P}_{\leq \hat{\mathbf{r}}}^{\text{HO}}(\mathcal{X}^{(t)}) \in \mathcal{M}_{\leq \mathbf{r}} \quad \text{with} \quad \text{rank}_{\text{tc}}(\tilde{\mathcal{X}}^{(t+1)}) \leq \mathbf{r}^{(t)}.$$

Figure 4 depicts the rank-decreasing procedure for $d = 3$. The detailed rank-decreasing procedure is illustrated in Algorithm 5

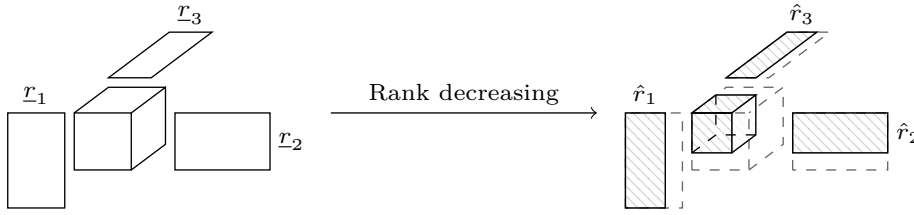


Fig. 4 Illustration of rank-decreasing procedure for $d = 3$

6.3 Rank-increasing procedure

Given $\mathcal{X}^{(t)} = \mathcal{G}^{(t)} \times_{k=1}^d \mathbf{U}_k^{(t)}$ returned by Algorithm 4 with initial guess $\tilde{\mathcal{X}}^{(t)}$, if $\mathcal{X}^{(t)}$ is an $\varepsilon_R^{(t)}$ -stationary point and $\mathbf{r}^{(t)} < \mathbf{r}$, it is reasonable to consider increasing the rank of $\mathcal{X}^{(t)}$ in pursuit of higher accuracy. As Remark 1 suggests, given a matrix $\mathbf{X} \in \mathbb{R}_+^{m \times n}$, adding a matrix in normal part $\mathbf{N}_{\leq \ell}(\mathbf{X})$ can increase the rank of \mathbf{X} . For Tucker tensors, similarly, we observe that

$$\mathbf{r}^{(t)} < \text{rank}_{\text{tc}}(\mathcal{X}^{(t)} + \mathcal{N}_{\leq \ell^{(t)}}^{(t)}) \leq \mathbf{r}$$

Algorithm 5 Rank-decreasing procedure

Input: $\mathcal{X}^{(t)} = \mathcal{G}^{(t)} \times_{k=1}^d \mathbf{U}_k^{(t)}$, $\Delta > 0$, $\rho_1 \in (0, 1)$.
 1: **for** $k = 1, \dots, d$ **do**
 2: Compute the singular values $\sigma_{1,k} \geq \dots \geq \sigma_{r_k^{(t)},k} > 0$ of $\mathbf{G}_{(k)}^{(t)}$.
 3: **end for**
 4: **repeat**
 5: Find $\hat{r}_k = \min\{i : \sigma_i < \Delta\sigma_1\}$ for $k = 1, \dots, d$.
 6: Compute $\hat{\mathcal{X}} = \mathbf{P}_{\leq \hat{\mathbf{r}}}^{\text{HO}}(\mathcal{X}^{(t)})$.
 7: Set $\Delta = \rho_1 \Delta$.
 8: **until** $f(\hat{\mathcal{X}}) \leq f(\mathcal{X}^{(t)})$
Output: $\tilde{\mathcal{X}}^{(t+1)} = \hat{\mathcal{X}}$ and Tucker rank $\underline{\mathbf{r}}^{(t+1)} = \hat{\mathbf{r}}$.

holds for all $\mathcal{N}_{\leq \ell^{(t)}}^{(t)} \in \mathcal{N}_{\leq \ell^{(t)}}(\mathcal{X}^{(t)})$ defined in (6.1) and $0 < \ell^{(t)} \leq \mathbf{r} - \underline{\mathbf{r}}^{(t)}$. Therefore, we can implement line search along $\mathcal{N}_{\leq \ell^{(t)}}^{(t)}$ with $\langle \mathcal{N}_{\leq \ell^{(t)}}^{(t)}, -\nabla f(\mathcal{X}^{(t)}) \rangle \geq 0$ to increase the rank of $\mathcal{X}^{(t)}$ and decrease the function value at the same time. Specifically, for any $\mathbf{U}_{k,1}^{(t)} \in \text{St}(\ell_k^{(t)}, n_k)$ with $(\mathbf{U}_{k,1}^{(t)})^\top \mathbf{U}_k^{(t)} = 0$, the direction

$$\mathcal{N}_{\leq \ell^{(t)}}^{(t)} := -\nabla f(\mathcal{X}^{(t)}) \times_{k=1}^d \mathbf{P}_{\mathbf{U}_{k,1}^{(t)}} \in \mathcal{N}_{\leq \ell^{(t)}}(\mathcal{X}^{(t)})$$

is always a descent direction. To ensure the convergence, we apply the Armijo backtracking line search (4.2). Subsequently, we yield a new tensor

$$\tilde{\mathcal{X}}^{(t+1)} = \mathcal{X}^{(t)} + s \mathcal{N}_{\leq \ell^{(t)}}^{(t)} \in \mathcal{M}_{\leq \mathbf{r}} \text{ with } \text{rank}_{\text{tc}}(\tilde{\mathcal{X}}^{(t+1)}) > \underline{\mathbf{r}}^{(t)}.$$

In the sense of tensor space, the rank-increasing procedure updates the tensor $\mathcal{X}^{(t)}$ to the tensor $\tilde{\mathcal{X}}^{(t+1)}$ in a larger tensor space,

$$\bigotimes_{k=1}^d \text{span}(\mathbf{U}_k^{(t)}) \longrightarrow \bigotimes_{k=1}^d \left(\text{span}(\mathbf{U}_k^{(t)}) + \text{span}(\mathbf{U}_{k,1}^{(t)}) \right).$$

A geometric illustration of the rank-increasing procedure for $d = 3$ is depicted in Fig. 5. Algorithm 6 summarizes the proposed rank-increasing procedure.

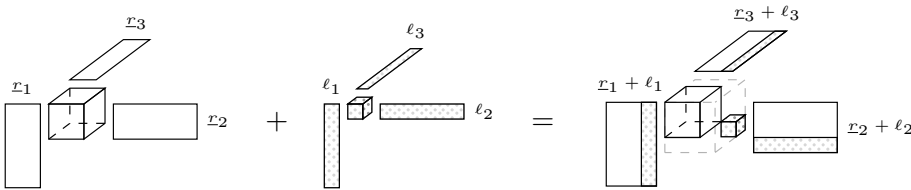


Fig. 5 Illustration of rank-increasing procedure for $d = 3$

Algorithm 6 Rank-increasing procedure**Input:** $\mathcal{X}^{(t)} = \mathcal{G}^{(t)} \times_{k=1}^d \mathbf{U}_k^{(t)}, \ell^{(t)}$.1: Select $\mathbf{U}_{1,1}^{(t)}, \dots, \mathbf{U}_{d,1}^{(t)}$.2: Compute $\hat{\mathcal{G}}^{(t)} = -\nabla f(\mathcal{X}^{(t)}) \times_{k=1}^d (\mathbf{U}_{k,1}^{(t)})^\top$.3: Choose stepsize s by Armijo backtracking line search (4.2).4: Merge the cores $\bar{\mathcal{G}}^{(t)} = \text{diag}(\hat{\mathcal{G}}^{(t)}, s\hat{\mathcal{G}}^{(t)})$, and the factor matrices $\bar{\mathbf{U}}_k^{(t)} = [\mathbf{U}_k^{(t)} \ \mathbf{U}_{k,1}^{(t)}]$.**Output:** Rank-increased tensor $\tilde{\mathcal{X}}^{(t+1)} = \bar{\mathcal{G}}^{(t)} \times_{k=1}^d \bar{\mathbf{U}}_k^{(t)}$ with Tucker rank $\mathbf{r}^{(t)} + \ell^{(t)}$.**Algorithm 7** Tucker rank-adaptive method for (1.1) (TRAM)**Input:** Initial guess $\mathcal{X}^{(0)} = \tilde{\mathcal{X}}^{(0)} \in \mathcal{M}_{\leq \mathbf{r}}$ with $\text{rank}_{\text{tc}}(\mathcal{X}^{(0)}) = \text{rank}_{\text{tc}}(\tilde{\mathcal{X}}^{(0)}) = \mathbf{r}^{(0)}$; parameters $\varepsilon_R^{(0)} > 0, \rho_R \in (0, 1)$; rank-decreasing parameters $\Delta > 0, \rho_1 \in (0, 1)$; rank-increasing parameter $\{\ell^{(t)}\}_{t \geq 0}$; backtracking parameters $\rho, a \in (0, 1), s_{\min} > 0$.1: **while** the stopping criteria are not satisfied **do**2: Compute $\mathcal{X}^{(t)}$ by Algorithm 4 with initial guess $\tilde{\mathcal{X}}^{(t)}$ and threshold $\varepsilon_R^{(t)}$. Obtain the Riemannian gradient $\mathcal{T}^{(t)} = \text{grad}f(\mathcal{X}^{(t)})$.3: **if** Algorithm 4 is terminated by detecting rank deficiency **then**4: Apply rank-decreasing procedure (Algorithm 5) to $\mathcal{X}^{(t)}$ and yield $\tilde{\mathcal{X}}^{(t+1)}$.5: **if** $\text{rank}_{\text{tc}}(\tilde{\mathcal{X}}^{(t+1)}) = \mathbf{r}^{(t)}$ **then**

6: Break.

7: **end if**8: **else**9: **if** $\mathbf{r}^{(t)} = \mathbf{r}$ **then**10: Set $\tilde{\mathcal{X}}^{(t+1)} = \mathcal{X}^{(t)}$ and $\varepsilon_R^{(t+1)} = \rho_R \varepsilon_R^{(t)}$.11: **else**12: Compute $\mathcal{N}_{\leq \ell^{(t)}}^{(t)} = \hat{\mathcal{G}}^{(t)} \times_{k=1}^d \mathbf{U}_{k,1}^{(t)}$ by lines 1–2 in Algorithm 6.13: **if** $\|\mathcal{N}_{\leq \ell^{(t)}}^{(t)}\|_F \geq \varepsilon_1 \|\mathcal{T}^{(t)}\|_F$ and $\varepsilon_2 \|\nabla f(\mathcal{X}^{(t)})\|_F \leq \|\mathcal{T}^{(t)}\|_F$ **then**14: Apply rank-increasing procedure (Algorithm 6) and yield $\tilde{\mathcal{X}}^{(t+1)}$.15: **else if** $\varepsilon_2 \|\nabla f(\mathcal{X}^{(t)})\|_F > \|\mathcal{T}^{(t)}\|_F$ **then**16: Update $\tilde{\mathcal{X}}^{(t+1)} = \text{P}_{\leq \mathbf{r}}^{\text{HO}}(\mathcal{X}^{(t)} - s^{(t)} \nabla f(\mathcal{X}^{(t)}))$ as a restart, where $s^{(t)}$ is computed by Armijo backtracking line search (4.2).17: **else**18: Set $\tilde{\mathcal{X}}^{(t+1)} = \mathcal{X}^{(t)}$ and $\varepsilon_R^{(t+1)} = \rho_R \varepsilon_R^{(t)}$.19: **end if**20: **end if**21: **end if**22: $t = t + 1$.23: **end while****Output:** $\mathcal{X}^{(t)}$

6.4 Tucker rank-adaptive method

We propose the Tucker rank-adaptive method (TRAM) to solve the optimization problem (1.1), as listed in Algorithm 7.

The method begins with the execution of Algorithm 4 using an initial guess of $\tilde{\mathcal{X}}^{(t)}$ and returns a result $\mathcal{X}^{(t)}$. Depending on different properties of $\mathcal{X}^{(t)}$, the rank adjustment proceeds as follows. If $\mathcal{X}^{(t)}$ is found to be rank-deficient, then the rank-decreasing procedure in Algorithm 5 is activated to prevent the potential rank degeneracy. If not, one can consider increasing the rank to improve the accuracy.

To this end, we first check

$$\|\mathcal{N}_{\leq \ell^{(t)}}^{(t)}\|_F \geq \varepsilon_1 \|\mathcal{T}^{(t)}\|_F \quad \text{and} \quad \varepsilon_2 \|\nabla f(\mathcal{X}^{(t)})\|_F \leq \|\mathcal{T}^{(t)}\|_F \quad (6.2)$$

with $\mathcal{T}^{(t)} := \text{grad}f(\mathcal{X}^{(t)})$, which implies that rank increasing does work. We implement the rank-increasing procedure in Algorithm 6 to increase the rank; otherwise, in view of (3.2) and Fig. 3, we observe that

$$\mathcal{T}_{\mathcal{X}^{(t)}} \mathcal{M}_{\mathbf{r}^{(t)}} + \mathcal{N}_{\leq \ell^{(t)}}(\mathcal{X}^{(t)}) \subsetneq \mathcal{T}_{\mathcal{X}^{(t)}} \mathcal{M}_{\leq \mathbf{r}}.$$

Therefore, we check the restart criterion

$$\varepsilon_2 \|\nabla f(\mathcal{X}^{(t)})\|_F \geq \|\mathcal{T}^{(t)}\|_F. \quad (6.3)$$

If the criterion holds, we resort to line search along $-\nabla f(\mathcal{X}^{(t)})$ as a restart in a similar fashion as the GRAP method in Algorithm 2.

6.5 Convergence results

Let $\{\mathcal{X}^{(t)}\}_{t \geq 0}$ be an infinite sequences generated by Algorithm 7. Note that in view of Algorithms 4–5, $\mathcal{X}^{(t+1)}$ satisfies

$$f(\mathcal{X}^{(t+1)}) \leq f(\tilde{\mathcal{X}}^{(t+1)}) \leq f(\mathcal{X}^{(t)}),$$

i.e., $\{f(\mathcal{X}^{(t)})\}_{t \geq 0}$ is nonincreasing. Subsequently, we prove the following global convergence of TRAM.

Lemma 2 *Let $\{\mathcal{X}^{(t)}\}_{t \geq 0}$ be an infinite sequence generated by Algorithm 7. Assume that f is bounded below from f^* . Then, it holds that*

$$\liminf_{t \rightarrow \infty} \|\mathcal{P}_{\mathcal{T}_{\mathcal{X}^{(t)}} \mathcal{M}_{\mathbf{r}^{(t)}}}(-\nabla f(\mathcal{X}^{(t)}))\|_F = 0.$$

Proof See Appendix C. □

By using Lemma 2, we can prove a stronger result as follows.

Theorem 5 *Let $\{\mathcal{X}^{(t)}\}_{t \geq 0}$ be an infinite sequence generated by Algorithm 7. Assume that f is bounded below from f^* . Then, it holds that*

$$\liminf_{t \rightarrow \infty} \|\mathcal{P}_{\mathcal{T}_{\mathcal{X}^{(t)}} \mathcal{M}_{\leq \mathbf{r}}}(-\nabla f(\mathcal{X}^{(t)}))\|_F = 0.$$

Proof Let $\{\tilde{\mathcal{X}}^{(t)}\}_{t \geq 0}$ be an infinite sequence generated by Algorithm 7. It follows from Lemma 2 that there exists a subsequence $\{\mathcal{X}^{(t_j)}\}_{j \geq 0}$, such that $\|\mathcal{T}^{(t_j)}\|_F < \varepsilon_R^{(t_j)}$ and $\lim_{j \rightarrow \infty} \|\mathcal{T}^{(t_j)}\|_F = 0$. Assume that $\|\nabla f(\mathcal{X}^{(t_j)})\|_F \geq \varepsilon_0$ holds for all $j \geq 0$ and some $\varepsilon_0 > 0$. Otherwise, the result is ready.

We aim to prove that $\text{rank}_{\text{tc}}(\mathcal{X}^{(t_j)}) = \mathbf{r}$ for sufficiently large j by contradiction. Since $\|\mathcal{T}^{(t_j)}\|_F$ converges to 0 and (6.3), the restart in line 16 will be continuously executed for sufficiently large j , it follows from the backtracking line search in line 16 that

$$f(\mathcal{X}^{(t_j)}) - f(\tilde{\mathcal{X}}^{(t_j+1)}) \geq s_{\min} a \|\nabla f(\mathcal{X}^{(t_j)})\|_F^2 \geq s_{\min} a \varepsilon_0^2,$$

which contradicts to the fact that $f(\mathcal{X}^{(t_j)}) - f(\tilde{\mathcal{X}}^{(t_j+1)})$ converges to 0.

Therefore, it holds that $\text{rank}_{\text{tc}}(\tilde{\mathcal{X}}^{(t_j)}) = \mathbf{r}$ for sufficiently large j . Consequently,

$$\lim_{j \rightarrow \infty} \|\mathcal{P}_{\mathcal{T}_{\mathcal{X}^{(t_j)}} \mathcal{M}_{\leq \mathbf{r}}}(-\nabla f(\mathcal{X}^{(t_j)}))\|_F = \lim_{j \rightarrow \infty} \|\mathcal{T}^{(t_j)}\|_F = 0.$$

□

6.6 Practical implementation details of TRAM

In practice, the TRAM method is implemented by following the flowchart in Fig. 6.

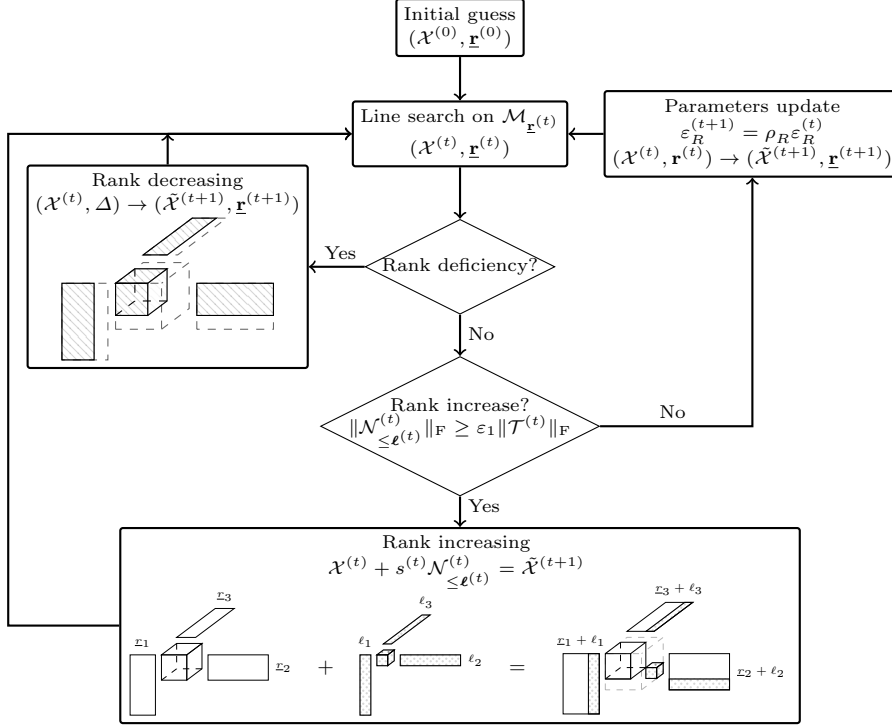


Fig. 6 A flowchart of the practical Tucker rank-adaptive method

Specifically, we notice that applying restart in Algorithm 7 can be computationally disadvantageous, as it involves dealing with full tensors. This scenario arises when $\mathcal{N}_{\leq \ell^{(t)}}^{(t)}$ is rejected by (6.2). Instead, we opt to tighten the stopping criteria by setting $\varepsilon_R^{(t+1)} = \rho_R \varepsilon_R^{(t)}$ and proceed with the RGD method again.

Additionally, let $\{\mathcal{Y}^{(i)}\}_{i \geq 0}$ be a sequence generated by RGD with $\mathcal{Y}^{(0)} = \tilde{\mathcal{X}}^{(t)}$. In practice, the ratio $\sigma_{\min}(\mathbf{Y}_{(k)}^{(i)})/\sigma_{\max}(\mathbf{Y}_{(k)}^{(i)})$ is computed for every point $\mathcal{Y}^{(i)} = \mathcal{G}^{(i)} \times_{k=1}^d \mathbf{U}_k^{(i)} \in \mathcal{M}_{\mathbf{r}^{(t)}}$ in Algorithm 4 to detect the rank deficiency. We observe that

$$\mathbf{Y}_{(k)}^{(i)} = \mathbf{U}_k^{(i)} \mathbf{G}_{(k)}^{(i)} (\mathbf{V}_k^{(i)})^\top = \mathbf{U}_k^{(i)} \check{\mathbf{U}}_k^{(i)} \check{\Sigma}(\check{\mathbf{V}}_k^{(i)})^\top (\mathbf{V}_k^{(i)})^\top$$

is a SVD of $\mathbf{Y}_{(k)}^{(i)}$, where $\check{\mathbf{U}}_k^{(i)} \check{\Sigma}(\check{\mathbf{V}}_k^{(i)})^\top$ is the SVD of $\mathbf{G}_{(k)}^{(i)}$. Therefore, it holds that

$$\frac{\sigma_{\min}(\mathbf{Y}_{(k)}^{(i)})}{\sigma_{\max}(\mathbf{Y}_{(k)}^{(i)})} = \frac{\sigma_{\min}(\mathbf{G}_{(k)}^{(i)})}{\sigma_{\max}(\mathbf{G}_{(k)}^{(i)})}.$$

We can benefit from it and avoid the explicit large-size construction of $\mathcal{Y}^{(i)}$ to carry out the rank detection by employing a small-size $\mathcal{G}^{(i)}$.

7 Numerical experiments

In this section, we test the performance of the proposed GRAP (Algorithm 2), rfGRAP (Algorithm 3), TRAM (Algorithm 7) and other existing methods on the tensor completion problem. Specifically, given a partially observed tensor $\mathcal{A} \in \mathbb{R}^{n_1 \times \dots \times n_d}$ on an index set $\Omega \subseteq [n_1] \times \dots \times [n_d]$. The goal of Tucker tensor completion is to recover the tensor \mathcal{A} from its entries on Ω based on the low-rank Tucker decomposition. The optimization problem can be formulated on the Tucker tensor variety $\mathcal{M}_{\leq \mathbf{r}}$, i.e.,

$$\begin{aligned} \min \quad & \frac{1}{2} \|\mathbf{P}_\Omega(\mathcal{X}) - \mathbf{P}_\Omega(\mathcal{A})\|_F^2 \\ \text{s. t.} \quad & \mathcal{X} \in \mathcal{M}_{\leq \mathbf{r}}, \end{aligned}$$

where \mathbf{P}_Ω is the projection operator onto Ω , i.e., $\mathbf{P}_\Omega(\mathcal{X})(i_1, \dots, i_d) = \mathcal{X}(i_1, \dots, i_d)$ if $(i_1, \dots, i_d) \in \Omega$, otherwise $\mathbf{P}_\Omega(\mathcal{X})(i_1, \dots, i_d) = 0$ for $\mathcal{X} \in \mathbb{R}^{n_1 \times \dots \times n_d}$. The *sampling rate* is denoted by $p := |\Omega|/(n_1 n_2 \dots n_d)$.

7.1 Implementation details

First, we introduce all the default settings and implementation details. In general, the tensor-related implementation of proposed methods is based on the Tensor-Toolbox v3.4¹. All experiments are performed on a workstation with two Intel(R) Xeon(R) Processors Gold 6330 (at 2.00GHz×28, 42M Cache) and 512GB of RAM running Matlab R2019b under Ubuntu 22.04.3. The codes of proposed methods are available at <https://github.com/JimmyPeng1998>.

Computing projections Given a tensor $\mathcal{T} \in \mathbb{R}^{n_1 \times \dots \times n_d}$ and $\mathcal{X} = \mathcal{G} \times_{k=1}^d \mathbf{U}_k$ with $\text{rank}_{\text{tc}}(\mathcal{X}) = \mathbf{r}$, the proposed methods involve the projections onto the tangent cone $\mathcal{T}_{\mathcal{X}}\mathcal{M}_{\leq \mathbf{r}}$ and Tucker tensor varieties $\mathcal{M}_{\mathbf{r}}$. We provide the computational details of two projections, $\tilde{\mathbf{P}}_{\mathcal{T}_{\mathcal{X}}\mathcal{M}_{\leq \mathbf{r}}}(\mathcal{T})$ and $\mathbf{P}_{\leq \mathbf{r}}^{\text{HO}}(\mathcal{T})$. In practice, we never manipulate a large full tensor \mathcal{X} with $n_1 \dots n_d$ number of parameters in $\tilde{\mathbf{P}}_{\mathcal{T}_{\mathcal{X}}\mathcal{M}_{\leq \mathbf{r}}}(\mathcal{T})$ and $\mathbf{P}_{\leq \mathbf{r}}^{\text{HO}}(\mathcal{T})$ but core tensor and unfolding matrices.

The approximate projection $\tilde{\mathbf{P}}_{\mathcal{T}_{\mathcal{X}}\mathcal{M}_{\leq \mathbf{r}}}(\mathcal{T})$ in (3.12) involves choosing appropriate matrices $\tilde{\mathbf{U}}_{k,1} \in \text{St}(r_k - r_k, n_k)$ with $\tilde{\mathbf{U}}_{k,1}^\top \mathbf{U}_k = 0$ for $k \in [d]$. One possible approach is to randomly generate $\tilde{\mathbf{U}}_{k,1}$ and then orthogonalize the matrix $[\mathbf{U}_k \ \tilde{\mathbf{U}}_{k,1}]$. Another approach is to select $\tilde{\mathbf{U}}_{k,1}$ as the leading $r_k - r_k$ singular vectors of $\mathbf{P}_{\mathbf{U}_k}^\perp \mathbf{A}_{\neq k} \in \mathbb{R}^{n_k \times r - r_k}$, where $\mathbf{A}_{\neq k} := \left(\mathcal{T} \times_{j \neq k} \mathbf{U}_j^\top \right)_{(k)}$. Subsequently, the approximate projection onto $\mathcal{T}_{\mathcal{X}}\mathcal{M}_{\leq \mathbf{r}}$ can be computed by Algorithm 1. These two approaches of choosing $\tilde{\mathbf{U}}_{k,1}$ are also adopted to selecting $\{\mathbf{U}_{k,1}\}_{k=1}^d$ in Algorithm 6. Additionally, the orthogonal projection onto the tangent space is computed by GeomCG toolbox². Note that if $\text{rank}_{\text{tc}}(\mathcal{X}^{(t)}) = \mathbf{r}$ in GRAP method, the projection onto the tangent cone is also computed by GeomCG toolbox for fair comparison since $\mathcal{T}_{\mathcal{X}^{(t)}}\mathcal{M}_{\leq \mathbf{r}} = \mathcal{T}_{\mathcal{X}^{(t)}}\mathcal{M}_{\mathbf{r}}$.

¹ Tensor-Toolbox v3.4: <http://www.tensortoolbox.org/>

² GeomCG toolbox: <https://www.epfl.ch/labs/anchp/index-html/software/geomcg/>.

For the projection $P_{\leq \mathbf{r}}^{\text{HO}}(\mathcal{T})$ in (2.7), in view of Algorithms 2, we consider \mathcal{T} being in the form of $\mathcal{T} = \mathcal{X} + \mathcal{V}$ with $\mathcal{V} \in \mathcal{T}_{\mathcal{X}} \mathcal{M}_{\leq \mathbf{r}}$. We observe from (3.2) that

$$\mathcal{T} = \mathcal{X} + \mathcal{V} \in \bigotimes_{k=1}^d (\text{span}(\mathbf{U}_k) + \text{span}(\mathbf{U}_{k,1}) + \text{span}(\mathbf{U}_{k,2} \mathbf{R}_{k,2})) \subseteq \mathcal{M}_{\leq (\mathbf{r} + \mathbf{r})}.$$

Therefore, the tensor \mathcal{T} admits a Tucker decomposition $\mathcal{T} = \tilde{\mathcal{G}} \times_{k=1}^d \tilde{\mathbf{U}}_k \in \mathcal{M}_{\tilde{\mathbf{r}}}$ with some $\tilde{\mathbf{r}} \leq \mathbf{r} + \mathbf{r}$. Instead of implementing HOSVD directly to the full tensor $\mathcal{T} \in \mathbb{R}^{n_1 \times \dots \times n_d}$, we exploit its low-rank structure and apply HOSVD to the core tensor $\tilde{\mathcal{G}} \in \mathbb{R}^{\tilde{r}_1 \times \dots \times \tilde{r}_d}$ of \mathcal{T} , which is much smaller. Specifically, denote the rank- \mathbf{r} HOSVD of $\tilde{\mathcal{G}}$ by $(\tilde{\mathcal{G}} \times_{k=1}^d \tilde{\mathbf{U}}_k^{\top}) \times_{k=1}^d \tilde{\mathbf{U}}_k$, where $\tilde{\mathbf{U}}_k \in \text{St}(r_k, \tilde{r}_k)$ is the leading r_k singular vectors of $\tilde{\mathbf{G}}_{(k)}$. Therefore, it holds that

$$P_{\leq \mathbf{r}}^{\text{HO}}(\mathcal{T}) = ((\tilde{\mathcal{G}} \times_{k=1}^d \tilde{\mathbf{U}}_k^{\top}) \times_{k=1}^d \tilde{\mathbf{U}}_k) \times_{k=1}^d \tilde{\mathbf{U}}_k = (\tilde{\mathcal{G}} \times_{k=1}^d \tilde{\mathbf{U}}_k^{\top}) \times_{k=1}^d (\tilde{\mathbf{U}}_k \tilde{\mathbf{U}}_k).$$

Note that $\tilde{\mathbf{U}}_k \tilde{\mathbf{U}}_k^{\top} \in \text{St}(r_k, n_k)$ since $(\tilde{\mathbf{U}}_k \tilde{\mathbf{U}}_k^{\top})^{\top} (\tilde{\mathbf{U}}_k \tilde{\mathbf{U}}_k) = \mathbf{I}_{r_k}$. This technique is also adopted to the rank-decreasing procedure and the retraction in the Riemannian gradient descent method (Algorithm 4) on $\mathcal{M}_{\mathbf{r}}$.

Exact line search on tangent cone Similar to the optimization on fixed-rank manifold of Tucker tensors [KSV14], given a point $\mathcal{X}^{(t)}$ and a descent direction $\mathcal{V}^{(t)} \in \mathcal{T}_{\mathcal{X}^{(t)}} \mathcal{M}_{\leq \mathbf{r}}$, the solution of the optimization problem

$$s_0^{(t)} = \arg \min_{s \geq 0} \|P_{\Omega}(\mathcal{X}^{(t)} + s\mathcal{V}^{(t)}) - P_{\Omega} \mathcal{A}\|_{\text{F}}^2$$

enjoys a closed-form

$$s_0^{(t)} = \frac{\langle P_{\Omega} \mathcal{V}^{(t)}, P_{\Omega}(\mathcal{A} - \mathcal{X}^{(t)}) \rangle}{\langle P_{\Omega} \mathcal{V}^{(t)}, P_{\Omega} \mathcal{V}^{(t)} \rangle} \geq 0.$$

The computation of $P_{\Omega} \mathcal{V}^{(t)}$ is implemented in a `MEX` function. We adopt $s_0^{(t)}$ as an initial stepsize of Armijo backtracking line search in (4.2).

Compared methods For Tucker-based methods, we compare the proposed methods with a Riemannian conjugate gradient method (GeomCG) [KSV14], and a Riemannian conjugate gradient method on quotient manifold under a preconditioned metric³ (Tucker-RCG) [KM16] for optimization on fixed-rank manifold.

We also compare the proposed methods with other candidates based on different tensor formats. For CP decomposition, we choose the graph-based alternating minimization method⁴ by Guan et al. [Gua+20], denoted by CP-AltMin. We consider the Riemannian conjugate gradient method⁵ in [Ste16] for tensor train completion, denoted by TT-RCG. For tensor completion in tensor ring decomposition, we consider the Riemannian gradient descent method (TR-RGD)⁶ under a preconditioned metric proposed by Gao et al. [GPY23].

³ Available at: <https://bamdevmishra.in/codes/tensorcompletion/>.

⁴ Available at: <https://gitlab.com/ricky7guanyu/tensor-completion-with-regularization-term>.

⁵ TTeMPS toolbox: <https://www.epfl.ch/labs/anchp/index-html/software/tttemp/>.

⁶ LRTCTR toolbox: <https://github.com/JimmyPeng1998/LRTCTR>

Stopping criteria The performance of all methods is evaluated by the training and test errors

$$\varepsilon_{\Omega}(\mathcal{X}) := \frac{\|P_{\Omega}(\mathcal{X}) - P_{\Omega}(\mathcal{A})\|_F}{\|P_{\Omega}(\mathcal{A})\|_F} \quad \text{and} \quad \varepsilon_{\Gamma}(\mathcal{X}) := \frac{\|P_{\Gamma}(\mathcal{X}) - P_{\Gamma}(\mathcal{A})\|_F}{\|P_{\Gamma}(\mathcal{A})\|_F},$$

where Γ is a test set different from the training set Ω . We terminate the methods if: 1) the training error $\varepsilon_{\Omega}(\mathcal{X}^{(t)}) < 10^{-12}$; 2) the relative change of the training error $(\varepsilon_{\Omega}(\mathcal{X}^{(t)}) - \varepsilon_{\Omega}(\mathcal{X}^{(t-1)}))/\varepsilon_{\Omega}(\mathcal{X}^{(t-1)}) < 10^{-8}$; 3) maximum iteration number is reached; 4) time budget is exceeded.

Default settings of proposed methods The default settings of the proposed methods are reported below. We set $\rho_R = 0.5$, $\varepsilon_R^{(0)} = 0.1$, rank-decreasing parameters $\Delta = 0.01$ and $\rho_1 = 0.5$, and rank-increasing parameters $\ell = (1, 1, \dots, 1)$ and $\varepsilon_1 = 0.01$ in TRAM. The backtracking parameters are set to be $\rho = 0.5$, $a = 10^{-4}$ and $s_{\min} = 10^{-10}$. Additionally, the maximum iteration number of fixed-rank line search in the TRAM method is set to be 5.

7.2 Experiments on synthetic data

We test the recovery performance of Tucker-based methods on synthetic data. To this end, given $\mathbf{r}^* = (r_1^*, \dots, r_d^*)$, we consider a synthetic low-rank tensor \mathcal{A} generated by

$$\mathcal{A} = \mathcal{G}^* \times_{k=1}^d \mathbf{U}_k^*,$$

where the entries of $\mathcal{G}^* \in \mathbb{R}^{r_1^* \times \dots \times r_d^*}$ and $\mathbf{U}_k^* \in \mathbb{R}^{n_k \times r_k^*}$ are sampled from the normal distribution $\mathcal{N}(0, 1)$. Then, \mathbf{U}_k^* is orthogonalized by the QR decomposition. We set $d = 3$, $n_1 = n_2 = n_3 = 400$, the size of test set $|I| = pn_1n_2n_3$, and $r_1^* = r_2^* = r_3^* = 6$. The initial guess $\mathcal{X}^{(0)}$ is generated in a same fashion with given rank $\mathbf{r}^{(0)}$. A method is terminated if the training error $\varepsilon_{\Omega}(\mathcal{X}^{(t)}) \leq 10^{-12}$ or it exceeds the time budget 200s.

Test with true rank First, we examine the performance of Tucker-based methods with true rank, i.e., $\mathbf{r} = \mathbf{r}^* = (6, 6, 6)$. To ensure a fair comparison, we compare the proposed methods with GeomCG and Tucker-RCG with initial guess $\mathcal{X}^{(0)} \in \mathcal{M}_{\mathbf{r}}$. Figure 7 reports the test error of Tucker-based methods with sampling rate $p = 0.01, 0.05$. First, we observe that GRAP and TRAM methods are comparable to GeomCG and Tucker-RCG. Second, rfGRAP method requires more iterations than other candidates, since it only adopts partial information about the tangent cone to avoid retraction.

Test with under-estimated initial rank In contrast with the Riemannian methods on $\mathcal{M}_{\mathbf{r}}$, the proposed methods can adopt any initial guess $\mathcal{X}^{(0)} \in \mathcal{M}_{\leq \mathbf{r}}$. Therefore, we compare the proposed methods under different initial ranks $\mathbf{r}^{(0)} = (r^{(0)}, r^{(0)}, r^{(0)})$ for $r^{(0)} = 1$ and 5. The sampling rate is chosen as $p = 0.05$. Note that we still run GeomCG and Tucker-RCG on $\mathcal{M}_{\mathbf{r}^{(0)}}$. The test error is reported in Fig. 8. We observe from Fig. 8 that the proposed GRAP and rfGRAP methods have favorably comparable performance than TRAM. A rank-increasing procedure is required to find the true rank \mathbf{r}^* in the TRAM method. In addition, the proposed TRAM

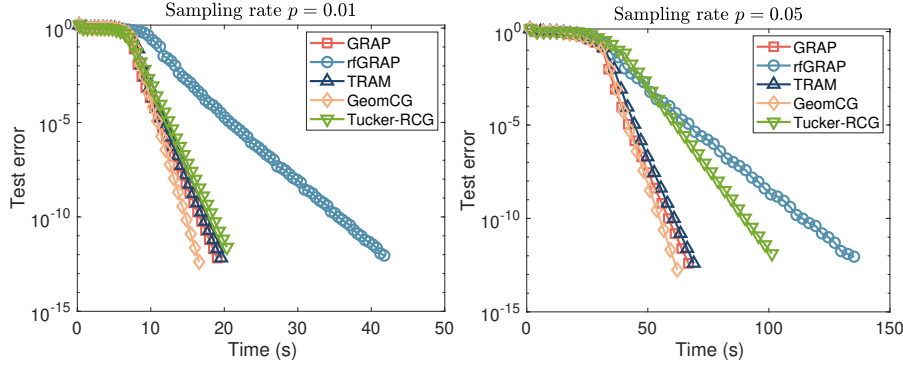


Fig. 7 The recovery performance under sampling rate $p = 0.01, 0.05$

can successfully find the true rank \mathbf{r}^* . However, since $\mathbf{r}^{(0)} < \mathbf{r}^*$, the GeomCG and Tucker-RCG methods can only obtain a poor low-rank approximation of the data tensor \mathcal{A} . Therefore, the rank-increasing procedure does allow us to search in a larger space with higher accuracy.

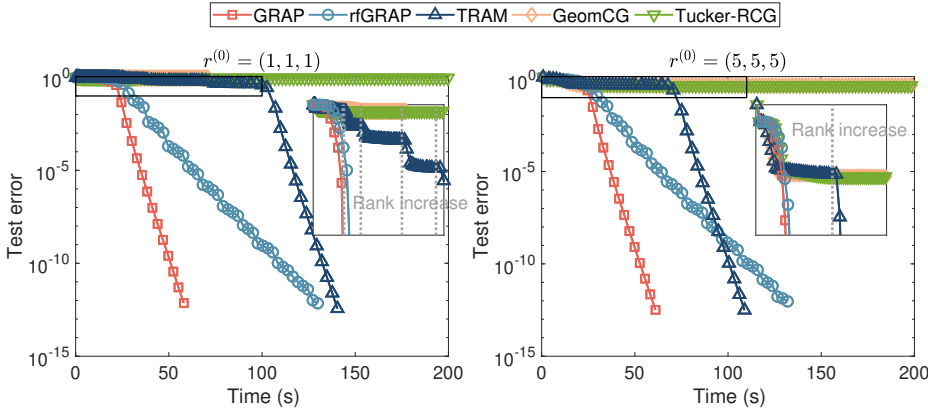


Fig. 8 Test error under different initial ranks $\mathbf{r}^{(0)} = (1, 1, 1)$ and $\mathbf{r}^{(0)} = (5, 5, 5)$

Test with over-estimated rank We test the performance of Tucker-based methods under a set of over-estimated ranks $\mathbf{r} = (r, r, r)$ with $r = 7, 8, 9, 10, 11, 12 > r^* = 6$. We set the sampling rate $p = 0.01$. To ensure a fair comparison to GeomCG and Tucker-RCG(Q), the initial guess $\mathcal{X}^{(0)}$ is generated from $\mathcal{M}_{\mathbf{r}}$. The numerical results are reported in Figs. 9 and 10. First, we observe from Fig. 9 that the proposed TRAM method converges while other candidates fail to recover the data tensor due to the over-estimated rank parameter. Second, the right figure in Fig. 9 suggests that TRAM successfully recovers the true Tucker rank of the data tensor \mathcal{A} under all selections of rank parameter. Therefore, the TRAM performs better than the other candidates. Additionally, Figure 10 provides history of the singular

values of the unfolding matrices $\mathbf{X}_{(1)}^{(t)}$, $\mathbf{X}_{(2)}^{(t)}$, and $\mathbf{X}_{(3)}^{(t)}$ in TRAM for $\mathbf{r} = (8, 8, 8)$. The proposed TRAM method indeed detects the disparity between the leading six singular values and the subsequent two singular values. The rank-decreasing procedure is activated to reduce the rank parameter to the true rank \mathbf{r}^* .

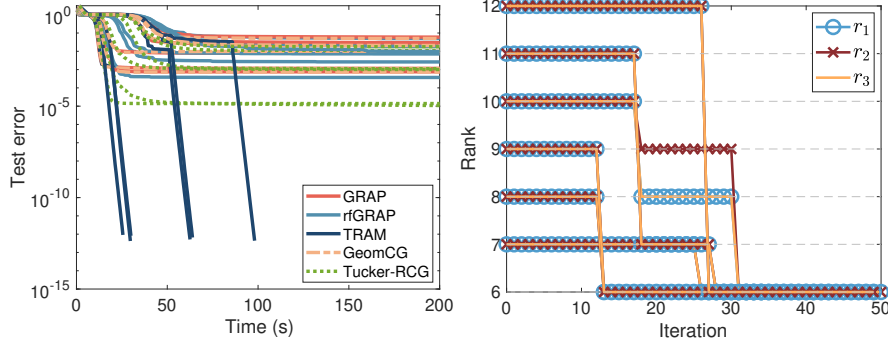


Fig. 9 Numerical results on synthetic dataset under over-estimated rank parameter of Tucker-based methods. Left: test error. Right: rank update of TRAM

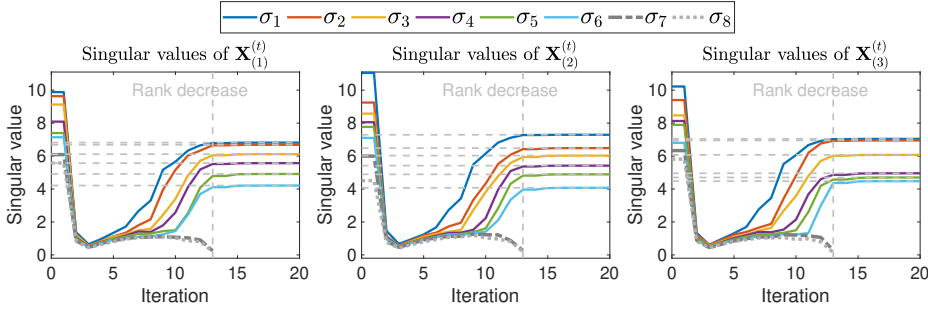


Fig. 10 The history of singular values of unfolding matrices $\mathbf{X}_{(1)}^{(t)}$, $\mathbf{X}_{(2)}^{(t)}$, and $\mathbf{X}_{(3)}^{(t)}$ for $\mathbf{r} = (8, 8, 8)$ in TRAM

7.3 Experiments on hyperspectral images

In this experiment, we test the performance of proposed methods and other candidates on hyperspectral images, which is formulated as a third order tensor $\mathcal{A} \in \mathbb{R}^{n_1 \times n_2 \times n_3}$. Mode three of \mathcal{A} represents the reflectance level under n_3 wavelength values of light. Mode one and two represents the reflectance level of light under different wavelengths. We select the “Ribeira Hotel Image” (Ribeira⁷) with size $249 \times$

⁷ Image source: hsi_32.mat from https://figshare.manchester.ac.uk/articles/dataset/Fifty_hyperspectral_reflectance_images_of_outdoor_scenes/14877285.

329×33 from “50 reduced hyperspectral reflectance images” by Foster [FR22], and “220 Band AVIRIS Hyperspectral Image” (AVIRIS⁸) with size $145 \times 145 \times 220$. Figure 11 shows the twenty-fourth frame of two hyperspectral images.



Fig. 11 The twenty-fourth frame of two images. Left: “Ribeira”. Right: “AVIRIS”

We evaluate the recovery performance of image completion by the peak signal-to-noise ratio (PSNR) defined by

$$\text{PSNR} := 10 \log_{10} \left(n_1 n_2 n_3 \frac{\max(\mathcal{A})}{\|\mathcal{X} - \mathcal{A}\|_{\text{F}}^2} \right),$$

where $\max(\mathcal{A})$ denotes the largest element of \mathcal{A} . Additionally, the relative error

$$\text{relerr} := \frac{\|\mathcal{X} - \mathcal{A}\|_{\text{F}}}{\|\mathcal{A}\|_{\text{F}}}$$

is also reported. The sampling rate is $p = 0.1$. We test the Tucker-based methods under the rank parameter $\mathbf{r} = (r, r, r)$ with $r = 5, 10, 15, \dots, 30$. To ensure a fair comparison, a method is terminated if it reaches the maximum iteration number 250, which is the same as [KM16, §5].

Figure 12 and Table 1 illustrate the recovery results of Tucker-based methods. We observe from Fig. 12 that the low-rank structure along mode three is detected by TRAM, i.e., there exists similarity among different wavelength values of light in the image tensor \mathcal{A} . It is worth noting that the last rank obtained from TRAM under $\mathbf{r} = (15, 15, 15)$ in “Ribeira” image is $(15, 15, 6)$, which coincides with the rank selection in [KSV14, §4.3.1]. Moreover, Table 1 reports a quantified recovery result. The proposed GRAP and rfGRAP are comparable to GeomCG and Tucker-RCG. Specifically, the proposed TRAM method reaches the highest PSNR and the lowest relative error under most rank parameters.

7.4 Experiments on “MovieLens 1M” dataset

We consider tensor completion on the real-world dataset “MovieLens 1M”⁹, which consists of 1000209 movie ratings from 6040 users on 3952 movies from September

⁸ Available at <https://purrr.purdue.edu/publications/1947/1>.

⁹ Available at <https://grouplens.org/datasets/movielens/1m/>.

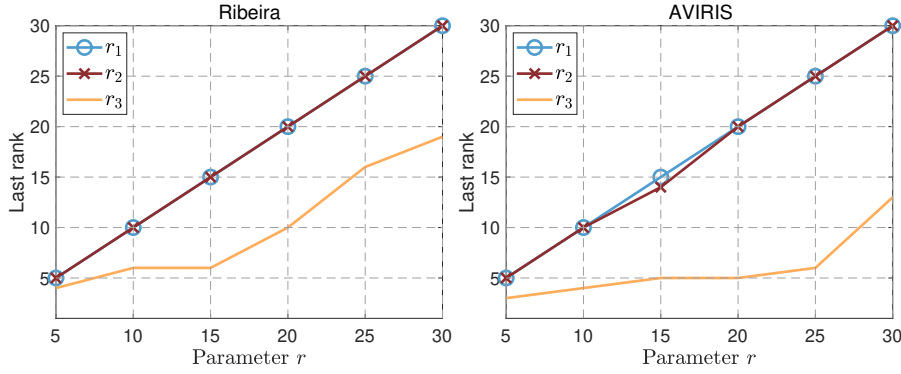


Fig. 12 The last rank obtained from TRAM for “Ribeira” and “AVIRIS” images under different parameters $\mathbf{r} = (r, r, r)$

Table 1 Relative error and PSNR on “Ribeira” and “AVIRIS” image

Tucker rank \mathbf{r} (r_1, r_2, r_3)	Results	GRAP	rfGRAP	TRAM	GeomCG	Tucker-RCG
“Ribeira”						
(5, 5, 5)	PSNR	24.9351	24.9325	24.9351	24.9351	24.9350
	relerr	0.2984	0.2985	0.2984	0.2984	0.2984
(10, 10, 10)	PSNR	26.8481	26.8482	26.8648	26.8483	26.8482
	relerr	0.2394	0.2394	0.2389	0.2394	0.2394
(15, 15, 15)	PSNR	28.3451	28.3450	28.4127	28.3451	28.3451
	relerr	0.2015	0.2015	0.1999	0.2015	0.2015
(20, 20, 20)	PSNR	29.3908	29.3934	29.5197	29.3917	29.3924
	relerr	0.1786	0.1786	0.1760	0.1786	0.1786
(25, 25, 25)	PSNR	30.2324	30.1852	30.3897	30.2315	30.2332
	relerr	0.1621	0.1630	0.1592	0.1622	0.1621
(30, 30, 30)	PSNR	30.7088	30.7182	30.9921	30.7579	30.7566
	relerr	0.1535	0.1533	0.1486	0.1526	0.1527
“AVIRIS”						
(5, 5, 5)	PSNR	31.7181	31.7181	31.6955	31.7181	31.7181
	relerr	0.0835	0.0835	0.0837	0.0835	0.0835
(10, 10, 10)	PSNR	33.7393	33.7393	33.7517	33.7393	33.7394
	relerr	0.0661	0.0661	0.0660	0.0661	0.0661
(15, 15, 15)	PSNR	35.1308	35.1157	35.1427	35.1144	35.1251
	relerr	0.0564	0.0564	0.0563	0.0565	0.0564
(20, 20, 20)	PSNR	36.1776	36.1777	36.5438	36.1781	36.1780
	relerr	0.0500	0.0500	0.0479	0.0500	0.0500
(25, 25, 25)	PSNR	36.6010	36.6430	37.5433	36.6142	36.6002
	relerr	0.0476	0.0473	0.0427	0.0475	0.0476
(30, 30, 30)	PSNR	36.3106	36.4263	37.4879	36.1278	36.1505
	relerr	0.0492	0.0485	0.0430	0.0502	0.0501

19th, 1997 to April 22nd, 1998. By choosing one week as a period, these movie ratings are formulated as a third-order tensor \mathcal{A} of size $6040 \times 3952 \times 150$. We randomly select 80% of the known ratings as a training set Ω and the rest 20% ratings are test set Γ . The rank parameter is set to be $\mathbf{r} = (r, r, r)$ with $r = 1, 2, \dots, 15$. In addition, we not only compare the performance of the proposed methods to other Tucker-based methods, but also to other methods including CP-AltMin,

TT-RCG, and TR-RGD. To ensure a close number of parameters in different tensor decompositions, we choose the CP rank 9, tensor train rank $(1, 4, 4, 1)$, and $(3, 3, 3)$ in tensor ring completion. The initial guess $\mathcal{X}^{(0)}$ for the proposed methods is generated in the same fashion as section 7.2 by Tucker decomposition. Then, the initial guesses for other methods are transformed by CP-ALS [KB09, Fig. 3.3], TT-SVD [Ose11, Theorem 2.1], and TR-SVD [Zha+16, Algorithm 1] from $\mathcal{X}^{(0)}$. Note that initial guesses under different tensor formats have a comparable number of parameters. A method is terminated if it exceeds the time budget of 3000s.

Figures 13 and 14 demonstrate the numerical results on the “MovieLens 1M” dataset. We observe that: 1) the proposed methods are favorably comparable to GeomCG and Tucker-RCG with lower test error under different rank parameters \mathbf{r} ; 2) The test error of the TRAM method is less sensitive when \mathbf{r} increases, while the test error of the other candidates begins increasing; 3) Fig. 13(b) presents the last rank obtained from TRAM. The proposed TRAM method indeed adaptively finds an appropriate rank $\mathbf{r}^{(t)}$ and reveals the low-rank structure of the categories of movies in mode two of the “MovieLens 1M” data tensor \mathcal{A} .

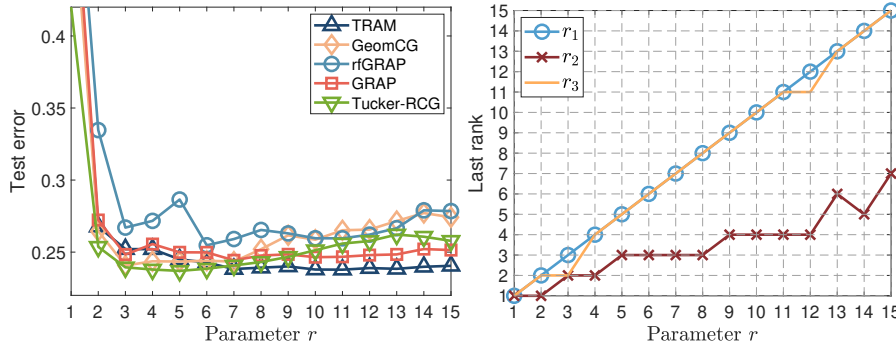


Fig. 13 Test error and the last rank obtained from TRAM under different rank parameters $\mathbf{r} = (r, r, r)$. Left: test error. Right: last rank of TRAM

Moreover, we compare the Tucker-based methods with other methods under rank parameter $\mathbf{r} = (9, 9, 9)$. We observe from Fig. 14(a) that the proposed methods are favorably comparable to other candidates, and the TRAM method performs better than the other candidates. Figure 14(b) demonstrates that under the rank parameter $\mathbf{r} = (9, 9, 9)$, the parameter $\mathbf{r}^{(t)}$ is reduced to $(9, 4, 9)$. This reduction signifies the identification of four distinct categories of movies within the “MovieLens 1M” by TRAM.

8 Conclusion and perspectives

In this paper, we have conducted a thorough investigation of the geometry of Tucker tensor varieties and have developed novel geometric and rank-adaptive methods for optimization on Tucker tensor varieties. We observe that the geometry of Tucker tensor varieties is closely connected but much more intricate to the

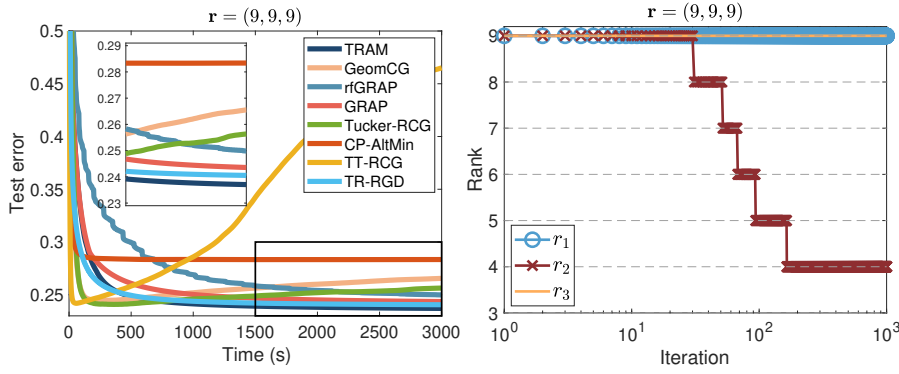


Fig. 14 Numerical results on “MovieLens 1M” dataset under rank parameter $\mathbf{r} = (9, 9, 9)$. Left: test error. Right: rank update in iterations

matrix varieties. All of the results can elegantly boil down to the known ones in matrix varieties via geometric illustration figures. Furthermore, the heart of optimization on Tucker tensor varieties is the metric projection. By leveraging the established geometry, we have proposed approximate projections to circumvent the explicit computation of metric projections. Surprisingly, we have observed the retraction-free search directions by using partial information of the tangent cone. Numerical experiments on tensor completion suggest that the proposed methods perform better than existing state-of-the-art methods across various rank parameter selections. In general, when a reliable rank parameter estimation is available, we recommend the GRAP and rfGRAP methods to bypass the lengthy process of rank parameter selection. Conversely, in scenarios where the rank parameter is uncertain, the TRAM method is advised since it adaptively identifies an appropriate rank. To the best of our knowledge, this study represents the first endeavor to explore optimization on Tucker tensor varieties.

In the future, we intend to adopt the proposed methods for optimization on Tucker tensor varieties to other applications, e.g., dynamic low-rank tensor approximation and low-rank solution of high-dimensional partial differential equations. In addition, it is interesting but challenging to design *apocalypse-free* methods on tensor varieties that is guaranteed to converge to a stationary point.

Declaration

The authors declare that the data supporting the findings of this study are available within the paper. The authors have no competing interests to declare that are relevant to the content of this article.

A Proof of Proposition 2

Proof Since $P_{\leq \mathbf{r}}^{\text{HO}}$ is a contraction mapping, the mapping $t \mapsto R_{\mathcal{X}}(t\mathcal{V})$ is continuous. Then, it suffices to prove $\lim_{t \rightarrow 0+} (R_{\mathcal{X}}^{\text{HO}}(t\mathcal{V}) - \mathcal{X} - t\mathcal{V})/t = 0$. Since $\mathcal{V} \in T_{\mathcal{X}}\mathcal{M}_{\leq \mathbf{r}}$, it follows from [OW04, Proposition 2] that there exists an analytic arc $\gamma : [0, \epsilon) \rightarrow \mathcal{M}_{\leq \mathbf{r}}$ such that $\dot{\gamma}(0) = \mathcal{V}$.

Moreover, since $P_{\leq \mathbf{r}}(\mathcal{X} + t\mathcal{V})$ is the metric projection of $\mathcal{X} + t\mathcal{V}$ onto $\mathcal{M}_{\leq \mathbf{r}}$, it holds that

$$\|\mathcal{X} + t\mathcal{V} - P_{\leq \mathbf{r}}(\mathcal{X} + t\mathcal{V})\|_F \leq \|\mathcal{X} + t\mathcal{V} - \gamma(t)\|_F.$$

By using the quasi-optimality (2.8), we have

$$\|\mathcal{X} + t\mathcal{V} - R_{\mathcal{X}}^{\text{HO}}(t\mathcal{V})\|_F \leq \sqrt{d}\|\mathcal{X} + t\mathcal{V} - P_{\leq \mathbf{r}}(\mathcal{X} + t\mathcal{V})\|_F \leq \sqrt{d}\|\mathcal{X} + t\mathcal{V} - \gamma(t)\|_F = o(t),$$

and thus $R_{\mathcal{X}}^{\text{HO}}$ is a retraction mapping. \square

B Proof of Proposition 4

Proof \mathcal{X}^* admits the Tucker decomposition $\mathcal{G}^* \times_1 \mathbf{U}_1^* \cdots \times_d \mathbf{U}_d^*$, where $\mathcal{G}^* \in \mathbb{R}^{r_1 \times r_2 \times \cdots \times r_d}$, $\mathbf{U}_k^* \in \text{St}(r_k, n_k)$ for $k \in [d]$. Consider the k_0 -th unfolding $\mathbf{X}_{(k_0)}^* = \mathbf{U}_{k_0}^* \mathbf{G}_{(k_0)}^* (\mathbf{V}_{k_0}^*)^\top \in \mathbb{R}^{n_{k_0} \times n_{-k_0}}$, where $\mathbf{V}_{k_0}^* := (\mathbf{U}_j^*)^{\otimes j \neq k_0}$. Since $r_{k_0} < n_{k_0}$ and $r_{-k_0} < n_{-k_0}$, there exists $\mathbf{u} \in \mathbb{R}^{n_{k_0}} \setminus \{0\}$ and $\mathbf{v} \in \mathbb{R}^{n_{-k_0}} \setminus \{0\}$, such that $(\mathbf{U}_{k_0}^*)^\top \mathbf{u} = 0$ and $(\mathbf{V}_{k_0}^*)^\top \mathbf{v} = 0$.

Consider the sequence $\mathcal{X}^{(t)} \in \mathcal{M}_{\leq \mathbf{r}}$ defined by $\mathcal{X}^{(t)} = \mathcal{G}^{(t)} \times_{k=1}^d [\mathbf{U}_k^* \mathbf{U}_{k,1}]$, where $\mathbf{U}_{k,1} \in \text{St}(r_k - r_k, n_k)$ with $\mathbf{U}_{k,1}^\top \mathbf{U}_k^* = 0$, $\mathcal{G}^{(t)}(i_1, \dots, i_d) := \mathcal{G}^*(i_1, \dots, i_d)$ if $(i_1, \dots, i_d) \leq \mathbf{r}$, $\mathcal{G}^{(t)}(i_1, \dots, i_d) := \frac{1}{t} \bar{\mathcal{G}}(i_1 - r_1, \dots, i_d - r_d)$ if $(i_1, \dots, i_d) > \mathbf{r}$, $\mathcal{G}^{(t)}(i_1, \dots, i_d) := 0$ otherwise; and $\bar{\mathcal{G}} \in \mathbb{R}^{(r_1 - r_1) \times (r_2 - r_2) \times \cdots \times (r_d - r_d)}$ satisfying $\text{rank}_{\text{tc}}(\bar{\mathcal{G}}) = \mathbf{r} - \mathbf{r}$. Then, it holds that $\text{rank}_{\text{tc}}(\mathcal{X}^{(t)}) = \mathbf{r}$ and $\mathcal{X}^{(t)}$ converges to \mathcal{X}^* .

Consider the function $f(\mathcal{X}) = \mathbf{u}^\top \mathbf{X}_{(k_0)}^* \mathbf{v}$. Since \mathcal{X}^* is rank-deficient but the gradient $\nabla f(\mathcal{X}) = \text{ten}_{(k_0)}(\mathbf{u}\mathbf{v}^\top) \neq 0$, it follows from Corollary 2 that \mathcal{X}^* is not a stationary point. Moreover, for all $\mathcal{X}^{(t)} \in \mathcal{M}_{\mathbf{r}}$, we have

$$\begin{aligned} P_{T_{\mathcal{X}^{(t)}} \mathcal{M}_{\leq \mathbf{r}}}(-\nabla f(\mathcal{X}^{(t)})) &= P_{T_{\mathcal{X}^{(t)}} \mathcal{M}_{\mathbf{r}}}(-\nabla f(\mathcal{X}^{(t)})) \\ &= -\left(\text{ten}_{(k_0)}(\mathbf{u}\mathbf{v}^\top) \times_{k=1}^d (\mathbf{U}_k^*)^\top\right) \times_{k=1}^d \mathbf{U}_k^* \\ &\quad - \sum_{k=1}^d \mathcal{G}^{(t)} \times_k \left(P_{\mathbf{U}_k^*}^\perp(\text{ten}_{(k_0)}(\mathbf{u}\mathbf{v}^\top) \times_{j \neq k} (\mathbf{U}_j^*)^\top)_{(k)} (\mathcal{G}_{(k)}^{(t)})^\dagger\right) \times_{j \neq k} \mathbf{U}_j^* \\ &= -\mathcal{G}^{(t)} \times_{k_0} \left(P_{\mathbf{U}_{k_0}^*}^\perp \mathbf{u}\mathbf{v}^\top \mathbf{V}_{k_0}^* (\mathcal{G}_{(k_0)}^{(t)})^\dagger\right) \times_{j \neq k_0} \mathbf{U}_j^* \\ &= 0, \end{aligned}$$

where we use (2.9) and $\text{ten}_{(k_0)}(\mathbf{u}\mathbf{v}^\top) \times_{j \neq k} (\mathbf{U}_j^*)^\top = 0$ for $k \neq k_0$.

Hence, the triplet $(\mathcal{X}^*, \{\mathcal{X}^{(t)}\}, f)$ is an apocalypse. \square

C Proof of Lemma 2

Proof Let $\{\tilde{\mathcal{X}}^{(t)}\}_{t \geq 0}$ be an infinite sequence generated by Algorithm 7. First, we claim that there are infinite many t such that $\|\mathcal{T}^{(t)}\|_F \leq \varepsilon_R^{(t)}$. Otherwise, according to the stopping criteria of Algorithm 4, it always returns rank-deficient points for sufficiently large t . Hence, the rank-decreasing procedure will be executed continuously, which leads to a contradiction to the fact that rank is finite. Additionally, we claim that the update of parameters in lines 10 and 18 is executed finitely. If not, $\varepsilon_R^{(t+1)} = \rho_R \varepsilon_R^{(t)}$ is executed infinitely and thus $\lim_{t \rightarrow \infty} \varepsilon_R^{(t)} = 0$, implying $\liminf_{t \rightarrow \infty} \|P_{T_{\mathcal{X}^{(t)}} \mathcal{M}_{\mathbf{r}}}(-\nabla f(\mathcal{X}^{(t)}))\|_F = 0$.

Consequently, there exists a subsequence $\{\mathcal{X}^{(t_j)}\}_{j \geq 0}$ satisfying $\|\mathcal{T}^{(t_j)}\|_F \leq \varepsilon_R^{(t_j)}$. We aim to prove that $\|\mathcal{T}^{(t_j)}\|_F$ converges to 0. Since f is bounded below, it holds that

$$0 \leq \lim_{j \rightarrow \infty} f(\mathcal{X}^{(t_j)}) - f(\tilde{\mathcal{X}}^{(t_j+1)}) \leq \lim_{j \rightarrow \infty} f(\mathcal{X}^{(t_j)}) - f(\mathcal{X}^{(t_j+1)}) = 0.$$

Subsequently, we proceed to discuss two scenarios (rank-increasing procedure and restart) regarding the update of $\mathcal{X}^{(t_j)}$ for sufficiently large j : 1) if the rank-increasing procedure in line 14 is executed, it follows from the backtracking line search in Algorithm 6 and (6.2) that

$$\begin{aligned} f(\mathcal{X}^{(t_j)}) - f(\tilde{\mathcal{X}}^{(t_j+1)}) &\geq s_{\min} a \langle \mathcal{N}_{\leq \ell^{(t_j)}}^{(t_j)}, -\nabla f(\mathcal{X}^{(t_j)}) \rangle \\ &= s_{\min} a \|\mathcal{N}_{\leq \ell^{(t_j)}}^{(t_j)}\|_{\mathbb{F}}^2 \\ &\geq s_{\min} a \varepsilon_1^2 \|\mathcal{T}^{(t_j)}\|_{\mathbb{F}}^2; \end{aligned}$$

2) if the restart in line 16 is executed, the search direction $-\nabla f(\mathcal{X}^{(t_j)})$ is adopted. Therefore, it holds that

$$\begin{aligned} f(\mathcal{X}^{(t_j)}) - f(\tilde{\mathcal{X}}^{(t_j+1)}) &\geq s_{\min} a \|\nabla f(\mathcal{X}^{(t_j)})\|_{\mathbb{F}}^2 \\ &\geq s_{\min} a \|\mathcal{T}^{(t_j)}\|_{\mathbb{F}}^2. \end{aligned}$$

In summary, we have

$$\|\mathcal{T}^{(t_j)}\|_{\mathbb{F}}^2 \leq \frac{f(\mathcal{X}^{(t_j)}) - f(\tilde{\mathcal{X}}^{(t_j+1)})}{s_{\min} a \min\{\varepsilon_1^2, 1\}}$$

for sufficiently large j and thus it converges to 0. \square

References

- [AMS09] P.-A. Absil, Robert Mahony, and Rodolphe Sepulchre. *Optimization Algorithms on Matrix Manifolds*. Princeton University Press, 2009. DOI: [10.1515/9781400830244](https://doi.org/10.1515/9781400830244).
- [BAC19] Nicolas Boumal, Pierre-Antoine Absil, and Coralia Cartis. “Global rates of convergence for nonconvex optimization on manifolds”. In: *IMA Journal of Numerical Analysis* 39.1 (2019), pp. 1–33. DOI: [10.1093/imanum/drx080](https://doi.org/10.1093/imanum/drx080).
- [BEU23] Markus Bachmayr, Henrik Eisenmann, and André Uschmajew. “Dynamical low-rank tensor approximations to high-dimensional parabolic problems: existence and convergence of spatial discretizations”. In: *arXiv preprint arXiv:2308.16720* (2023).
- [Bou23] Nicolas Boumal. *An Introduction to Optimization on Smooth Manifolds*. Cambridge University Press, 2023. DOI: [10.1017/9781009166164](https://doi.org/10.1017/9781009166164). URL: <https://www.nicolasboumal.net/book>.
- [BV06] Winfried Bruns and Udo Vetter. *Determinantal Rings*. Vol. 1327. Springer, 2006. URL: <https://link.springer.com/content/pdf/10.1007/BFb0080378.pdf>.
- [DDV00] Lieven De Lathauwer, Bart De Moor, and Joos Vandewalle. “A multilinear singular value decomposition”. In: *SIAM Journal on Matrix Analysis and Applications* 21.4 (2000), pp. 1253–1278.
- [Don+22] Shuyu Dong et al. “New Riemannian preconditioned algorithms for tensor completion via polyadic decomposition”. In: *SIAM Journal on Matrix Analysis and Applications* 43.2 (2022), pp. 840–866. DOI: [10.1137/21M1394734](https://doi.org/10.1137/21M1394734).
- [FR22] David H Foster and Adam Reeves. “Colour constancy failures expected in colourful environments”. In: *Proceedings of the Royal Society B* 289.1967 (2022), p. 20212483. DOI: [10.1098/rspb.2021.2483](https://doi.org/10.1098/rspb.2021.2483).

- [GA22] Bin Gao and P.-A. Absil. “A Riemannian rank-adaptive method for low-rank matrix completion”. In: *Computational Optimization and Applications* 81 (2022), pp. 67–90. doi: [10.1007/s10589-021-00328-w](https://doi.org/10.1007/s10589-021-00328-w).
- [GKS20] Kathrin Glau, Daniel Kressner, and Francesco Statti. “Low-rank tensor approximation for Chebyshev interpolation in parametric option pricing”. In: *SIAM Journal on Financial Mathematics* 11.3 (2020), pp. 897–927. doi: [10.1137/19M1244172](https://doi.org/10.1137/19M1244172).
- [GKT13] Lars Grasedyck, Daniel Kressner, and Christine Tobler. “A literature survey of low-rank tensor approximation techniques”. In: *GAMM-Mitteilungen* 36.1 (2013), pp. 53–78. doi: [10.1002/gamm.201310004](https://doi.org/10.1002/gamm.201310004).
- [GPY23] Bin Gao, Renfeng Peng, and Ya-xiang Yuan. “Riemannian preconditioned algorithms for tensor completion via tensor ring decomposition”. In: *arXiv preprint arXiv:2302.14456* (2023).
- [Gua+20] Yu Guan et al. “Alternating minimization algorithms for graph regularized tensor completion”. In: *arXiv preprint arXiv:2008.12876* (2020).
- [Hit28] Frank L Hitchcock. “Multiple invariants and generalized rank of a p-way matrix or tensor”. In: *Journal of Mathematics and Physics* 7.1-4 (1928), pp. 39–79.
- [HS95] Uwe Helmke and Mark A Shayman. “Critical points of matrix least squares distance functions”. In: *Linear Algebra and its Applications* 215 (1995), pp. 1–19. doi: [10.1016/0024-3795\(93\)00070-G](https://doi.org/10.1016/0024-3795(93)00070-G).
- [HU19] Seyedehsormayeh Hosseini and André Uschmajew. “A gradient sampling method on algebraic varieties and application to nonsmooth low-rank optimization”. In: *SIAM Journal on Optimization* 29.4 (2019), pp. 2853–2880. doi: [10.1137/17M1153571](https://doi.org/10.1137/17M1153571).
- [KB09] Tamara G Kolda and Brett W Bader. “Tensor decompositions and applications”. In: *SIAM Review* 51.3 (2009), pp. 455–500. doi: [10.1137/07070111X](https://doi.org/10.1137/07070111X).
- [KL10] Othmar Koch and Christian Lubich. “Dynamical tensor approximation”. In: *SIAM Journal on Matrix Analysis and Applications* 31.5 (2010), pp. 2360–2375. doi: [10.1137/09076578X](https://doi.org/10.1137/09076578X).
- [KM16] Hiroyuki Kasai and Bamdev Mishra. “Low-rank tensor completion: a Riemannian manifold preconditioning approach”. In: *Proceedings of The 33rd International Conference on Machine Learning*. Ed. by Maria Florina Balcan and Kilian Q. Weinberger. Vol. 48. Proceedings of Machine Learning Research. New York, New York, USA: PMLR, June 2016, pp. 1012–1021. URL: <https://proceedings.mlr.press/v48/kasai16.html>.
- [KNW86] Arie Kapteyn, Heinz Neudecker, and Tom Wansbeek. “An approach to n-mode components analysis”. In: *Psychometrika* 51.2 (1986), pp. 269–275. doi: [10.1007/BF02293984](https://doi.org/10.1007/BF02293984).
- [KSV14] Daniel Kressner, Michael Steinlechner, and Bart Vandereycken. “Low-rank tensor completion by Riemannian optimization”. In: *BIT Numerical Mathematics* 54.2 (2014), pp. 447–468. doi: [10.1007/s10543-013-0455-z](https://doi.org/10.1007/s10543-013-0455-z).
- [KSV16] Daniel Kressner, Michael Steinlechner, and Bart Vandereycken. “Pre-conditioned low-rank Riemannian optimization for linear systems with tensor product structure”. In: *SIAM Journal on Scientific Computing* 38.4 (2016), A2018–A2044. doi: [10.1137/15M1032909](https://doi.org/10.1137/15M1032909).

- [Kut18] Benjamin Kutschan. “Tangent cones to tensor train varieties”. In: *Linear Algebra and its Applications* 544 (2018), pp. 370–390. DOI: <https://doi.org/10.1016/j.laa.2018.01.012>.
- [LKB23] Eitan Levin, Joe Kileel, and Nicolas Boumal. “Finding stationary points on bounded-rank matrices: A geometric hurdle and a smooth remedy”. In: *Mathematical Programming* 199.1–2 (2023), pp. 831–864. DOI: [10.1007/s10107-022-01851-2](https://doi.org/10.1007/s10107-022-01851-2).
- [LQ23] Ziyang Luo and Liqun Qi. “Optimality conditions for Tucker low-rank tensor optimization”. In: *Computational Optimization and Applications* (2023), pp. 1–24. DOI: [10.1007/s10589-023-00465-4](https://doi.org/10.1007/s10589-023-00465-4).
- [Mis+14] Bamdev Mishra et al. “Fixed-rank matrix factorizations and Riemannian low-rank optimization”. In: *Computational Statistics* 29 (2014), pp. 591–621. DOI: [10.1007/s00180-013-0464-z](https://doi.org/10.1007/s00180-013-0464-z).
- [OA23] Guillaume Ollier and P.-A. Absil. “An apocalypse-free first-order low-rank optimization algorithm with at most one rank reduction attempt per iteration”. In: *SIAM Journal on Matrix Analysis and Applications* 44.3 (2023), pp. 1421–1435. DOI: [10.1137/22M1518256](https://doi.org/10.1137/22M1518256).
- [OGA23] Guillaume Ollier, Kyle A Gallivan, and P.-A. Absil. “First-order optimization on stratified sets”. In: *arXiv preprint arXiv:2303.16040* (2023).
- [Ose11] Ivan V Oseledets. “Tensor-train decomposition”. In: *SIAM Journal on Scientific Computing* 33.5 (2011), pp. 2295–2317. DOI: [10.1137/090752286](https://doi.org/10.1137/090752286).
- [OUV23] Guillaume Ollier, André Uschmajew, and Bart Vandereycken. “Gauss-Southwell type descent methods for low-rank matrix optimization”. In: *arXiv preprint arXiv:2306.00897* (2023).
- [OW04] Donal B O’Shea and Leslie C Wilson. “Limits of tangent spaces to real surfaces”. In: *American Journal of Mathematics* 126.5 (2004), pp. 951–980. DOI: [10.1353/ajm.2004.0040](https://doi.org/10.1353/ajm.2004.0040).
- [Pen+14] Y. Peng et al. “Decomposable Nonlocal Tensor Dictionary Learning for Multispectral Image Denoising”. In: *2014 IEEE Conference on Computer Vision and Pattern Recognition*. 2014, pp. 2949–2956.
- [Ste16] Michael Steinlechner. “Riemannian optimization for high-dimensional tensor completion”. In: *SIAM Journal on Scientific Computing* 38.5 (2016), S461–S484. DOI: [10.1137/15M1010506](https://doi.org/10.1137/15M1010506).
- [SU15] Reinhold Schneider and André Uschmajew. “Convergence results for projected line-search methods on varieties of low-rank matrices via Łojasiewicz inequality”. In: *SIAM Journal on Optimization* 25.1 (2015), pp. 622–646. DOI: [10.1137/140957822](https://doi.org/10.1137/140957822).
- [SWC12] Uri Shalit, Daphna Weinshall, and Gal Chechik. “Online learning in the embedded manifold of low-rank matrices”. In: *Journal of Machine Learning Research* 13.2 (2012). URL: <https://www.jmlr.org/papers/volume13/shalit12a/shalit12a.pdf>.
- [TT23] Tianyun Tang and Kim-Chuan Toh. “Solving graph equipartition SDPs on an algebraic variety”. In: *Mathematical Programming* (2023), pp. 1–49. DOI: [10.1007/s10107-023-01952-6](https://doi.org/10.1007/s10107-023-01952-6).
- [Tuc+64] Ledyard R Tucker et al. “The extension of factor analysis to three-dimensional matrices”. In: *Contributions to Mathematical Psychology* 110119 (1964).

- [UV13] André Uschmajew and Bart Vandereycken. “The geometry of algorithms using hierarchical tensors”. In: *Linear Algebra and its Applications* 439.1 (2013), pp. 133–166.
- [UV20] André Uschmajew and Bart Vandereycken. “Geometric methods on low-rank matrix and tensor manifolds”. In: *Handbook of Variational Methods for Nonlinear Geometric Data*. Springer, 2020, pp. 261–313. URL: https://link.springer.com/chapter/10.1007/978-3-030-31351-7_9.
- [Van13] Bart Vandereycken. “Low-rank matrix completion by Riemannian optimization”. In: *SIAM Journal on Optimization* 23.2 (2013), pp. 1214–1236. DOI: [10.1137/110845768](https://doi.org/10.1137/110845768).
- [Ver+23] Charlotte Vermeylen et al. “Rank estimation for third-order tensor completion in the tensor-train format”. In: *2023 31st European Signal Processing Conference (EUSIPCO)*. IEEE, 2023, pp. 965–969.
- [VT03] M Alex O Vasilescu and Demetri Terzopoulos. “Multilinear subspace analysis of image ensembles”. In: *2003 IEEE Computer Society Conference on Computer Vision and Pattern Recognition, 2003. Proceedings.* Vol. 2. IEEE, 2003, pp. II–93. DOI: [10.1109/CVPR.2003.1211457](https://doi.org/10.1109/CVPR.2003.1211457).
- [Wan+23] Yifan Wang et al. “Solving high dimensional partial differential equations using tensor neural network and a posteriori error estimators”. In: *arXiv preprint arXiv:2311.02732* (2023).
- [Zha+16] Qibin Zhao et al. “Tensor ring decomposition”. In: *arXiv preprint arXiv:1606.05535* (2016). URL: <https://arxiv.org/abs/1606.05535>.
- [Zho+16] Guifang Zhou et al. “A Riemannian rank-adaptive method for low-rank optimization”. In: *Neurocomputing* 192 (2016), pp. 72–80. DOI: [j.neucom.2016.02.030](https://doi.org/10.1016/j.neucom.2016.02.030).